SPECIAL CONSIDERATIONS IN ESTIMATING DETECTION LIMITS

By

CHRISTOPHER LEONIDAS STEVENSON

A DISSERTATION PRESENTED TO THE GRADUATE SCHOOL
OF THE UNIVERSITY OF FLORIDA IN PARTIAL FULFILLMENT
OF THE REQUIREMENTS FOR THE DEGREE OF
DOCTOR OF PHILOSOPHY

UNIVERSITY OF FLORIDA

1991

ACKNOWLEDGEMENTS

There have been many group members who have been supportive throughout the past years, and who have made this time much more interesting. Most particularly I would like to thank Joe Simeonsson and Giuseppe Petrucci for their invaluable friendship and help in the lab; Giuseppe especially was helpful in keeping me alert through his constant prowling about for unwatched lab equipment. Joe also kept me on my toes -- he dogged my trail from North Carolina to Florida, and kept showing up at every residence I ever had in Gainesville.

By far the three people most influential on me during my stay here have been three outstanding scientists and teachers: Benny Smith, Nico Omenetto, and Jim Winefordner. It would be fortunate indeed to have come into contact with any one of these three during graduate school; having worked with all of them has been an unforgettable experience. I especially would like to thank Jim for his support and encouragement, and the opportunity to be a part of his group.

Finally, my deepest love and gratitude go to my family, who have never faltered in their support. Nothing would have been possible without the tremendous love of my parents and sister. Maybe someday I may even move back to California.

TABLE OF CONTENTS

Abstract of Dissertation Presented to the Graduate School
of the University of Florida in Partial Fulfillment of the
Requirements for the Degree of Doctor of Philosophy

SPECIAL CONSIDERATIONS IN ESTIMATING DETECTION LIMITS

By

Christopher Leonidas Stevenson

December 1991

Chairperson: James D. Winefordner
Major Department: Chemistry

A valuable figure of merit in evaluating and comparing analytical techniques is the limit of detection (LOD), which represents the minimum detectable concentration or amount of analyte in a sample. The factors which influence the value of the LOD are theoretically evaluated through the application of estimation theory and propagation of errors to the LOD concept. Equations are derived which can be used to estimate the magnitude of the random fluctuations which result from the use of sample statistics in the estimation of the LOD. The resulting confidence intervals can be used to evaluate and compare the true LOD values of analytical systems, and to determine the most efficient procedure for quick estimation of LOD. Monte Carlo simulations of typical analytical situations are used to evaluate the effectiveness of the derived equations.

Application of conventional detection limit theory is not straightforward when considering laser spectroscopic methods which are capable of detecting single atoms or molecules in the laser beam. Theoretical considerations in the detection and evaluation of these methods are addressed based on a model of a typical laser spectroscopic experiment with destructive and nondestructive detection methods. Computer simulations are used to verify the application of the theory of single atom detection (SAD) to typical experimental situations, as well as to discuss the scope of SAD methods and the various possible signal processing methods which can be used to continuously monitor and count the atoms or molecules which flow through the laser beam.

CHAPTER 1
INTRODUCTION

Any analytical technique designed to determine the concentration or amount of analyte in a given sample from the magnitude of the resulting signal can be characterized by a limit of detection (LOD). The LOD is designed to give an indication of the lower limit of analyte concentration or amount that the given analytical technique can distinguish from the background noise, which is present even when the analyte is absent. The LOD is very often a significant characteristic of a given analytical procedure, since calculated LODs can be used for comparison and/or evaluation of the procedure relative to other analytical procedures. For example, the LOD may be used to indicate the improvement of the detecting power of a given analytical protocol; the improvement is measured by comparing the LOD to the values reported for the procedure in the past. Alternatively, a particular application may have certain sensitivity requirements; in this case, the reported LOD value may be used as a first basis of evaluation as to the suitability of the method for the application.

The importance of the LOD to characterize a given method's detection abilities signifies that great care must be taken when estimating and reporting LODs. The actual value for the LOD calculated for a given analytical procedure may vary widely due to either of two factors: (1) the method used to measure and calculate the

LOD; and (2) the use of different definitions to characterize a minimal detectable concentration/amount of analyte. Despite the effort made in the past two decades to define the LOD unambiguously, and to recommend guidelines for its measurement [1, 2], this diversity in definition and measurement protocol persists.

The random variation in calculated LOD is often intuitively sensed by practicing analytical chemists, who realize that LODs which are close (within a factor of 2 or 3) may not be statistically different. For example, if the same chemist determines the LOD of the same analytical technique two consecutive times, it is usually recognized that the same value for the LOD will not result. Additionally, if the LOD is measured on the next day by a different chemist, then it may be even more likely that another value will be obtained. This variability in calculated LOD is usually taken into account only in a general sense when comparing LODs from different methods; i.e., two LODs which are close are often considered equivalent. However, it would be desirable to know just how much might be of the variability in calculated LOD values might be due to random fluctuations in measurement, and how much due to actual differences in analytical conditions (sensitivity, background noise, etc).

The various different definitions used for the LOD were recognized and reconciled in the pioneering works of Kaiser [3] and Currie [4], and the situation has greatly improved since that time. However, there are now emerging laser spectroscopic methods which claim the ability to detect very small numbers of analyte atoms or molecules within the laser beam, all the way down to the level of single

atoms/molecules. The application of the LOD concept to these newer methods is not always obvious, but the comparison and evaluation of these methods needs consistent and appropriate definitions specifically designed to address the difficulties which result from the ability to detect small numbers of atoms.

The intent of this dissertation is to address both of the subjects discussed above. A review of some of the relevant concepts and past literature is presented in chapters 2 and 3; these chapters form the basis for the new work presented in the remainder of the dissertation. The variability of the calculated LODs will be addressed from a theoretical standpoint in chapter 4; in chapter 5, logical and precise definitions will be presented which are designed to clarify misunderstandings which may arise when attempting to define detection limits and other figures of merit for laser-based analytical methods capable of detecting single atoms/molecules. Later chapters serve to confirm, evaluate, and illustrate the concepts introduced in chapters four and five through the use of simple Monte Carlo computer simulations.

CHAPTER 2
THEORY OF LIMITS OF DETECTION

The limit of detection (LOD) is an analytical figure of merit (FOM) which gives the minimal concentration[1] of analyte in a sample which can be distinguished from the blank. The LOD of a procedure is only one of several possible FOMs. The purpose of FOMs is to objectively summarize important characteristics of the analytical procedure. Other than the LOD, there are a number of important FOMs, such as the linear dynamic range, the sensitivity of the technique, the resolution, the accuracy and precision of determination, the informing power of the method, price and time of analysis, interferences, and others which are less commonly used. The use and importance of many of these has been covered in reviews [5-7] and books [8-11] and will not be covered here other than to note that the LOD is only one of a group of FOMs which describe the total analytical procedure, although the LOD is one of the most important FOMs.

The present concept of the LOD has been promoted in several landmark papers [3, 4, 12]. These works mark the beginning of applying a statistical approach to the problem of determining the minimum detectable concentration of analyte for a given analytical procedure. This chapter will summarize all the relevant principles

---

[1]for convenience the term "concentration" will signify either analyte concentration or amount, whichever is appropriate.

of detection limits in both the signal domain and in the concentration domain. There will be no attempt at a comprehensive review of past literature; these have been presented in various review articles and textbooks [8, 10, 11, 13-16].

Analyte Signal Detection

Signal Detection Limit

Any instrumental analytical method is indirect in the sense that the "result" of a single analysis is a mean instrument response in the signal domain (e.g., current, charge, potential difference) rather than a direct reading of the analyte concentration in the sample. In a steady-state measurement, the response of the instrument for a given sample is measured for a certain time T_m, and the average response during this time is taken as a single measurement of the sample. The relation of a given measurement to the concentration of analyte is found through a calibration of the response function of the instrument; for the present time, however, we will only be concerned with the instrument response in the signal domain.

In the absence of analyte in the sample, there may be a nonzero response during T_m due to the blank only. This response consists of a nonrandom component μ_b and random component characterized by the standard deviation σ_b. Although it is certainly possible to compensate for the non-random contribution of the blank, the random fluctuation σ_b will still contribute to uncertainty in the measured signal. For signals which are of the same magnitude as σ_b there is a need for some criterion to

decide when a given signal is due to the presence of analyte in the sample or when the measurement may be due to spurious fluctuations due to the background signal.

The minimal detectable signal in the steady state case is best illustrated through a simple example. A typical situation is shown in figure 1. The response as a function of time is shown for one measurement (where T_m = 1000 s in this case). Each individual value shown in fig. 1(a) fluctuates about the (unknown) mean μ_b with variance σ_x^2; the distribution of the values (population distribution) is shown in fig. 1(b). In the particular case shown in this figure, the population of individual readings in the blank is normally distributed with a mean of 50 mV and a standard deviation of 10 mV. The average value in fig. 1(a) during T_m is 50.259 mV; this is one measurement of the blank.

According to the central limit theorem [17], the blank measurements will be approximately normally distributed, no matter the form of the original distribution of individual values, with a standard deviation given by

$$\sigma_b = \frac{\sigma_x}{\sqrt{N}} \qquad [2.1]$$

where

N = the number of individual measurements during T_m,

σ_x = the standard deviation of the individual signal values, and

σ_b = the standard deviation of the blank measurement.

The above equation holds if the fluctuation of measurement values due to the blank is characterized by "white" noise, rather than long-term drift (i.e., flicker noise). The

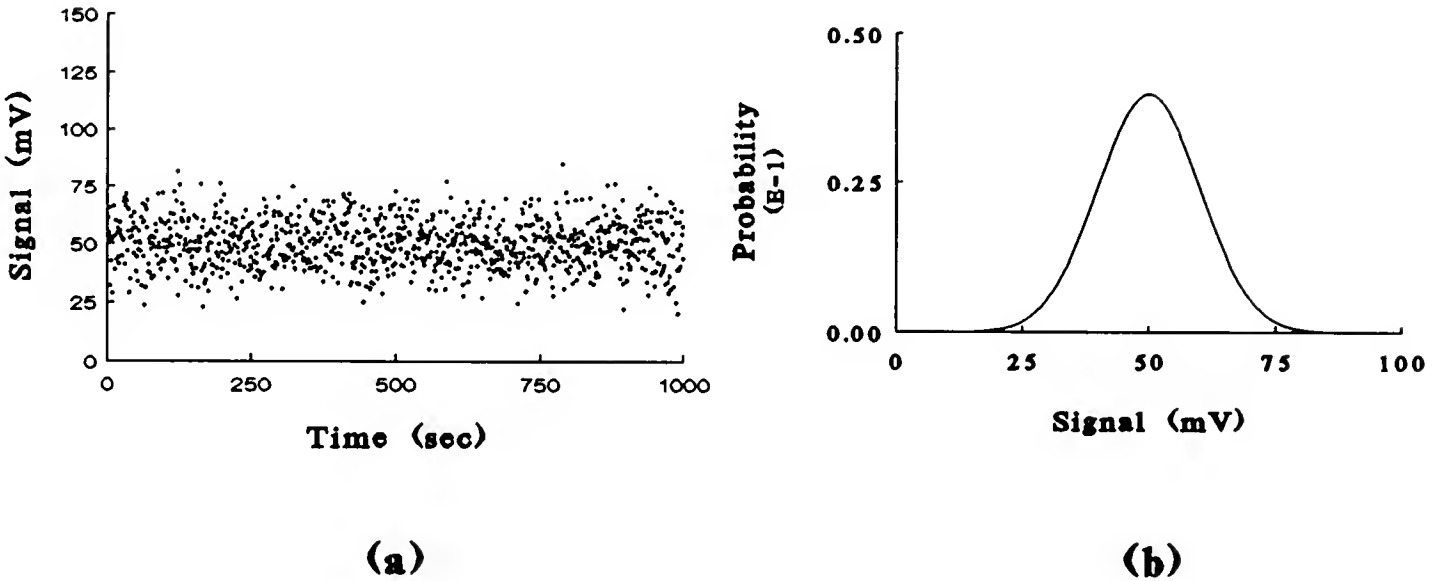

Figure 1. Example of a blank measurement. Conditions: T_m = 1000 s, data collected at 1 Hz.
(a) A single blank measurement, with signal of 50.259 mV.
(b) Population distribution of individual values within the blank measurements. The population mean is 50 mV, the standard deviation is 10 mV.

question now becomes, at what point is a sample measurement said to be "detected" above the blank noise. In other words, we seek a measurement value large enough so that the chance of the value belonging to the distribution of possible blank values is negligible.

The lowest value at which the measurement is considered to be due to a process other than blank noise is the signal detection limit, X_d. Since the standard deviation of blank measurements directly limits the ability to detect small signals, the detection limit is directly related to the value σ_b:

$$X_d = \mu_b + k\sigma_b \qquad [2.2]$$

where k is known as the confidence factor. The probability that a blank measurement can give rise to a measurement value greater than or equal to the detection limit is known as the type I error, or the probability of false positive error:

$$P(X_b \leq X_d) = \alpha \qquad [2.3]$$

where

α = the probability of type I error, and

X_b = one blank measurement (the mean during T_m).

The value of α is controlled by the confidence factor chosen in eqn. 2.2.

Choosing the Confidence Factor

According to the central limit theorem, if T_m is long enough it is usually reasonable to assume that the blank measurements follow a normal distribution $N(\mu_b,$

σ_b^2). In terms of the z-statistic,

$$z = \frac{X_b - \mu_b}{\sigma_b^2} \sim N(0,1) \qquad [2.4]$$

where the symbol ~ means "distributed as." With this in mind the confidence factor, k, can be chosen according to

$$k = z_{\alpha/2} \qquad [2.5]$$

where $z_{\alpha/2}$ is chosen from tables of the z-distribution. The factor k depends on the desired one-sided confidence level, given by the probability (1-α).

The detection limit is defined in eqn. 2.2 in terms of the population parameters μ_b and σ_b. However, these parameters are usually unknown and must be estimated by repeated measurements on the blank. The effect of substituting an estimate s_b^2 for σ_b^2 in the z-statistic is to broaden the distribution. In this case, the t-statistic must be used, with n-1 degrees of freedom, since

$$\frac{X_b - \mu_b}{s_b^2} \sim t_{n-1} \qquad [2.6]$$

where n is the number of blank measurements, each for time T_m, used to calculate s_b^2. In addition, the effect of using the estimated mean $\bar{X}_b$ for μ_b in the above statistic can be seen:

$$\frac{X_b - \overline{X_b}}{s_b^2 + s_b^2/n} \sim t_{n-2} \qquad [2.7]$$

where the denominator reflects the increased variance in the numerator. The above expression suggests that the confidence factor should be chosen according to

$$k = t_{n-2,\alpha/2}(1+1/n)^{1/2} \qquad [2.8]$$

Thus, the signal detection limit can be found by first choosing the desired confidence level α, making repeated measurements on the blank signal (at least 16-20 measurements are recommended), calculating the sample mean and standard deviation, and substituting in the above equation to find the value of k to use in eqn. 2.2. In practice, the (1/n) term in eqn. 2.8 is usually ignored and the t-factor is calculated with n-1 degrees of freedom. In essence, this is the same as ignoring the effect of using an estimate for the parameter μ_b; however, for typical values of n, the effect of ignoring the 1/n term in eqn. 2.8 is small.

The value recommended by IUPAC for the confidence factor is 3 [18]; with μ_b and σ_b known this would result in $\alpha = 0.0014$. Of course, even assuming a normal distribution of blank measurements, the true value of α would increase due to the imprecise nature of the estimates used for the population parameters. A non-normal distribution might inflate the type I error probability even further, although by Chebyshev's theorem [19] this probability cannot exceed 0.11 (for k=3) when the blank noise is due to random error alone. A recent publication points out that the true value of α cannot be accurately known due to various factors such as systematic error, long-term drift, and non-normal distributions of blank measurements [2]. Since strict interpretation of X_d and LOD in terms of α is usually difficult, a value of k=3 was recommended for consistency.

The detection limit for the example given earlier (fig. 1) is shown in fig. 2. Figure 2(a) shows X_d in terms of the probability distribution of the blank measurements, X_b, with k = 3. In order to get a better idea of the magnitude of the detection limit in comparison with the background fluctuation, figure 2(b) shows a signal at a level above the detection limit (55.102 mV), compared with a single blank measurement (50.259 mV). The signal shown is barely distinguishable from the blank measurement by eye.

There are two important points which should be made concerning the above discussion of X_d:

(1) If a single "measurement" actually consists of two measurements -- one on the sample, and one for blank subtraction, then the confidence factor should be multiplied by a factor of $\sqrt{2}$. Simultaneous blank subtraction is frequently used to account for long-term drift in μ_b.

(2) The discussion above was for steady state signals. The value of the detection limit will depend on the value of T_m chosen and so this value should always be given as part of the experimental procedure. Application of the above theory to the case of transient signals is straightforward in the case of peak detection, and σ_x is used in the above equations instead of σ_b. The correct detection limit value in the case of peak integration is somewhat less obvious, and will not be discussed here.

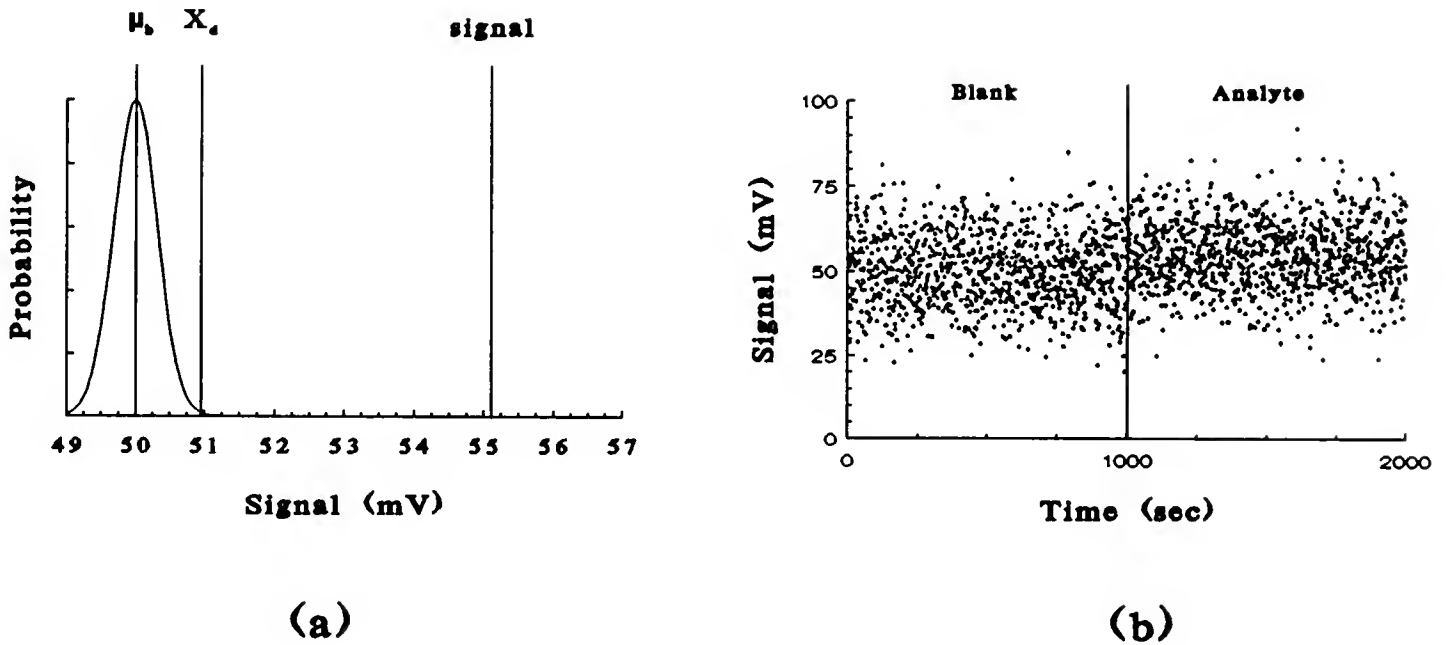

Figure 2. Example of a signal barely detectable above the background.
(a) Probability distribution of blank measurement, together with the signal detection limit and the value of the measured signal.
(b) Comparison of the signal measurement with the background measurement. The value of the blank measurement is 50.259 mV; the signal has a measurement value of 55.102 mV.

Minimum Detectable Concentration

The usefulness of the particular value of X_d for an analytical procedure is limited. Although knowledge of X_d is necessary for any analyst who wishes to detect the presence of a small signal as an indication of whether an analyte is present, it is very difficult to use X_d as a comparison between different methods, or between methods reported in the literature. Therefore, the value X_d must be transformed into a useful measure of a methods ability to detect the presence of small amounts of analyte. Before this can be done, the analytical procedure must be calibrated; i.e., the functional relationship between the measured signal and the analyte concentration must be known.

Calibration

The most commonly used method of calibration is by linear least-squares regression. Textbooks on regression give detailed theory on various types of regression analysis [20, 21]; this section will only cover the most basic type, simple first-order linear least-squares regression.

In many cases in analytical chemistry, a linear relation between the signal and the analyte concentration can be assumed over the range of interest, and the following model applies:

$$\begin{aligned} \mu_{y_i} &= \alpha_0 X_i + \mu_b \\ Y_i &= \alpha_0 X_i + \mu_b + \epsilon_i \end{aligned} \qquad [2.9]$$

where

μ_{Yi} is the true mean response at $X = X_i$;

α_0 and μ_b are the true slope and intercept of the calibration line;

Y_i is an observed (variable) response at $X = X_i$; and

ϵ_i is the true error of an observed response Y_i (the residual).

The first equation describes the true mean value of the signal at a given value of analyte concentration; the second equation describes the effect of the random variation in the observed measurement at $X=X_i$. The parameter described by α_0 is also known as the sensitivity of the analytical method.

Estimates of the parameters α_0 and μ_b are usually found by using least-squares estimators; equations for these estimators and conditions for their validity are readily available [20, 21]. Using these estimates, the model becomes

$$Y_i = a_0 X_i + \overline{X_b'} + e_i \qquad [2.10]$$

where

a_0 = the estimated slope;

$\bar{X}_b'$ = the estimated blank response (i.e., the intercept); and

e_i = the observed residual at $X = X_i$.

Of course, the estimators used are subject to variation σ_a and σ_b for the slope and intercept, respectively. The equations for the least-squares estimates and their estimated standard error, s_a and s_b, are readily available in textbooks, along with conditions for their validity [20, 21]; these values are usually automatically computed in regression software packages. The variability in the estimates for the parameters

of the linear model in eqn. 2.9 means that there will be uncertainty in a given predicted response value Y_i. It is possible to construct a confidence interval within which the true value of μ_{yi} will lie with 100(1-α)% reliability. This confidence interval is given by

$$Y_i \pm t_{\alpha/2,n-2} s \left(\frac{1}{N} + \frac{(X_i - \bar{X})^2}{S_{xx}} \right)^{1/2} \qquad [2.11]$$

where

$$S_{xx} = \sum (X_i - \bar{X})^2 \qquad [2.12]$$

and

s = standard deviation of response (assumed constant); and

N = number of points in calibration curve.

The interval above is likely to contain the true mean response at a given analyte concentration. An interval which describes where a future response at X = X_i is likely to fall with (1-α) probability is often called the prediction interval, and is given by:

$$Y_i \pm t_{\alpha/2,n-2} s \left(1 + \frac{1}{N} + \frac{(X_i - \bar{X})^2}{S_{xx}} \right)^{1/2} \qquad [2.13]$$

The relation between the two intervals for a typical calibration curve is shown in figure 3. The wider intervals are the prediction intervals.

Weighted least-squares regression. It should be noted that the above intervals were derived with the assumption of constant variance in the measurement response along the calibration curve. In analytical chemistry, however, there are a number of

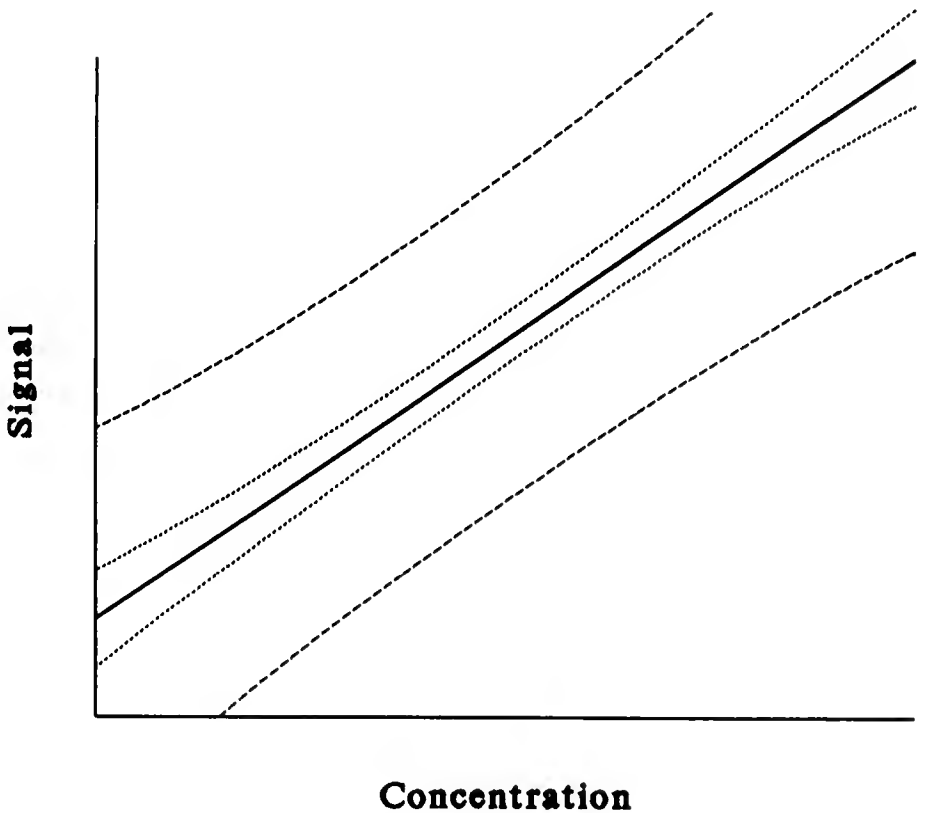

Figure 3. The confidence and prediction intervals of a fitted line. The narrower interval is the confidence interval.

techniques with large linear dynamic ranges, where it is likely that the noise on the signal increases with the concentration. An example was given recently for atomic emission in the inductively coupled plasma [22]. In addition, certain transformations of variables have the affect of skewing the error magnitude even if the assumption of constant variance were valid to begin with [23]. In these cases, weighted least-squares estimates must be used, particularly when it is important to obtain information on the sizes of the intervals given in the above equations.

One-point calibration curves. If it is only desired that an estimate of the sensitivity α_0 near X_d be required, then a single standard can be used so long as it is known that the linear model applies up to the standard concentration, and that the standard is reliable. In this case, the standard deviation of the sensitivity estimate is given by:

$$\sigma_a = \frac{\sigma_{y(c)}}{C} \qquad [2.14]$$

where

C = standard concentration, and

$\sigma_{y(c)}$ = standard deviation of response at C.

Of course, multiple measurements of the standard are needed to estimate $\sigma_{y(c)}$. Note that this fluctuation in response includes the uncertainty in both the blank and the signal measurements.

Limit of Detection

Once the analytical system has been calibrated, it is possible to define the limit of detection, LOD, as the analyte concentration which corresponds to the signal detection limit, X_d:

$$LOD = \frac{X_d - \mu_b}{\alpha_0} = \frac{k\sigma_b}{\alpha_0} \qquad [2.15]$$

where all the terms have been previously defined. The value of LOD thus defined can be used for comparisons between analytical procedures. Thus, in addition to the estimates for the blank mean and standard deviation necessary to estimate X_d, an estimate for the sensitivity must also be used to calculate the LOD.

The confidence factor, k, in the definition of LOD is chosen as described in the section on signal detection. However, the use of the calibration estimate of sensitivity introduces another source of variability which may serve to increase α, the probability of type I error. In the past, another approach to estimating LOD based on the calibration equation has been advocated in order to compensate for this extra uncertainty [24-27]. In this approach, the (1 - $\alpha/2$) prediction interval for the intercept (i.e., the response of the blank) from the calibration curve is used. The upper limit of this interval corresponds to X_d and the corresponding analyte concentration is the LOD. The procedure is illustrated in figure 4.

The prediction interval for the intercept can be found by using eqn. 2.13 with $X_i = 0$. The procedure is equivalent to using a value for the confidence factor, k, in eqn. 2.15 calculated as follows:

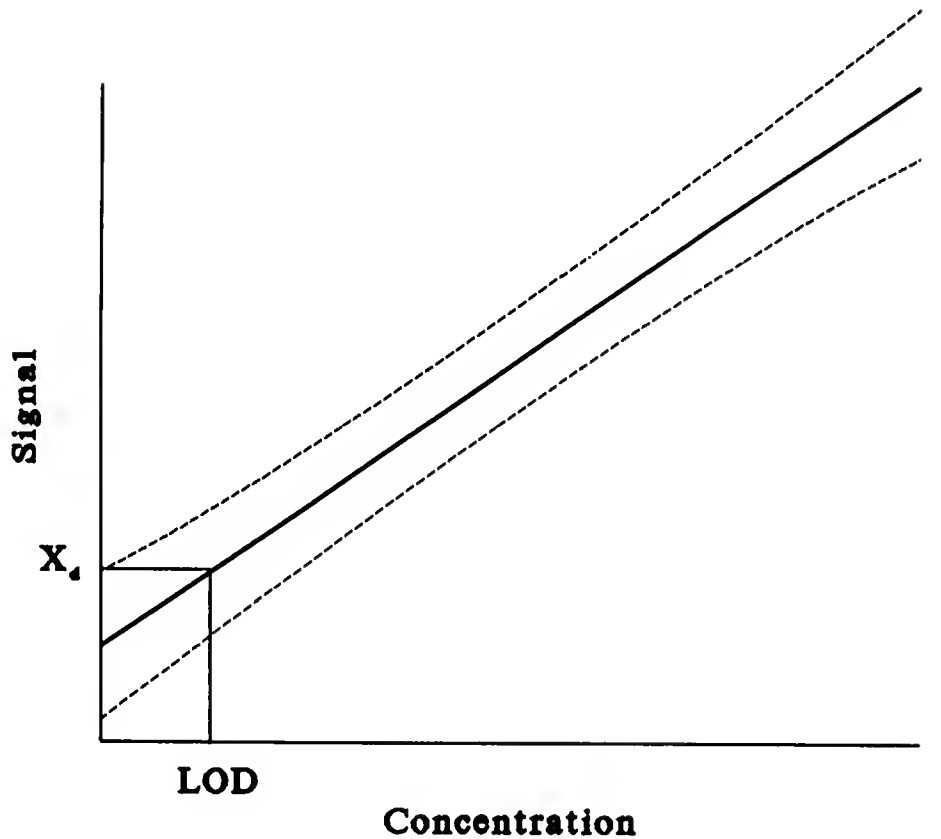

Figure 4. "Calibration band" method of determining the limit of detection. The prediction interval is shown in the figure.

$$k = t_{\alpha/2,N-2}\left(1 + \frac{1}{N} + \frac{\bar{X}^2}{S_{xx}}\right)^{1/2} \qquad [2.16]$$

The similarity between this equation and eqn. 2.8 can easily be seen; the 2nd and 3rd terms in the parenthesis account for the influence of the calibration conditions on the value of α. With this procedure for calculating the LOD, the k term (and hence the LOD) will depend on the calibration conditions such as the number and range of the concentrations of standards used in calibration, and the use of weighted or unweighted regression to estimate the prediction interval. Using the confidence factor in eqn. 2.16 compensates for possible change in α due to these calibration conditions.

Limit of Guaranteed Detection

IUPAC defines the LOD as "the minimum concentration or quantity detectable" and that it is "derived from the smallest measure that can be detected with reasonable certainty [i.e., the value of X_d]" [1]. This definition of LOD is deceptive since it can lead to the false assumption that if the analyte is present at or above the LOD value that it will always be detected -- i.e., result in a measurement above the signal detection limit. Conversely, if a given (unknown) sample does not give a detectable signal, then it might be falsely assumed that the analyte must be present at a concentration less than the LOD.

By the definition of LOD in eqn. 2.15, it is apparent that the mean response μ_{Yi} for the analyte present at a concentration equal to the LOD is the signal

detection limit, X_d. If the distribution of possible signal values is symmetrical about the mean, this means that in 50% of the measurements where an analyte is present in a sample at a concentration equal to the LOD, the resulting signal will not be detected. The probability that the signal due to the analyte present at a given concentration does not give rise to a detectable signal is known as the probability of type II error, ß, or the probability of a false negative. Thus, when the analyte is present at a concentration equal to the LOD, ß = 0.5.

The lack of a detectable signal does not mean that the analyte concentration level must be below the LOD value. It would be useful to know at what concentration level the analyte must be present in order to be detected with near certainty (i.e., with very low ß). The inadequate nature of the LOD figure of merit in this regard has been noted by several authors [3, 4, 14, 16]. It is possible to define a guaranteed signal detection limit, X_g, such that for the distribution of signal measurement values X_s, with a mean equal to X_g,

$$P(X_s<X_d) = \beta \qquad [2.17]$$

where the value of ß is chosen according to a predefined risk of type II error. The corresponding limit in the concentration domain is the limit of guaranteed detection, LOG, which is defined as follows:

$$LOG = \frac{X_g - \mu_b}{\alpha_0} = \frac{2k\sigma_b}{\alpha_0} \qquad [2.18]$$

where the second part of the equation can be used to calculate LOG if the standard deviation of the signal is the same as that of the blank; in such a situation, α = ß. Figure 5 shows the distributions of measurements for the blank and analyte concentrations equal to the LOD and LOG values with k=3. As can be seen, the LOG is a useful FOM since, if a given sample is not detected above X_d, the analyst can confidently state to the customer (with only ß probability of error) that the analyte is not present at a concentration at or above LOG.

Limit of Quantitation

One final FOM should be mentioned which is related to the limits of detection and guaranteed detection: the limit of quantitation (LOQ), sometimes called the limit of precision or the limit of determination [3, 4, 16]. Although the two limits, LOD and LOG, are important for the process of analyte detection, the analyst is frequently most interested in quantitation. It is obvious that the precision in quantitation is frequently degraded near the detection limit since the signal and the noise approach the same magnitudes. The quantitation limit, X_q, in the signal domain, is defined as

$$X_q = \mu_b + k_q\sigma_q \qquad [2.19]$$

where

σ_q = true standard deviation on the analyte signal, and

$1/k_q$ = desired relative standard deviation (RSD).

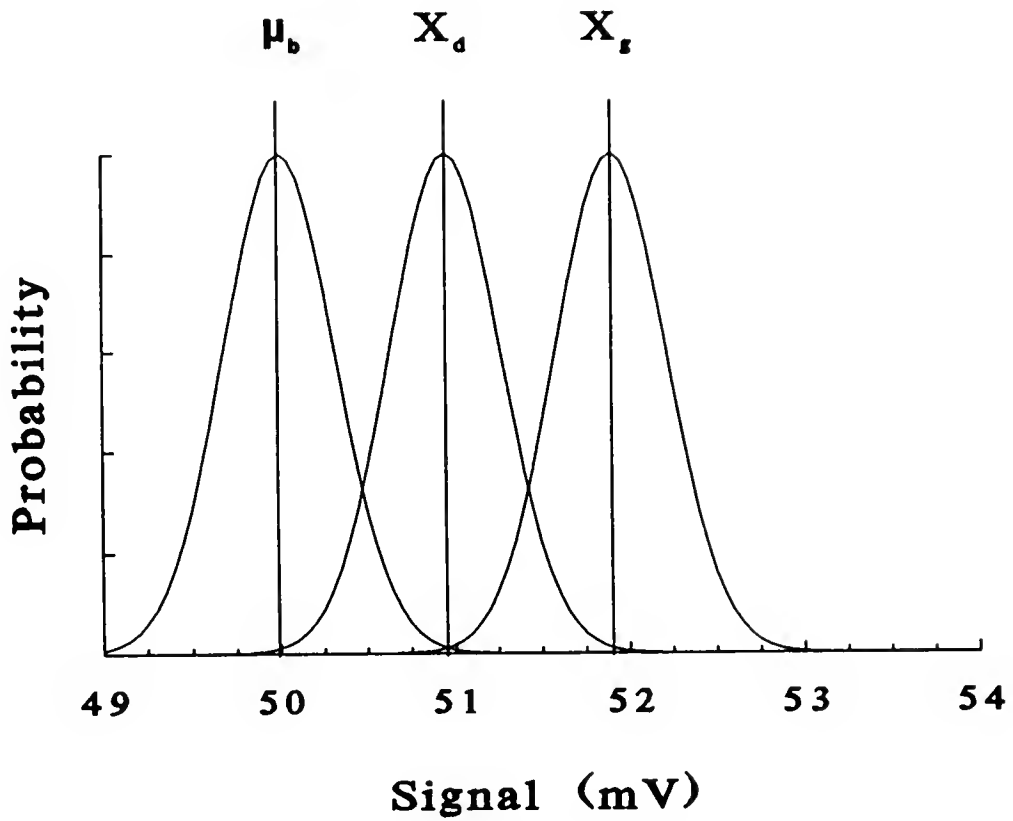

Figure 5. Distributions of signal of analyte concentrations equal to the LOD and the LOG. The LOG distribution is centered on X_g, the guaranteed detection limit in the signal domain.

Finding the corresponding value LOQ in the concentration domain is straightforward. The meaning of this limit is the LOQ is the lowest concentration of analyte which can be determined at a pre-defined level of precision (RSD). If it is assumed that σ is constant and 10% RSD is required, then

$$LOQ = \frac{10\sigma_b}{\alpha_0} \qquad [2.20]$$

The signal probability distribution (with 10% RSD) of analyte present at the LOQ is also shown in fig. 5.

Summary

The theory behind three related and useful figures of merit, the limit of detection, the limit of guaranteed detection, and the limit of quantitation, have been reviewed in this section. The purpose of the first two FOMs is to give some indication of the analytical procedure's ability to detect small amounts of analyte. Although the LOG is a more useful value in this regard, the LOD has been far more widely reported for various analytical procedures. From the standpoint of comparison of techniques' detection power, either FOM can be used as long as consistent definitions are used, all the relevant experimental detail is given (the measurement time and the electronic bandwidth are often ignored) and an appropriate experimental protocol is used to estimate values for σ_b and α_0. The procedure used to obtain these last two values should be given in any report of LOD or LOG as well.

CHAPTER 3
THE DETECTION OF INDIVIDUAL ATOMS OR MOLECULES

Laser Spectroscopic Methods of Analysis

Lasers have become a powerful and versatile tool in the arsenal of the physical and analytical spectroscopist. Lasers possess a number of unique and valuable properties such as high degrees of directionality, intensity, coherence, monochromaticity, and polarization; these qualities have opened up a realm of experiments previously impossible using only conventional light sources. In particular, in the field of ultra-trace analysis, the intensity and monochromaticity of the laser allow for the unique blend of very high sensitivity and selectivity, especially in the field of atomic spectroscopy.

The impact of lasers in spectroscopy can perhaps be appreciated by reviewing briefly some of the possible results of the interaction of an electromagnetic field with an atom or a molecule in the ground state, and some of the related methods which use these processes as basis for analysis. These processes are shown in fig. 6. Interaction of the ground state of the analyte with radiation at a specific frequency results in the production of the excited-state species A^* at a rate that is proportional to the spectral energy density of the radiation. Once in the excited state, some of the processes which can be detected for analysis are the production of radiation, charged

species, or heat dissipation into the surrounding medium. Since the number density of A^* (n_A^*) is directly proportional to the ground-state population present before irradiation, monitoring the events shown in the figure can give information related to the concentration of analyte initially present in the ground-state level. The processes and some related analytical techniques shown in the figure can be described as follows:

1. Stimulated absorption of incident radiation: atomic or molecular absorption spectroscopy, in which the attenuation of light irradiating the sample is monitored.
2. Stimulated emission from A^*: atomic and molecular stimulated emission spectroscopy. Methods based on this process have not been exploited, although techniques based on this method have been used to monitor flame species [28, 29].
3. Spontaneous emission from A^*: atomic and molecular fluorescence. Of course, atomic emission spectroscopy is also based on this process, although the excitation is not provided by a light source.
4. Collisional deactivation of A^*: photothermal spectroscopy, where the collisional heating of the surrounding medium is monitored.
5. Radiation-induced ionization: photoionization spectroscopy, in which the incident radiation produces the ion-electron pairs.

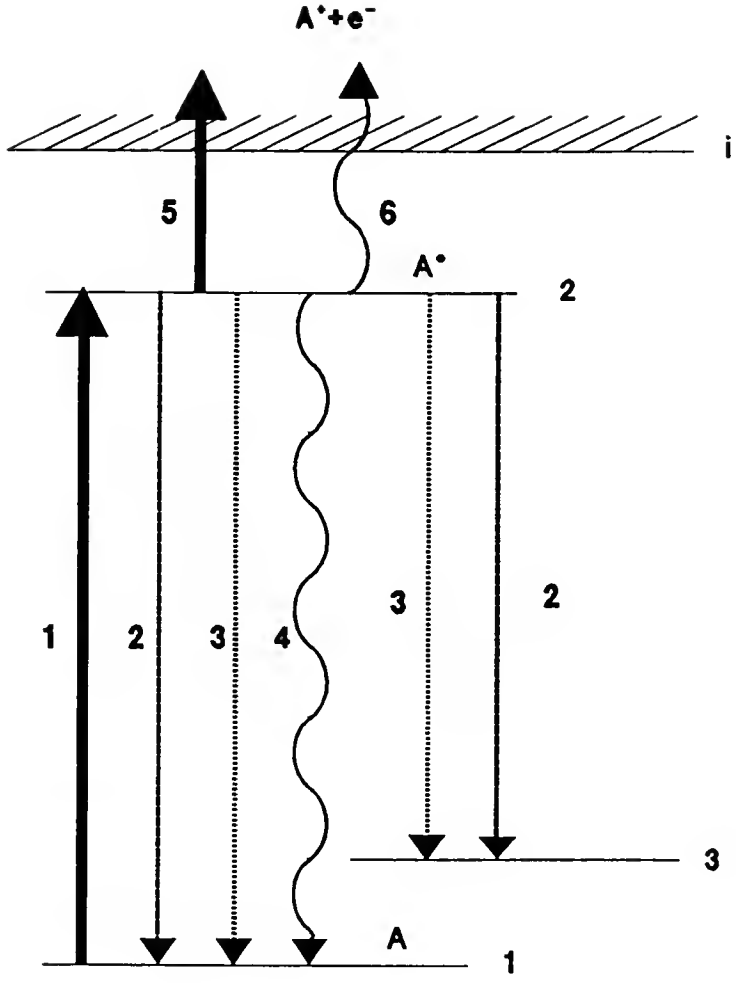

Figure 6. Excitation of analyte by interaction with electromagnetic radiation, and some of the processes that can occur as a result.

6. Collisionally induced ionization: optogalvanic spectroscopy, in which the enhance rate of production of analyte ion/electron pairs with irradiation is monitored in an external voltage field.

For a given volume of irradiated analyte, lasers can result in spectral energy densities that are roughly 4-10 orders of magnitude greater than most conventional sources. In the processes listed above, using the laser as the light source has resulted in a great enhancement in sensitivity and selectivity. Indeed, analytical techniques based on processes 2 and 4-6 are not practical without using lasers. Note that scattering processes and related techniques such as Raman spectroscopy, which have also become important analytical methods since the use of laser sources, are not listed in the figure.

Single Atom/Molecule Detection

Some of the analytical techniques outlined above are so sensitive and selective that it is possible to detect analyte-specific events when only a few atoms or molecules interact with the laser. Indeed, laser-based methods capable of detecting single atoms or molecules were first reported over a decade ago [30-32]. Interpreting these methods in terms of the concepts of detection limits, as reviewed in chapter 2, has not proven to be straightforward. Laser-based techniques in which the sensitivity is high enough (and the noise is low enough) that individual species can be detected

shall be called single-atom detection (SAD) methods.[1] Strict requirements for techniques to be termed SAD will be outlined in chapter 5; all others which possess detection limits of only a few atoms can be called near-SAD methods.

Past SAD Experiments: A Sampling of Applications and Techniques

Why be concerned with the ability to detect single atoms? Certainly it would seem that the vast majority of analytical methods, even those based on laser-induced processes for ultra-trace analysis, would fall far short of requiring the capability of SAD. However, there are several beneficial reasons to being aware of the particular concepts which apply to (near-)SAD techniques; these are now briefly outlined.

First of all, there are applications in physics and chemistry, including analytical chemistry, which do in fact require a capability of SAD. Even if the goal is not quantitation of analyte, the capability of a laser-based method to detect single atoms often must be evaluated, and many of the concepts of SAD theory apply.

Current ultra-trace laser spectroscopic methods are getting ever closer to the SAD regime of analysis. The LODs reported in conventional bulk analysis often translate into very few atoms in the laser during the measurement time. In addition, for some of the methods, the selectivity is so great that it is possible to reduce the noise to almost nonexistent levels; many of the concepts from SAD theory are relevant in these cases.

---

[1]The term "SAD" will be used even though the detected species may be atoms, molecules, ions or radicals. The term "atom" in reference to SAD techniques will apply to all such species as well.

Finally, the ultimate goal of an analytical method is the detection of single atoms. The ability to quantitate the amount of analyte in a sample at the atomic level certainly represents this ultimate goal in chemical analysis, and many unique and interesting experiments in analysis and other fields would no doubt result from such an ability.

Applications of SAD

This is by no means meant to be an exhaustive list of possible applications of SAD. There have been reports in the literature of possible applications of SAD techniques [33-36]; this list covers some of these as well as various others. The applications listed here specifically call for the ability to detect the signal due to single atoms.

Physical applications

1. It is possible to observe and measure the transport, diffusion or otherwise, of individual atoms through the volume defined by the laser beam, as well as other statistical mechanics applications in which the fluctuations in various atomic/molecular processes must be monitored. The observation of the gas-phase reactions of individual atoms or molecules [37] might be included in this type of application.
2. The (mean) lifetimes of various excited states of individual atoms or molecules can be reported and studied in various environments. This

information is usually only available as an ensemble average over many atoms/molecules.

3. The spectroscopic features of free atoms or ions [37, 38] can be studied; the spectroscopy of molecules in various sites in a solid matrix can also be investigated [39-42].
4. Sorting of individual species (atoms, ions, molecules) requires the ability to "tag" and detect them with the laser. This is an example of Maxwell's sorting demon [35, 43].
5. The detection of rare events, such as solar neutrinos, by their effect on individual atoms [33, 34, 44].
6. The observation of the orientation of individual species in clusters. SAD has been applied to clusters of ions in a laser-cooled ion trap [45].

Analytical applications

1. Detection of very low bulk concentration of analyte, where the limiting "noise" on the signal is due to the statistical appearance of individual atoms in the laser.
2. Detection of very rare isotopes and application in various related fields such as geochemistry and environmental analysis [43, 46] and cosmochemistry [35].
3. Application of SAD methods in surface analysis is necessary for even relatively "high" bulk and surface concentrations since very few analyte atoms will be analyzed at any time by combinations of sputtering methods with laser-based detection [47].

4. Detection of analyte in difficult matrices. Simple dilution is often an effective method of correction for matrix effects, but is limited by the sensitivity of the analytical technique. With the development of methods capable of SAD in large samples, the sample can be diluted to an arbitrarily high degree.

Techniques Capable of SAD

Techniques which have achieved (near-)SAD in the past can be broadly categorized as using either destructive or nondestructive methods of detection. In the former class, the atom is consumed during the detection process, producing at most one single "count"; in the second category, each atom can produce multiple detectable events during its interaction with the laser. In this work, most attention will be focused on two laser-based methods which have had the most success at detecting single atoms: resonance ionization spectroscopy (RIS) and related methods, and laser-induced fluorescence (LIF). These two methods can represent the two classes of SAD methods: RIS is almost always destructive, while with LIF it is frequently possible for each atom to emit many photons during its interaction with the laser.

Resonance ionization spectroscopy

Resonance ionization spectroscopy involves the laser-assisted production and subsequent detection of analyte ions. Production of ion-electron pairs using lasers can approach 100% efficiencies. Since the manipulation of charged particles is relatively easy and detection of these particles can also be highly efficient, it is not

surprising that there have been a number of (near-)SAD reports using RIS [31, 32, 43, 44, 48-54] as well as a number of review articles which cover various theoretical and practical aspects of the technique [35, 36, 55, 56].

There are two basic ways in which the ion has been produced through laser-induced processes; these are shown in figure 7. The method in fig. 7(a), direct photoionization by the laser, has been developed at Oak Ridge National Laboratories as outlined by Hurst and Payne [35]; the detection of the ion in a buffer gas has usually been achieved by a proportional counter. The process shown in fig. 7(b) involves excitation to a long-lived Rydberg level in a vacuum with subsequent field ionization, and detection by a secondary electron multiplier (with or without a mass spectrometer). The advantages of excitation to a Rydberg level is that less powerful lasers are necessary for saturation, which may result in a more general technique and less laser-induced background. The development of this method by Letokhov and Bekov has been outlined in a recent book [36].

Laser-induced fluorescence

Techniques of involving the detection of spontaneous emission of laser-excited analyte atoms have been characterized by extremely high selectivity and sensitivity. This high sensitivity has been accompanied by a number of reports of claiming SAD [30, 37, 38, 45, 57-69]. There are a large number of possible combinations of excitation/detection schemes using LIF; figure 8 shows three of them which represent the types of schemes which can be used.

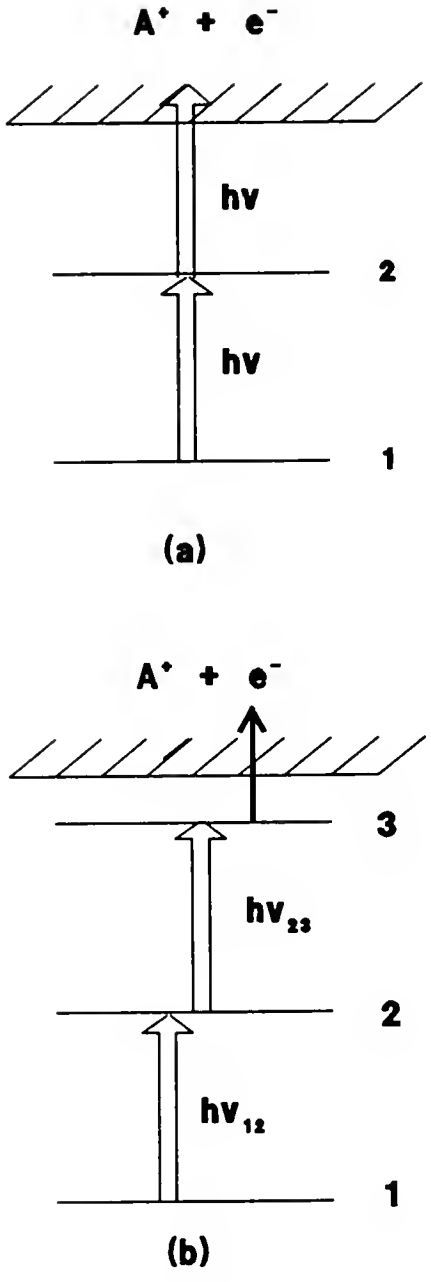

Figure 7. Two possible ionization methods for RIS.
(a) photoionization from an intermediate level.
(b) field ionization from a Rydberg level.

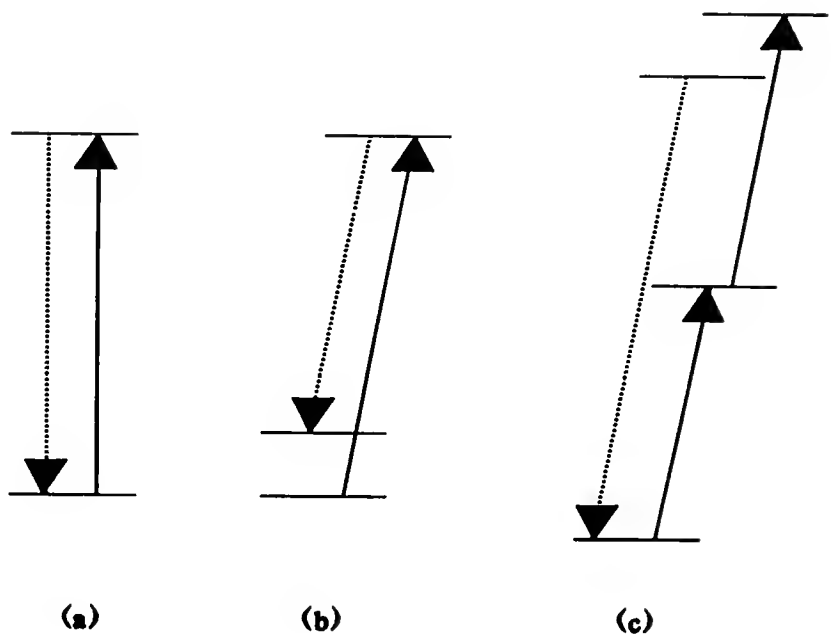

Figure 8. Three possible excitation/detection schemes for LIF.
(a) resonance LIF.
(b) direct-line LIF to discriminate against scatter.
(b) two-step excitation, detection at shorter wavelengths.

The technique of LIF can be either destructive or nondestructive, depending on the particular analyte, the environment and the time-scale of the interaction with the laser. The presence of a metastable level can act as an effective "trap" for atoms during the measurement; for example, if a scheme similar to the one shown in fig. 8(b) is used when the middle level has a very long lifetime and the analysis takes place in a vacuum, then LIF will be a destructive technique. Similarly, photodestruction of molecules by the laser may occur and effectively limit the emitted photons to a small number. On the other hand, when there is good collisional and optical coupling between all the levels involved in the excitation/detection scheme, then "cycling" of the atom back to the ground-state is possible, where the atom can then further interact with the laser.

CHAPTER 4
THE VARIABILITY OF ESTIMATED LIMITS OF DETECTION

The value of the LOD calculated for a given analytical procedure can vary due to a number of factors. In this chapter, these factors will be investigated, and the variation in calculated LOD due to random fluctuations will be theoretically evaluated. Before proceeding further, however, a brief introduction to estimation theory is necessary to fully appreciate the concepts involved in calculating an LOD for a given analytical procedure.

Estimation Theory

Variables are defined in terms of the population parameters of their probability distribution, such as the mean, μ_x, and variance, σ_x^2, of the variable x. However, the true values of these parameters are very rarely known exactly and must be estimated from a sample of the population. Functions of the sample which provide such estimates are known as sample statistics; common sample statistics include the sample mean $\bar{x}$ and variance s_x^2. The value of a single sample statistic is also known as a point estimate of the corresponding population parameter.

The value of a point estimate depends upon the particular sample chosen; thus, point estimators are themselves variables, with properties dependent on the size of the sample chosen and the estimation function used. The theory of the behavior

of sample statistics as variable estimators of the population parameters is known as estimation theory. Besides the two already given, some other common estimators include least-square estimators (seen in chapter 2) for the calibration parameters of slope, α_0, and intercept, μ_b. Desirable characteristics of sample statistics include the property of being unbiased estimators, when the mean of the point estimates is the equal to the population parameter, and the property of efficiency, which is indicated by a low variance of the estimate. The standard deviation of the statistic is also known as the standard error.

If information is known about the standard deviation of the estimate, then it is possible to construct an interval about the point estimate within which the true value of the population parameter is likely to lie. Such an interval is known as the confidence interval. The probability that the parameter lies outside the interval, α, is inversely proportional to the size of the interval. Recall that confidence intervals were briefly mentioned earlier in relation to estimating the true analytical response from a calibration curve.

The Limit of Detection as a Population Parameter

The LOD was defined in equation 2.15 according to

$$LOD = \frac{k\sigma_b}{\alpha_0} \qquad [4.1]$$

where

k = the confidence factor,

σ_b = the standard deviation in blank measurement, and

α_0 = the analytical sensitivity.

In light of the previous discussion on estimation, it can be easily understood that since the LOD is defined in terms of population parameters, the LOD is itself a parameter of the analytical system, which can be estimated according to

$$\hat{LOD} = \frac{ks_b}{a_0} \qquad [4.2]$$

where

$\hat{LOD}$ = calculated estimate of true LOD value.

Thus, regardless of how the confidence factor k is chosen in the above equations, the value of $\hat{LOD}$ has a given variance associated with it. Since the true value of the LOD is frequently of great importance as a performance characteristic of a given analytical method, it is of interest to estimate this variance, σ^2_{LOD}. Estimating the variability of a given $\hat{LOD}$ would serve several purposes: (1) confidence intervals within which the true LOD value would lie could be calculated; (2) hypothesis tests with different $\hat{LOD}$ values can be made in order to determine if there is a significant difference; and (3) the influence of various experimental procedures on σ_{LOD} can be assessed. In many research laboratories, for example, calibration curves may only be used to provide an estimate of the sensitivity, α_0, to use in calculating $\hat{LOD}$. Time saving methods of providing this sensitivity estimate

which do not adversely affect the quality of the LOD estimate (ie increase σ_{LOD}) would be welcome.

Variability of $\hat{LOD}$

To derive an equation for σ_{LOD}, a propagation of errors approach can be used with eqn. 4.2:

$$\sigma_{LOD} = \left[\left(\frac{k}{a_0}\right)^2 \sigma^2(s_b) + \left(\frac{k s_b}{a_0^2}\right)^2 \sigma_a^2\right]^{1/2} \qquad [4.3]$$

To solve this equation, it is necessary to estimate the variance of s_b. The variance of this estimate can be related to the variance of the estimator for σ^2, again by propagation of errors:

$$\sigma^2(s_b^2) = (2s_b)^2 \sigma^2(s_b) \qquad [4.4]$$

The estimated variance, s^2_b, for n measurements is distributed as follows:

$$s_b^2 \sim \frac{\chi^2_{n-1}\sigma_b^2}{n-1} \qquad [4.5]$$

where the χ^2 distribution has a mean of (n-1) and a variance of 2(n-1) [70]. From this, we can deduce

$$\sigma^2(s_b^2) = \left(\frac{\sigma_b^2}{n-1}\right)^2 2(n-1) = \frac{2\sigma_b^4}{n-1} \qquad [4.6]$$

Now we can estimate the variance of the background standard deviation as

$$S_{s_b}^2 = \frac{s_b^2}{2(n-1)} \qquad [4.7]$$

Substituting this into eqn. 4.3 gives the following estimate for σ_{LOD}:

$$S_{LOD} = \left[\left(\frac{k}{a_0}\right)^2 \frac{s_b^2}{2(n-1)} + \left(\frac{ks_b}{a_0}\right)^2 \frac{s_b^2}{a_0^2}\right]^{1/2} \qquad [4.8]$$

where

s_a = estimate of the standard error of the slope (sensitivity), and

S_{LOD} = estimate for the standard error of $\hat{LOD}$.

Rearrangement allows for two useful forms of the above equation:

$$CV_{LOD}^2 = \frac{1}{2(n-1)} + CV_a^2 \qquad [4.9]$$

$$S_{LOD} = \hat{LOD}\left(\frac{1}{2(n-1)} + \frac{s_a^2}{a_0^2}\right)^{1/2} \qquad [4.10]$$

where

CV_x = the coefficient of variation of variable ($x = \sigma_x/\mu_x$), and

n = number of blank measurements to calculate s_b.

Both of the above equations are valid no matter how the confidence coefficient is chosen in calculating the LOD by eqn. 4.2

Confidence Limits and Comparing Values of LOD

The validity of the propagation of errors approach used to derive an equation depends on the following two conditions: (1) the errors in the slope and background variances must be independent; and (2) the term CV_a must be small (below about 0.10). Effects of violation of the first condition (i.e., including blank values in the calibration curve) are probably only slight when a reasonable number of points are included in the calibration set. The second restriction arises due to the non-linear relationship between the LOD and the slope; for high coefficients of variation of the latter, the propagation of errors approach breaks down [71]; effects of high CV_a values will be investigated in chapter 7.

Keeping the above two restrictions in mind, the utility of eqns. 4.9 and 4.10 are as follows. Equation 4.10 gives an indication of the expected fluctuation in LOD estimate due only to the variable nature of point estimates; this value can be used to construct confidence intervals within which the true LOD is likely to lie. Examination of eqn. 4.9 shows how the variability of $\hat{LOD}$ can be divided between the uncertainty in the estimates of s_b and s_a. For a given set of conditions used to calculate LOD, eqn. 4.9 can be used to determine the relative contribution of the two error sources. The method used to determine the confidence interval about $\hat{LOD}$ depends on the relative magnitude of the two terms. If the first term dominates, then most of the variation in the estimate is due to the uncertainty in estimating σ_b. This situation is probably the most common in analytical chemistry. In these cases, the χ^2 distribution can be used to construct confidence intervals on the $\hat{LOD}$ value

in the same manner as for the sample standard deviation [72]; Kaiser has demonstrated similar calculations [3]. For example, for a two-sided 95% interval and 20 measurements of the blank,

$$0.76\,(\hat{LOD}) \leq LOD \leq 1.46\,(\hat{LOD}) \qquad [4.11]$$

Confidence intervals for different numbers of blank measurements can easily be constructed by using the appropriate degrees of freedom. For comparison of $\hat{\text{LOD}}$ values obtained under similar conditions, F-tests can be used [72].

As the second term in eqn. 4.9 becomes more important, the distribution of $\hat{\text{LOD}}$ will come to approximate a normal distribution; in these cases, standard t-tables can be used to construct confidence intervals of the type $\hat{\text{LOD}} \pm kS_{LOD}$, and to compare LOD estimates with the t-test. In either case, eqn. 4.10 is valid and gives a good idea of the variability of a given value of $\hat{\text{LOD}}$ due to random fluctuation of the sample statistics.

Summary

Inspection of eqns. 4.1 and 4.2 leads to the conclusion that there are two sources of variation in calculated values of LOD: the first source is due to actual changes in population parameters σ_b and α_0 of the analytical technique -- a shift in alignment, slightly increased background noise, the presence of interferences, improved analytical methodology -- and the second source is due to the variability of the point estimates used in eqn. 4.2. The source and magnitude of the latter fluctuation in LOD can be seen by application of eqns. 4.9 and 4.10. One benefit of

viewing the calculated value of the LOD as an estimate of the true value of the LOD is that these two sources of fluctuation of LOD can be separated; if the LOD fluctuates by an amount much greater than the calculated value of S_{LOD} indicates, then the probable source of the change in the observed LOD is an actual change in the analytical parameters of the system. The performance and use of eqns. 4.9 and 4.10 will be further investigated in chapter 7.

CHAPTER 5
THEORY OF THE DETECTION AND COUNTING OF ATOMS

Introduction

Some of the practical aspects of detecting individual atoms or molecules with lasers were outlined in chapter 3. As stated in that chapter, certain laser-based methods have achieved high enough sensitivity so that single atom detection may be possible. In the literature there are reports of methods which were able to detect single atoms with very high S/N ratio [30, 37, 44]. However, most of the reports of SAD have had a comparatively low S/N ratio for each atom; in these cases, there is a question of whether or not single atoms can actually be detected above the background (if any background is present). Evaluation of these methods often involves the following questions:

1. Can individual atoms can be detected?
2. Under what conditions is single atom detection possible?
3. If it is possible to detect single atoms, is it also possible to count the numbers of atoms passing through the laser beam?
4. What are the characteristics of these (possible SAD) methods when utilized in a more conventional sense, ie to measure bulk concentration of analyte?

There are problems in applying the theory of detection limits summarized in chapter 2 in attempting to answer these questions. In comparison with practical aspects, theoretical considerations for (possible) SAD methods have received very little attention in the literature. There have been a handful of papers which have evaluated laser spectroscopic techniques with respect to the potential to detect atoms [73-78]; these include some theoretical discussion of SAD methods. Recently, several papers have attempted to deal with the problem of verifying that single molecules were being detected by LIF as they flow through the laser [65-68]. However, the work of Alkemade remains the only in-depth, systematic general theoretical treatment of SAD to date; this work is presented in two classic papers [79, 80] and has recently been reviewed and extended [81].

The purpose of this chapter is to answer the questions posed earlier which may arise for methods which produce a signal for individual atoms which might be detectable above the background noise. The concepts from chapter 2 are applied in a logical manner to SAD methods, and strict definitions and important figures of merit for (near-)SAD methods are presented. Several other important factors in evaluating possible SAD methods will also be discussed. The treatment of SAD in this chapter owes much to Alkemade's original treatment of the subject; many of the terms used are identical, although the meanings may have been modified. The intent of this treatment is to generalize Alkemade's pioneering work and to present a general theory of SAD in a form useful in the development of methods which may achieve the goal of detecting and counting atoms. Most of the concepts presented

are verified and further illustrated in chapter 8 through the use of computer models of SAD experiments.

Definition of an SAD Method

The definition of an SAD method is a generalization of Alkemade's four criteria for true SAD [80] and is the following:

> A method is an SAD method if each and every atom which interacts with the laser can be detected above the background noise.

The above definition will be re-stated in a more rigorous form later in this chapter; nevertheless, the general concept of an SAD method can be appreciated. Implicit in the above statement is that we are concerned only with the atoms which actually interact with the laser. Equally important is to notice the difference between a method in which some (but not all!) individual atoms can be detected above the background and an SAD method: it is not enough to simply have a certain *likelihood* of detecting single atoms, but *every* atom which is probed by the laser must be detected.

General Model of SAD Methods

The Poisson Process

Many of the processes involved in SAD methods will be assumed to be related to the Poisson distribution. These include the number of atoms probed by the laser, the detection probability of an atom, and the number of detected events per atom. To fully understand the nature and limitations of SAD model presented in this chapter, a firm grasp of the properties of Poisson variables is necessary [82, 83].

Experiments which measure the (variable) number of discrete occurrences of an event in a certain length of time, or in a given area of space, frequently deal with variables possessing a Poisson distribution. For a Poisson variable, the probability of X number of events occurring during a given fixed interval time or space, t, is given by:

$$P(X) = \frac{(\phi t)^X e^{-\phi t}}{X!} \qquad [5.1]$$

where

ϕ = flux of events per unit time/space, and

$\mu_x = \sigma_x^2 = \phi t$.

A variable which is truly a Poisson variable (characteristic of a Poisson process) possesses the following qualities:

1. The probability of an event occurring within the interval of time or space is small compared to the probability that it can occur elsewhere.

2. The probability of an individual event occurring within the length of time or space is independent of all other events which have occurred, either during that length of time/space, or outside it.

The Poisson distribution is closely related to several other distributions, including the uniform random distribution, and the Gamma and exponential distributions. This relationship can be understood by considering a Poisson variable in time. When a given event can occur randomly in time (i.e., the probability distribution of the time of occurrence is a uniform distribution), then the number of events during a given time interval follows a Poisson distribution. This is the basis of a typical Poisson process. For such a process, the probability distribution of the time interval, t, between events is given by an exponential distribution

$$P(t) = \phi\, e^{-\phi t} \qquad [5.2]$$

where the meaning of ϕ is the same as in eqn. 5.1. The mean time interval between events is given by ϕ^{-1}. The exponential distribution is a simplified form of the Gamma distribution. The variable in the Gamma distribution is the amount of time, t_ν, for a specified number, ν, of events to occur:

$$P(t_\nu) = \frac{\phi x^{\nu-1} e^{-\phi t_\nu}}{\int_0^\nu x^{\nu-1}\, e^{-t_\nu} dt_\nu} \qquad [5.3]$$

Typical SAD Experiment

The general form of a laser-based SAD method can be illustrated with the aid of figure 9. In the figure, analyte atoms flow past a region of interaction with a laser beam; atoms which interact with the laser produce a number of detectable events. The method of detection can be either destructive (e.g., ion detection in an atomic beam) or nondestructive (e.g., fluorescence detection of molecules in a flowing stream). The number of events detected during a measurement time T_m are counted. During this time, a certain volume of sample containing analyte, V_a, flows past the laser beam; for the analyte atoms within this volume there is a probability of entering a region in which it is possible to interact with the laser beam and emit detectable events. This volume is the probe volume, V_p, and is defined by the region of intersection of the flowing stream with the laser beam which can be viewed by the detector. A certain number N_p of atoms which enter V_p interact with the laser beam during T_m; a given atom interacts with the laser beam for time t_i. The atom's interaction time is a function of various factors such as the magnitude of T_m, the type of laser used (probed, continuous or modulated), and the atom's residence time, t_r, within V_p. The value of t_r is usually a variable, with mean τ_r, depending on such factors as velocity, diffusion, and size and shape of V_p. The atom's corresponding interaction time t_i may also be a variable, with mean τ_i, depending on the relative magnitude of T_m and τ_r, and the conditions of the experiment.

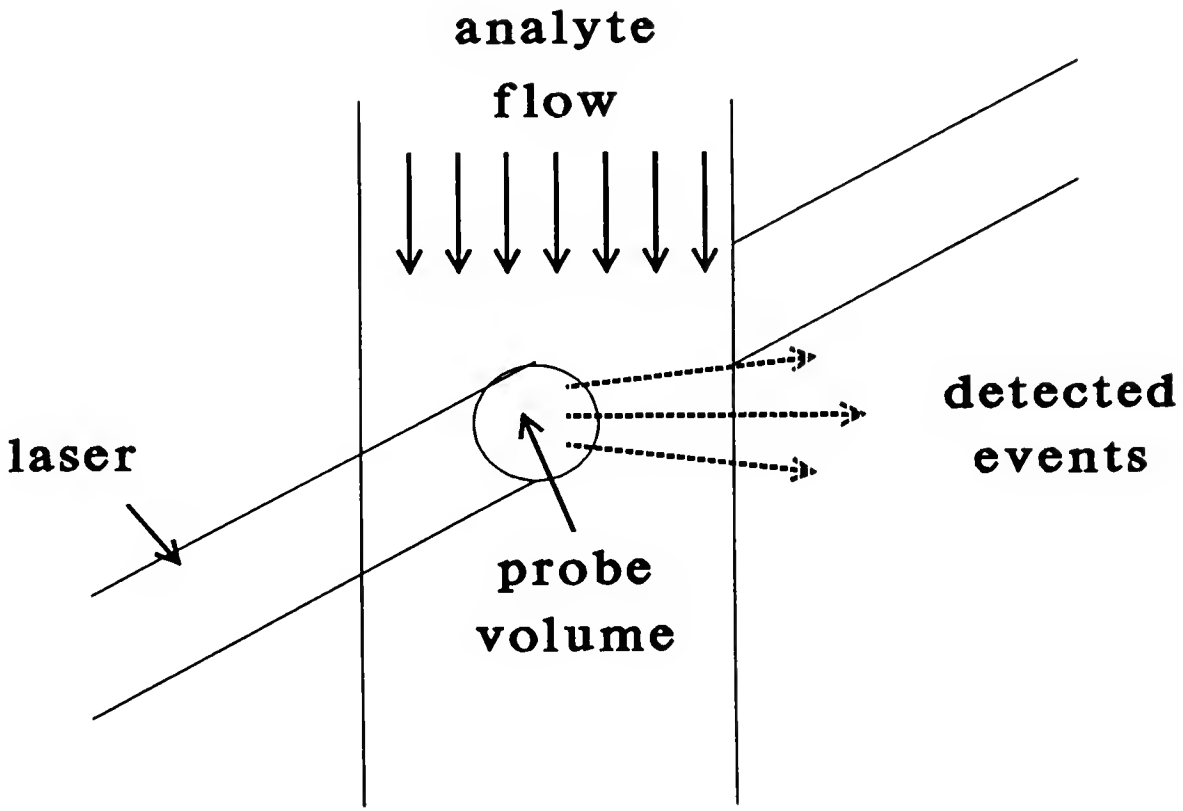

Figure 9. Illustration of the general model of an SAD experiment.

Detection efficiency: general definition

For the general layout of a typical SAD experiment as given above, it is convenient to define the detection efficiency of atoms which enter the probe volume. The detection efficiency, ϵ_d, is defined as the probability that any given atom, during its interaction with the laser, produces a signal that can be distinguished from the background which arises during the measurement time. Alkemade gives a similar definition for the detection efficiency [80], but there are two important differences: (1) Alkemade was only concerned with the case where there was no background noise; hence, ϵ_d was simply the probability that an atom which interacted with the laser produced at least one detectable event; (2) Alkemade's term only applied during a single probing time (e.g., one single laser pulse in a pulsed experiment) rather than during an atom's entire interaction time with the laser. One characteristic which the two definitions have in common is that they are only concerned with atoms which actually interact with the laser (i.e., atoms for which $t_i > 0$).

Signal production

This section will introduce terms relating to the signal detected during a single measurement; assumptions which will be made regarding the probability distribution of these signals in the SAD model will be discussed in the next section. During the measurement time T_m, there may be a certain (variable) number of background counts, I_b, with a mean given by

$$\mu_b = \phi_b T_m \qquad [5.4]$$

where

ϕ_b = mean flux of background noise (count/s)

μ_b = mean noise during T_m (counts).

The total signal, I_t, recorded during T_m is due to the contribution of noise and analyte signal. For nondestructive detection, this can be given as

$$I_t = I_b + \sum_{N_p} i_s \qquad [5.5]$$

where

i_s = number of detected events due to each individual atom which flows through V_p. This variable has a mean given by

$$\bar{i}_s = \phi_s t_i \qquad [5.6]$$

where

ϕ_s = mean flux of signal from a given atom (count s^{-1} $atom^{-1}$).

The mean total signal for a destructive technique is given by

$$\bar{I}_t = \mu_b + \epsilon_d N_p \qquad [5.7]$$

where N_p is the number of atoms which were probed during T_m and ϵ_d is the detection efficiency, the probability that a given atom will be detected.

The physical meaning of the term ϕ_s depends on the method used. If a nondestructive method such as cyclic LIF is used, the term refers to the actual rate of detected events from single atoms. For destructive methods, however, the meaning is obviously different since there can be no more than one detected event

per atom. In this case, the term is actually the reciprocal of the mean detection time of the atom within the laser. In other words, for a given atom which interacts with the laser within V_p the mean time until a detected event is produced is ϕ_s^{-1}. Theoretical expressions for ϕ_s for a number of cases for LIF and RIS can be found in the literature [78, 81, 84, 85].

Figure 9 has only shown one type of possible SAD experiment, specifically for a case where atoms continuously flow through V_p. Figure 10 depicts several alternative examples of SAD methods. As can be seen, various possible relative magnitudes of T_m and τ_r are possible: e.g., when a continuous-flow atomizer is used with a pulsed dye laser, if the detected events are counted for each pulse, then it is frequently true that $\tau_r >> T_m$, and the atoms are "frozen" during the measurement. This situation was termed the stationary case by Alkemade [80]. The nonstationary case occurs when the measurement time T_m is of the same magnitude or larger than the typical value of t_r. For example, in a heated cell, the atoms or molecules may be free to diffuse in and out of V_p during T_m; a case such as shown in fig. 9 with a continuous wave (CW) laser would be nonstationary.

Basic Assumptions for the SAD Model

Number of probed atoms, N_p

In a solution or sample which contains analyte atoms, it is often reasonable to assume that the analyte atoms are randomly distributed throughout the sample. Such being the case, it can be assumed that the appearance of analyte atoms in V_p

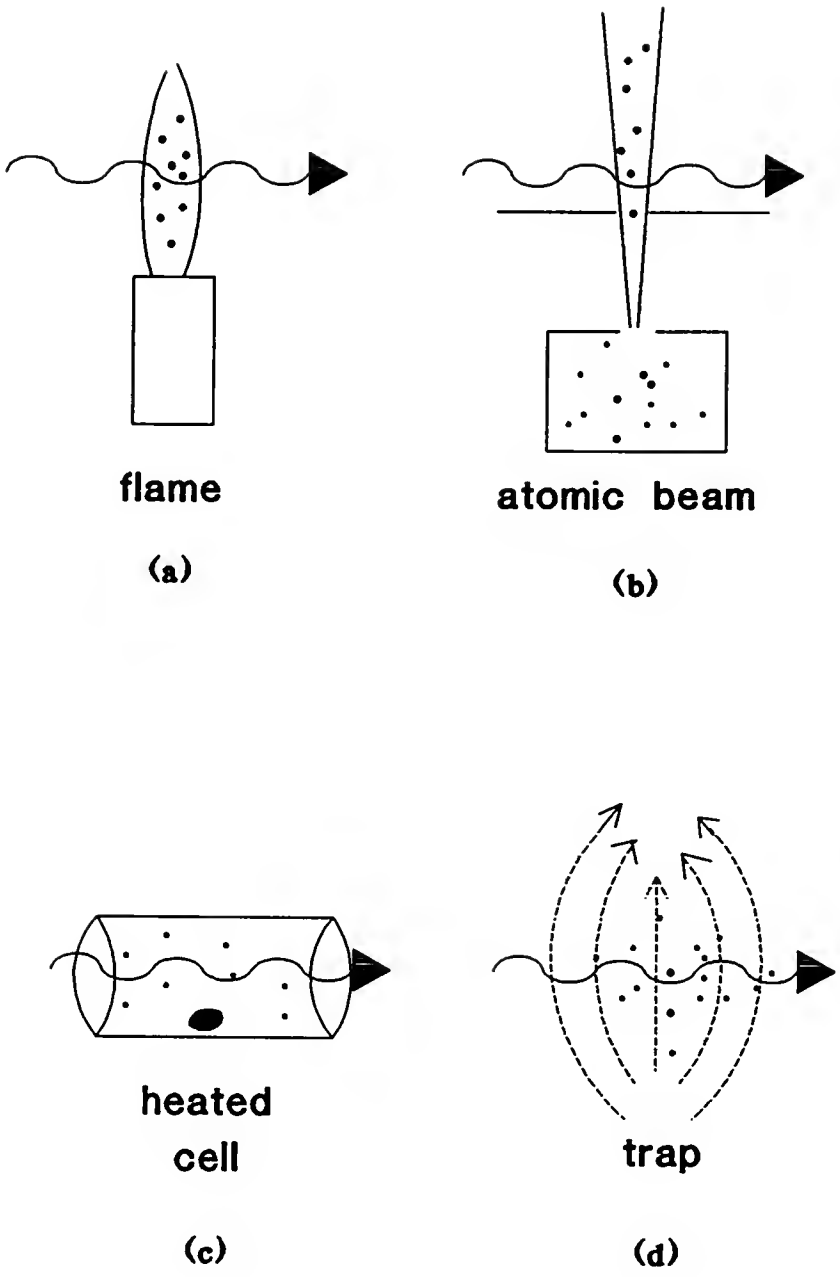

Figure 10. Examples of possible SAD methods. Typical examples of nonstationary methods are methods (a) and (b); methods such as (c) and (d) are often under stationary conditions during T_m.

is a Poisson process, and the number N_p is a Poisson variable governed by eqn. 5.1 with a mean which is dependent on V_p, T_m, and the analyte concentration. This assumption will almost always be valid in the absence of severe clustering effects or very small probe volumes (ie when analyte atoms cannot be treated as infinitely small); these cases violate the requirements of a Poisson process.

Number of detected events, I_t

The distribution of the background counts, I_b, will be assumed to follow a Poisson distribution. In other words, the limiting noise will be background shot noise. Even though this assumption is made for convenience (and applies in many counting situations), it is quite possible for the background noise SAD experiment to be flicker noise [69]; in such cases, the concepts in this and other chapters still apply, but with some slight modification.

The detection process in SAD methods will also be assumed to be a Poisson process. For nondestructive methods, such as cyclic LIF, this means that the number of counts per atom, i_s, detected during T_m, is a Poisson variable in time such as was described in an earlier section; all of the detected photons are randomly distributed during the atom's interaction time with the laser. Since I_b is also assumed to follow a Poisson distribution with a mean of $\mu_b = \phi_b T_m$, then when a single atom passes through V_p during T_m, I_t has a Poisson probability distribution with a mean of $\mu_b + \phi_s t_i$.

For a destructive detection method, such as RIS, the detection process is also a Poisson process, although in a more subtle way. A large number of atoms N_p all

interacting with the laser beam at one time would result in a mean flux ϕ_s of detected ions; the detection times of these ions are assumed to be uniform random variables, and the time intervals between detection follow an exponential distribution such as in eqn. 5.2, with mean time between detection of ϕ_s^{-1}. If this assumption is true, then the probability that at least one single ion will be detected by time t_i can be found by integrating the exponential distribution from t=0 to t=t_i:

$$P(0 \le t \le t_i) = 1 - e^{-\phi_s t_i} \qquad [5.8]$$

Since this is assumed to be a Poisson process, the production and detection of ions are independent events; thus, the above equation applies even if there is only one atom irradiated by the laser. However, the meaning of the ϕ_s term has changed, since a "flux" of ions is of course not possible with only one possible ion. As explained earlier, ϕ_s is now considered to be the reciprocal mean time to detection of the ion produced from the single atom. As with any Poisson process, the distribution of detection times is an exponential distribution. Note that eqn. 5.8 applies also for nondestructive detection, which is also assumed to be a Poisson process; in this case, the variable "detection time" is the time before one event due to a single atom is detected.

The mean signal due to N_p atoms irradiated during T_m was given in equation 5.7 as $\epsilon_d N_p$. We now consider the distribution of the signal produced: the number of detected ions, N_i, when a fixed number of atoms, N_p, are probed by the laser is given by the binomial distribution:

$$P(N_i) = \binom{N_p}{N_i} (\epsilon_d)^{N_i} (1-\epsilon_d)^{N_p-N_i} \qquad [5.9]$$

However, as explained above, N_p is assumed to be a Poisson variable; hence, the probability distribution of N_i will also follow a Poisson distribution, with mean $\epsilon_d \bar{N}_p$. Obviously, when only one atom crosses through V_p during T_m, the signal due to the analyte is either zero (not detected) or one (detected).

Variability of I_t

As described in the previous section, the detection process for the signal produced by atoms in the laser beam is considered to be a Poisson process. In this section, the variability in the total signal, represented by the value of the total variance, σ_t^2, will be investigated for cyclic LIF.

Equation 5.5 gives the total signal due to N_p atoms interacting with the laser beam during a measurement time T_m. Since the background is assumed to possess a Poisson probability distribution, and the number of detected photons from each individual atom also follows a Poisson distribution with a mean given by eqn. 5.6, it would seem that I_t should also be a Poisson distribution with mean and variance given by

$$I_t = \sigma_t^2 = \mu_b + \phi_s t_i \qquad [5.10]$$

However, eqn. 5.10 is only valid when both ϕ_s and t_i are constant for every atom which can interact with the laser. Although this can be true, depending on the experimental conditions, it can easily be the case that both ϕ_s and t_i are variables, with mean Φ_s and τ_i, respectively. The values of ϕ_s and t_i for a particular atom may

depend on the path of that atom through V_p. For example, ϕ_s depends upon the optical collection efficiency, and this may not be constant over the entire probe volume; another source of variation in ϕ_s with path is if the transition of the atom is not saturated, and the laser intensity is not constant throughout V_p. The interaction time, t_i, of an atom will not be constant if diffusion effects play a significant role during T_m, or if the shape of V_p is such that (for example) an atom travelling down the center of V_p will have a larger interaction time than one which skirts the edge.

Thus, although the number of detected photons from a given atom which interacts with the laser will follow a Poisson distribution with a mean given by eqn. 5.6, the overall distribution of photoelectrons due to a single atom, I_s, will have a mean given by

$$\bar{I}_s = \Phi_s \tau_i \qquad [5.11]$$

and I_s will *not* follow a Poisson distribution. The mean of the total signal can thus be written for the general LIF case:

$$\bar{I}_t = \phi_b T_m + N_p \Phi_s \tau_i \qquad [5.12]$$

The effect of having either ϕ_s or t_i variable is to increase the variance of I_t. The variance of I_t (for a fixed value of N_p) can be partitioned between the variance due to the Poisson detection process in both the background and signal counts ("shot noise") and the "extra" variance due to any variability in ϕ_s and t_i:

$$\sigma_t^2 = I_t + (N_p)^2 \sigma^2 (I_s) \qquad [5.13]$$

where the second term in the equation is due to the "extra" variance. Of course, when ϕ_s and t_i can both be assumed to be reasonably constant, then this term approaches zero and I_t will be approximately Poisson.

Note that this section only discussed the case of LIF. Of course, similar considerations are involved in any technique based on destructive detection. The case of variable interaction time and LIF detection will be addressed in chapter 8.

Signal Detection Limit for the SAD Model

With the SAD model and definition as given above, the application of detection limit theory is as follows. For a given measurement time T_m, the distribution of I_b is Poisson with mean and variance μ_b. From eqn. 2.3 , the signal detection limit X_d is set according to a pre-defined tolerance (denoted by α, the probability for type I error) for false positives:

$$P(I_b \geq X_d) = \alpha \qquad [5.14]$$

A value for α must be chosen before the experiment; the value of X_d is set so that the observed probability of one or more false counts during T_m (due to background noise) is at or below this level. Note that, since I_b is a discrete variable, the value of α will not be uniformly decreased by increasing the value of X_d. If I_b is a Poisson variable then estimating the mean μ_b during T_m and application of eqn. 5.1 will allow X_d to be set through the use of tables of the Poisson probability distribution [86].

If it is found that, for given values of T_m and α,

$$P(I_b>0) \leq \alpha \qquad [5.15]$$

then there is essentially no background noise during T_m; this is called the intrinsic-noise limit, since the only noise on the analyte signal is due to variance of the signal itself. At the intrinsic limit, a single count (or more) indicates the presence of analyte; the value of X_d is one count.

Detection Efficiency of a near-SAD Method

The general definition for the detection efficiency, ϵ_d, has been given previously as that probability of a given atom will result in a signal detectable above the background noise. Now we can state more clearly that the detection efficiency is defined such that, when a single atom interacts with the laser during T_m,

$$\epsilon_d = P(I_t \geq X_d) \qquad [5.16]$$

where X_d is chosen according to a pre-defined tolerance for false positives. At the intrinsic limit, the detection efficiency is limited by the noise inherent on the signal itself. Since we have assumed a Poisson detection process for both destructive and nondestructive detection, we can see from eqn. 5.8 that, for $\mu_b = 0$, the probability that an atom entering V_p will be detected is given by:

$$\epsilon_d = 1 - \exp(-\phi_s t_i) \qquad [5.17]$$

This equation is equivalent to the one used by Alkemade [80], who was only concerned with the intrinsic-limited case. When noise is indeed present, however, eqn. 5.16 must be used.

Requirements for SAD

General Requirement

The general definition of an SAD method, given earlier, is that the method detects each and every atom which interacts with the laser with near-certainty. This requirement is now given in a more succinct form: *an SAD method is a method in which*

$$\epsilon_d \geq 1 - \beta \qquad [5.18]$$

where the detection efficiency is defined in eqn. 5.16 and ß is the probability of type II error (false negative) as described in chapter 2. The highest allowable value of ß must be decided prior to the evaluation of the (possible) SAD method.

The application of the above general requirement for SAD is different in the cases of RIS and cyclic LIF. The difference between the two as SAD methods can best be understood by studying figure 11 for fixed N_p and equivalent detection efficiencies. The intrinsic-limited case is shown in the figure, and ϵ_d can be calculated by using eqn. 5.17. It is assumed that ϕ_s and t_i are constant for all N_p atoms in both cases (such a situation is reasonable for an atomic beam experiment with a pulsed dye laser and a small V_p).

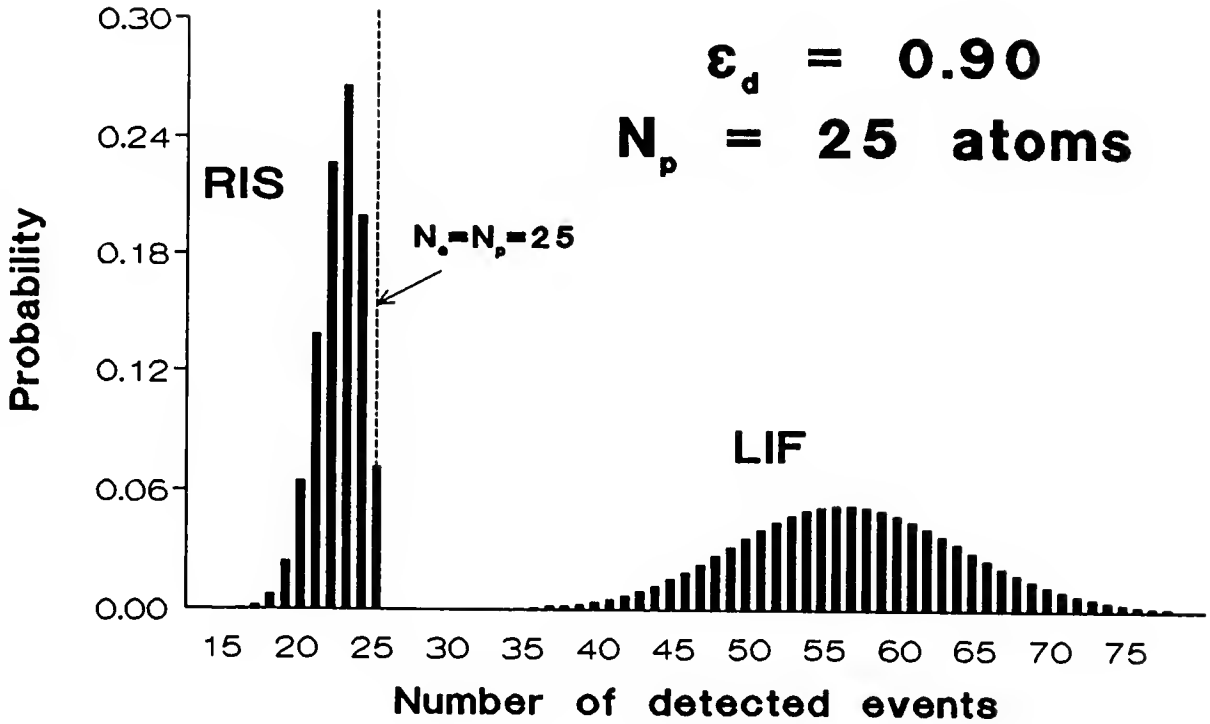

Figure 11. Probability distributions for the signal counts for RIS and LIF experiments with $N_p = 25$ atoms and $\epsilon_d = 0.90$. The RIS signal follows a binomial distribution, and the LIF distribution is a Poisson. It is assumed that ϕ_s and t_i are constant for all 25 atoms.

Achieving SAD with RIS (Destructive Detection)

With a destructive method such as RIS, a single atom can only give rise to one count at the most. The detection efficiency in this case is simply the binomial probability of "success" (eqn. 5.9) -- for RIS, the probability that the given atom will be ionized during its interaction time t_i. This probability is given in eqn. 5.8 for a Poisson process. However, the only way in which the requirement for SAD will be met as set forth in eqn. 5.18 is if $X_d = 1$; i.e., the intrinsic-limited case. Thus, for true SAD using RIS (or any other destructive technique) the following two conditions must hold (from eqns. 5.15, 5.17 and 5.18):

$$P(I_b>0) \leq \alpha$$
$$e^{-\phi_s t_i} \leq \beta$$

Note that the second condition assumes constant ϕ_s and t_i. The effect of variable values of these parameters on the overall detection efficiency must be taken into account if necessary.

Achieving SAD with LIF (Nondestructive Detection)

Guaranteed detection limit (X_g). Recall that the concept of a guaranteed signal detection limit, X_g, was introduced in chapter 2. The value of X_g is helpful in clarifying the requirements for a nondestructive technique to be a true SAD method. For a given value of X_d, the value X_g is defined so that the probability of a variable in a distribution with mean X_g being less than X_d is negligible (less than a desired

probability ß of type II error). If both the background and the signal are described by Poisson probability distributions, it is easy enough to assign values to X_d and X_g for any value of μ_b by using tables of Poisson values [86]. Table 1 shows these values for a number of cases, and different values of α and ß. The procedure in determining these signal detection limits is as follows: from the value of μ_b, X_d is chosen so that $P(I_b \geq X_d) \approx \alpha$. From this value of X_d, a Poisson distribution is found such that $P(X \geq X_d) \approx 1\text{-}ß$. The mean of this distribution is X_g.

If it is assumed that both ϕ_s and t_i are constant, then if X_g is found from Poisson tables as described, the requirement for SAD by LIF is

$$\bar{i}_s \geq X_g - \phi_b T_m \qquad [5.19]$$

Figure 12 shows a situation with $\mu_b = 1$ count and SAD is possible by LIF detection ($\alpha = ß = 0.0014$). When $\mu_b = 1$ count during T_m, $X_d = 6$ counts and $X_g = 16$ counts; thus, by eqn. 15, SAD is possible with $\bar{i}_s \geq 15$ counts/atom. Note from table 1 that even in the intrinsic-limited case ($\mu_b = 0$), a value of $\bar{i}_s = 6.6$ counts/atom is needed for SAD by LIF (at the 99.86% confidence level).

Summary: Requirements for SAD

The basic requirement for SAD by any laser-based method is given by eqn. 5.18. The practical consequences of this requirement for both destructive and nondestructive cases have also been discussed in this section. True SAD is possible with destructive detection only at the intrinsic-limit; however, SAD is possible by nondestructive means even in the presence of noise if the sensitivity is high enough.

Table 1
The Two Limits for an SAD Experiment

Mean blank level (μ_b)	Detection limit (X_d) $\alpha \leq 0.0014$ ($\alpha \leq 0.05$)	Guaranteed limit (X_g) $\beta \approx 0.0014$ ($\beta \approx 0.05$)
0.00	1 (1)	6.6 (3.3)
0.05	2 (1)	8.9 (3)
0.25	4 (2)	12.6 (4.7)
1.00	6 (4)	16 (7.8)
5.00	14 (10)	28 (16)
10.00	22 (16)	39 (23)
100.00	132 [130][a] 117 [117][a]	[169][a] [136][a]

The limits are given for the signal domain, with all the signals given as counts.

[a]The values in the square brackets were found by assuming a Gaussian distribution with the appropriate k values. At these higher signal levels, the Poisson distribution can be approximated by a Gaussian with $\mu = \sigma^2$.

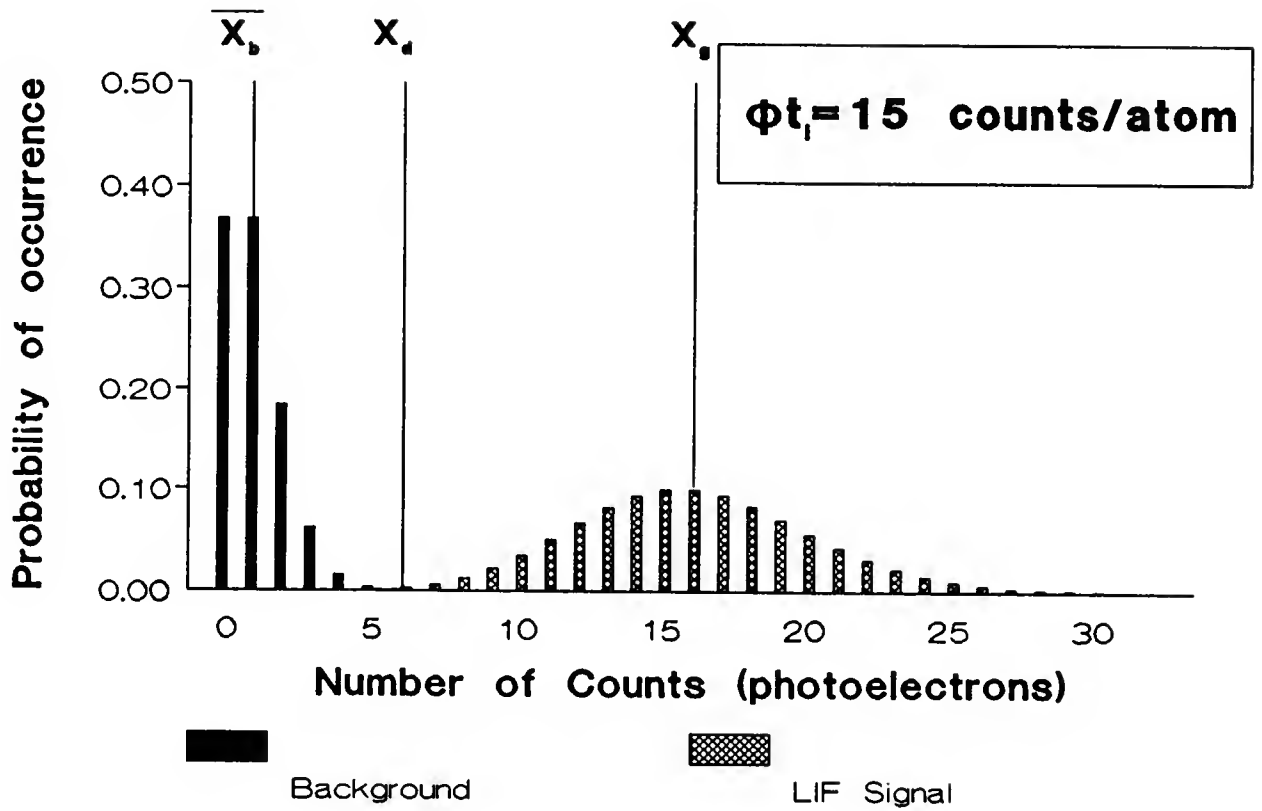

Figure 12. Guaranteed detection of a single atom in the presence of noise by LIF. The background distribution describes the situation when no atom passes through V_p during the measurement; when $N_p = 1$ atom the signal distribution has a mean of X_g and is almost certain to give rise to a detectable signal.

It should be emphasized that it is possible for a given technique to detect individual atoms and still not be a true SAD method; for example, with $\mu_b = 0$ the requirement for SAD (at the 99.86% confidence level) with LIF is 6.6 counts/atom (assuming ϕ_s and t_i constant); however, if $\bar{i}_s = 1$ count/atom, then individual atoms would still be detected quite often ($\epsilon_d = 0.632$). This is an example of a near-SAD method, where detection of an atom in the laser beam during T_m is *possible* (and perhaps likely) but not certain.

Detection Efficiency as a FOM. Notice that even though the detection limit theory of chapter 2 was applied to the SAD case in the signal domain, it is somewhat difficult to speak of near-SAD and SAD methods in terms of LOD.[1] Intuitively, it is not possible to have LOD < 1 atom, or as a non-integral number of atoms. This would seem to indicate that LOD (and LOG) is not an ideal FOM for the evaluation and comparison of (near-) SAD methods, as it is for more conventional methods. Another possible FOM is to compare S/N for one (or more) atoms, where S/N is the ratio of the mean signal due to one atom to the background noise. A more informative FOM than S/N for near-SAD methods is the detection efficiency, ϵ_d. This parameter contains information about the magnitudes of both the mean signal and the background noise, as well as the noise on the signal due to single atoms. Improvements in near-SAD methods should be evaluated by improvements in the value of ϵ_d rather than an increase in S/N (which may be at a cost to ϵ_d if there is

[1]with LOD in terms of numbers of atoms in the laser beam, not bulk concentration (this aspect will be discussed later).

an increased variance in the signal due to one atom). Once SAD has been achieved ($\epsilon_d \approx 1$), then improvements in the SAD method would best be described in terms of increases in S/N due to single atoms.

Precision of Counting Atoms

Thus far in this chapter we have treated the likelihood of detecting single atoms. However, the question remains as to whether it is possible to precisely count the number of atoms which pass through the laser if $N_p > 1$ atom. Recall that in chapter 2, a FOM called the limit of quantitation (LOQ) was introduced which specified an analyte concentration above which it was possible to determine an unknown sample with a predefined degree of precision (usually with RSD = 0.10, following the suggestion of Kaiser [3]). For an SAD method, it is possible to define a similar FOM in terms of atoms which pass through the laser beam during T_m; in this section, a related FOM shall be investigated: the minimum sensitivity, $(\tilde{i}_s)_c$, necessary to count atoms with a pre-defined precision at all levels of N_p.

Precision of Signal

In the measurement of a fixed N_p in the SAD model,[2] the signal distributions in the LIF and RIS experiments are given by the Poisson and binomial distributions,

---

[2]it is assumed that ϕ_s and t_i are constant throughout the section on precision of counting atoms.

and by substituting the appropriate values for σ from these distributions, the following equations are obtained for the intrinsic-limited case:

$$RIS: \qquad RSD = \sqrt{\left(\frac{1-\epsilon_d}{\epsilon_d N_p}\right)} \qquad [5.20(a)]$$

$$LIF: \qquad RSD = \frac{1}{\sqrt{N_p \Phi \mathcal{S} t_i}} \qquad [5.20(b)]$$

From eqn. 5.20(a), it can be calculated that for a precision of 10% or better with RIS it is necessary that $\epsilon_d \geq 0.99$. Since the RSD improves as N_p increases for RIS, an RIS method with this detection efficiency or better is capable of counting atoms for any value of N_p.

The situation for LIF is different, however, since many events can be detected from a single atom. Substituting $N_p = 1$ atom in eqn. 5.20(b) results in a requirement of 100 photoelectrons/atom for RSD = 0.10 with $N_p = 1$. Thus, it would seem that for precise counting of atoms with LIF, a sensitivity of at least 100 photoelectrons/atom during t_i is required at the intrinsic limit. This is a far more stringent requirement than the 6.6 photoelectrons/atom which are necessary for SAD (at the 99.86% level).

There is a problem, however, when the RSD is calculated using the above formula that stems from the difference between the precision of signal measurement, RSD_m, and the precision of counting atoms, RSD_c, when using a nondestructive SAD method. This problem does not arise with RIS since, when SAD is possible, it is

essentially true that every atom gives rise to a single count; thus, the signal exactly follows the number of atoms.

Consider the situation for LIF with 100 photoelectrons/atom, shown in figure 13. This figure illustrates the difference between the signal precision and the counting precision. Although, by eqn. 5.20(b), this situation corresponds to $RSD_m = 0.1$ for $N_p = 1$ atom, it is obvious that there is very little possibility of incorrectly counting atoms when $N_p = 1$ since there is almost no overlap between the distributions. Obviously, the value for RSD_m is not a reflection of the counting precision of the LIF method.

Counting Precision

This section is concerned with nondestructive detection only, since the requirements for precise counting by RIS are essentially the same as the requirements for SAD. For a nondestructive technique, the value of N_p is estimated according to the following equation:

$$N_m = RND\left(\frac{I_t - \mu_b}{\bar{i}_s}\right)$$

where the RND function rounds the expression in the parentheses to the nearest whole number, and the integer N_m is the number of measured atoms (i.e., the estimate for N_p). We can define the counting precision, RSD_c, as

$$RSD_c = \frac{\sigma(N_m)}{N_p} \qquad [5.22]$$

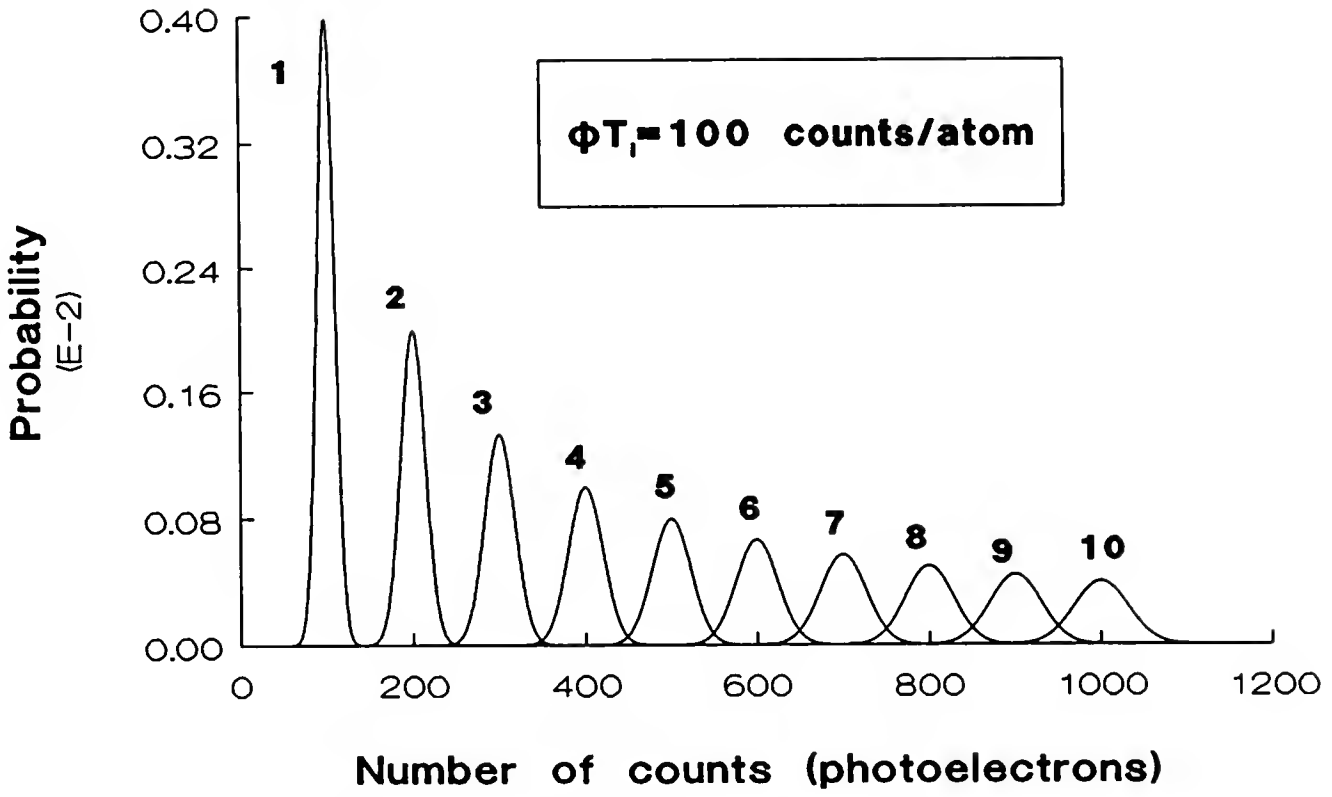

Figure 13. The distribution of signal counts for values of N_p from 1 to 10 atoms. The RSD of the individual distributions is given by eqn. 5.20(b).

where $\sigma(N_m)$ is the standard deviation in the number of measured atoms *with fixed* N_p.

The difference between RSD_c and RSD_m can be seen in figure 14, which shows the signal probability distribution with $\mu_b = 0$ counts, $\bar{i}_s = 20$ counts/atom and $N_p = 5$ atoms. The top axis displays the values of N_m which would be calculated at a given signal value using eqn. 5.21. The dashed lines in the figure show the portions of the probability distribution which would result in values of 4, 5, or 6 atoms for N_m. Notice that N_m is an integer; thus, a signal of 75 photoelectrons, for example, would result in a value of $N_m = 4$ atoms (and not 3.75 atoms!) as the best estimate for the true value of N_p.

Calculation of RSD_c

In order to investigate the counting precision of an SAD method, and calculate a value of $(\bar{i}_s)_c$ for a given background, the theoretical value of RSD_c for various fixed N_p must be determined. The theoretical value of RSD_c is not as easily calculated as for RSD_m in eqn. 5.20. To do so, an expression for $\sigma(N_m)$ in eqn. 5.22 must be found for given conditions of N_p, sensitivity and noise. From the definition of the variance of a discrete variable [87], it is known that

$$\sigma^2(N_m) = \sum_{N_m} (N_m - N_p)^2 \, P(N_m) \qquad [5.23]$$

where $P(N_m)$ is the probability distribution of N_m. This probability distribution can be written as

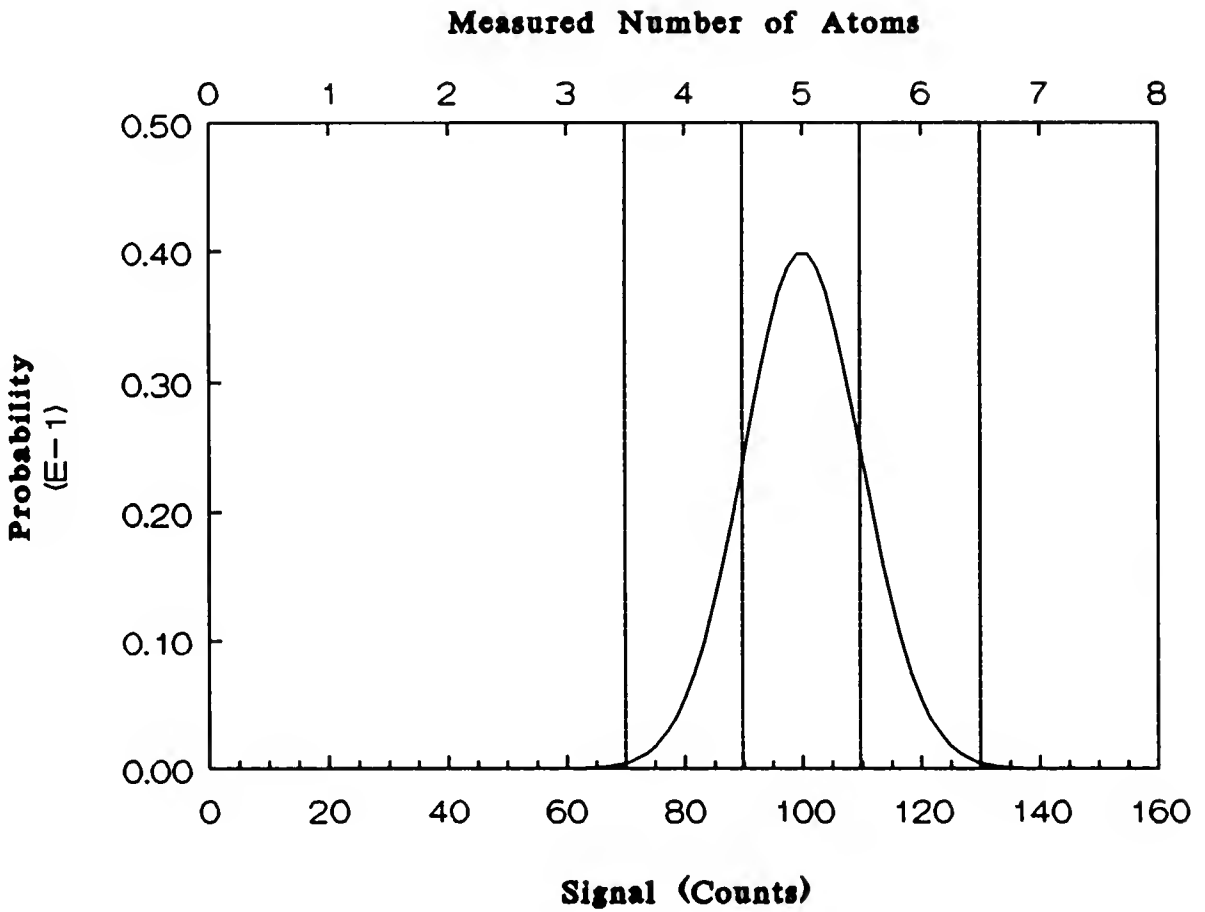

Figure 14. Illustration of the difference between the measurement precision of the signal, RSD_m, and the counting precision, RSD_c.

$$P(N_m) = \sum_{I_t=X_l}^{X_u} P(I_t) \qquad [5.24]$$

where the summation limits, X_l and X_u are found as follows.

For $N_m = 0$:

$$X_l = 0$$
$$X_u = X_d - 1$$

For $N_m = 1$:

$$X_l = X_d$$
$$X_u = INT[(N_m - 0.5)\phi_s f_i + \mu_b]$$

For $N_m > 1$:

$$X_l = INT[(N_m - 0.5)\phi_s f_i + \mu_b] + 1$$
$$X_u = INT[(N_m + 0.5)\phi_s f_i + \mu_b]$$

In all cases the INT function represents the integral part of the expression in the parentheses.

The above expressions are tedious to solve manually; a computer program can be written to evaluate these expressions for the SAD model for various values of N_p, μ_b and ϕ_s to determine $(\bar{i}_s)_c$ if the distribution of I_t is known. The results, and comparison of the theoretical value with the observed value of RSD_c from computer simulations, are presented in chapter 8. For the intrinsic limit the above equations give a value of $(\bar{i}_s)_c = 35$ counts/atom for $RSD_c \leq 0.1$ for all values of N_p.

In any practical situation, the value of RSD_c would be almost impossible to determine since N_p would not be fixed but would be a variable that would change for

different measurements (according to a Poisson distribution for the model presented in this chapter). Nevertheless, the purpose behind this section is to illustrate that for a nondestructive technique such as LIF, the requirement of SAD is not sufficient to count atoms during T_m to an arbitrary precision (unlike the case with a destructive SAD method). There is an additional increase in sensitivity required before this is possible by LIF.

Scope of an SAD Method

Effect of the Measurement Time on an SAD Method

The requirements for an SAD method have been presented; as an illustration of what an "SAD method" means in a more conventional analytical situation, let us assume that somehow the flow of atoms can be directed so that every atom in a given sample interacts with the laser. If the technique is capable of SAD, does this mean that the method possesses infinite detection capabilities? In other words, can any concentration of analyte in the sample can be detected?

The general SAD model presented the requirements for an SAD method *for a given measurement time*, T_m. The meaning and limitation of this requirement should be very clear: a method which is truly capable of SAD is capable of detecting above the background noise every atom which crosses the laser during T_m. Thus, in partial answer to the above questions, it is not possible to simply state that a given technique is an "SAD method" without stating the conditions under which this is possible -- most particularly the measurement time, T_m. A simple numerical example

with SAD by pulsed LIF will illustrate this point and serve to answer the above questions.

Numerical example: LIF with pulsed lasers

Let us imagine the interaction of a beam with a pulsed dye laser, where stationary conditions apply.[3] During a single laser pulse it is found that $\mu_b = 0.25$ counts; i.e., there is one "noise" count every four laser pulses on the average. During a single laser pulse (T_m is the pulse duration), we can say for the SAD model presented in this chapter that $X_d = 3$ ($\alpha = 0.00216$) and $X_g = 10.8$ ($\beta = 0.00143$). Thus, from eqn. 5.19, we see that if $\bar{i}_s = 10.55$ counts/atom, then SAD is possible during a single laser pulse.

Thus, this is a true SAD technique. Now suppose that a given sample is analyzed and will take 10,000 laser shots to completely flow past the laser. Again, assume that every atom in the sample interacts with the laser for time t_i. Is it possible to reliably detect a single atom in the sample with the technique just described?

The answer is no, because the scope of the above SAD method is only a single laser pulse. When T_m is changed to 10,000 laser shots, the requirements for SAD will change. If $X_d = 3$ counts is used as a criterion to distinguish the presence of analyte atoms from the background noise, then from the value of α for one laser

---

[3]each atom interacts with the laser for one pulse only and t_i is fixed. It is assumed that ϕ_s is constant as well. It will be assumed that the number of detected events (ie photoelectrons above a discriminator level) can be unambiguously counted. In reality, this may not be so easy with typical pulsed dye laser experiments.

pulse, we see that during T_m = 10,000 shots there will be 216 false positives on the average. Obviously it would be impossible to detect a single atom with this value for X_d.

With the new value of T_m, we must choose X_d high enough so that α is at the desired value. When μ_b = 0.25 counts/pulse and the background follows a Poisson distribution it can be calculated that

$$P(I_b \geq 7) = 9.734 \times 10^{-9}$$

so that for 10,000 shots with X_d = 7 counts, α = 0.000973, an acceptable level. This value of X_d gives X_g = 18 (ß=0.001043); the requirement to detect a single atom in the sample is that $\bar{i}_s$ = 17.25 counts/atom, instead of 10.55 counts/atom.

This simple illustration shows that a given SAD method has a certain "scope" -- i.e., a certain value of T_m over which the technique can detect a single atom. Beyond this measurement time, the method can no longer detect single atoms with the required values of α and ß. If the sensitivity of the method is very high, however, the scope of the SAD method (measurement time over which SAD is possible) may be so long as to be practically infinite. In other words, X_d can be set so high that it is extremely unlikely that I_b will ever exceed X_d during a single laser pulse, no matter how many pulses are counted. If SAD is still possible with such an X_d value, then the method is truly capable of detecting a single analyte atom in any (reasonable) size sample.

Counting precision, RSD_c. The value of RSD_c, and the requirement for precise counting of N_p in each laser pulse depends only on the value μ_b (and on the

variability of I_t; however, we assume ϕ_s and t_i are constant). Thus, increasing the length of T_m does not affect the value of minimum sensitivity necessary to precisely count the number of atoms present in each laser pulse.

Continuous Monitoring of Atoms

One of the most promising methods of achieving SAD is by using continuous lasers with LIF detection (CW-LIF). This method has been used in the past to detect single molecules [62, 65-68] and atoms [59, 60, 63] as they flow through the laser. The evaluation of near-SAD methods based on CW-LIF is a task which must be carefully approached. This section will discuss some possible signal-processing methods which apply the general SAD theory discussed thus far. In chapter 8, some of the methods and ideas discussed in this section will be demonstrated.

Signal Processing Methods

Simple integration over the measurement time, T_m

Most analyses based on atomic or molecular fluorescence of bulk analyte in a sample solution, in the simplest case, will integrate the signal for the measurement time and the sum (or its normalized analog, the average) will be the measurement value. This situation was depicted in fig. 1 and fig. 2. Such an approach is of course possible with a method based on CW-LIF. Application of the SAD theory when using this "simple integration" signal processing method is straightforward: the detection efficiency is measured for a given value of X_d (chosen for the pre-defined

tolerance to false positive detection) and eqn. 5.18 is used to determine if SAD is possible during T_m.

The simple integration method is very inefficient when $T_m >> \tau_i$ since the mean signal due to a single analyte atom will never exceed $\Phi_s \tau_i$ while the mean blank value will increase linearly with T_m. In addition, there is no temporal information on the exact time the atom is in the laser beam; it is only known that the atom entered V_p sometime during T_m. Nevertheless, there may be certain situations in which the simplicity of the method has its advantages. In the analysis of discrete samples which flow quickly through the laser beam (e.g.,in LIF of analyte atoms atomized in a furnace, or in flow injection analysis), then SAD may be possible when T_m is chosen so that the entire sample is analyzed.

Far more efficient methods for the analysis of continuously flowing analyte solution through V_p are based on the use of a time "window," of length t_w, applied repeatedly during T_m. Three such methods will be presented here. Their common feature is that the only the number of photoelectron counts within the window t_w are considered at any one time, and the duration of t_w is chosen to be of the magnitude of τ_r. Thus, the S/N ratio due to single analyte atoms is increased.

Sequential Application of Time Window ($t_w < \tau_r$)

It may be that the sensitivity of the CW-LIF method is so high that it is still possible to detect the presence of a single atom even if $t_w \approx \tau_r/10$. The S/N due to a single atom would decrease relative to a situation in which $t_w = \tau_r$; however, if

SAD is still possible by eqn. 5.18, then this is the best method to use. Such situations have only rarely been reported in the literature [30, 37].

The application of this method is simply the use of sequential integrations for time t_w for the entire measurement time T_m. In choosing the value of X_d for t_w it should be remembered that X_d should be high enough so that the total number of false positives from T_m/t_w windows will be at the desired tolerance level. The disadvantage of this method is that higher sensitivity is required to achieve SAD than by either of the next two methods which use a time window. However, if this sensitivity is available, then the method is very simple to use and can count atoms in real time as they traverse the laser beam. For CW-LIF which is on the borderline of becoming a true SAD method and does not have a high enough sensitivity for this method, one of the following two methods can be used.

Photon burst method

This method has been reported in the literature as a method of recording spectra of single atoms in an atomic beam [61, 63]. Figure 15 demonstrates how the "photon burst" method may be applied to CW-LIF. A single photoelectron count triggers open the gate, which is pre-set to count the photoelectrons for the gate time t_w. The number of photoelectrons (including the trigger pulse) constitutes the "signal" during t_w. The gate duration is set so that $t_w \approx \tau_r$. The photon burst method can be implemented during real time so that bursts above a pre-set value (X_d) can signal the presence of an analyte atom in the laser beam. Alternately, the number of counts from all the photon bursts can be stored in a computer and analyzed later; only the

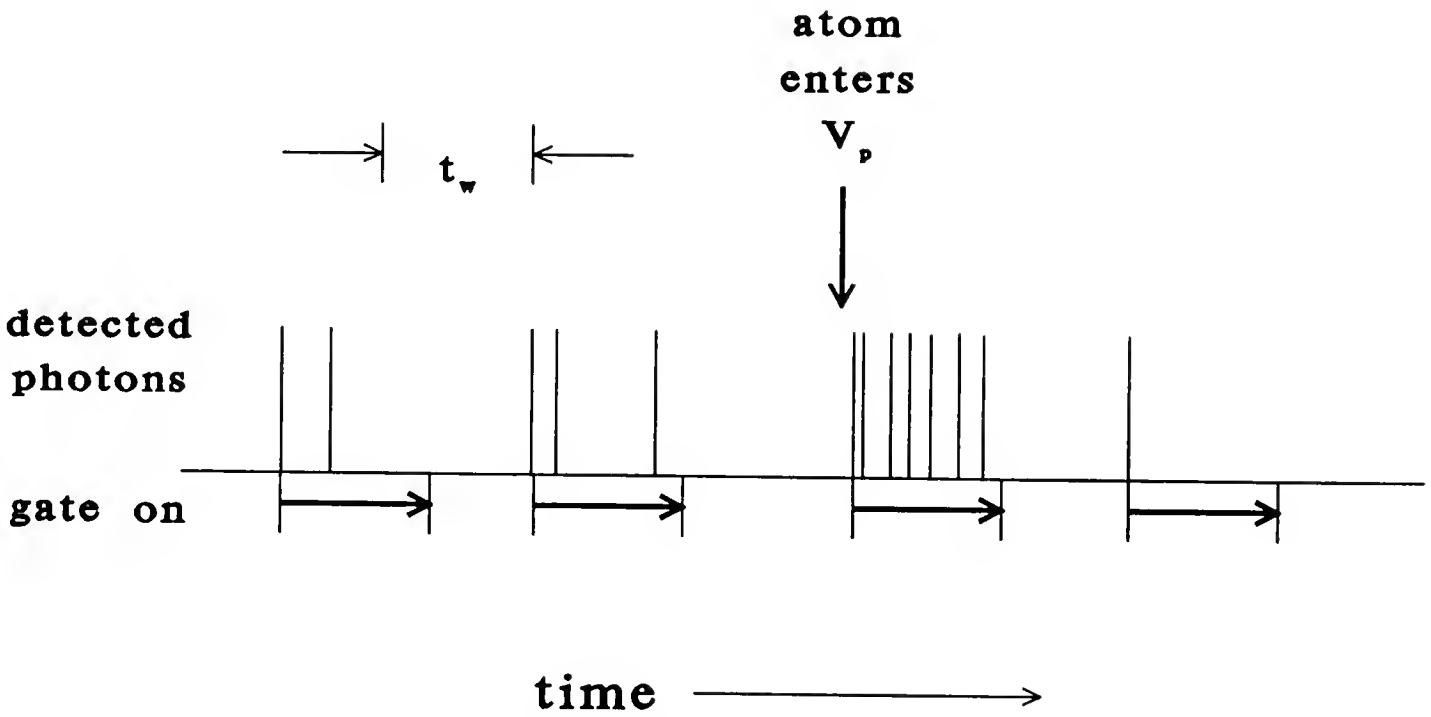

Figure 15. Demonstration of the photon burst method. A single detected photoelectron triggers the gate to open for a set time, t_w. The number of counts detected within t_w, including the trigger count, constitutes the burst signal. Bursts due to atoms, such as the one shown, will be larger than those due to background noise for near-SAD methods.

bursts with a sum equal to or greater than X_d can be considered due to analyte atoms with 1-α probability of false positive. All the normal requirements given previously for an SAD method apply. The advantage of the photon burst method over simple integration is that only the noise during t_w can contribute to false positives, and consequently a lower value of X_d can be chosen and the sensitivity necessary for SAD is not as high.

False positives during T_m. As explained previously, as T_m increases, it is frequently necessary to increase X_d to keep the probability of a false positive during T_m down to an acceptable value. For the "simple integration" and "sequential window" methods above, it is relatively easy to determine the value of α for given values of X_d and T_m. The theoretically calculated value of α (assuming a Poisson distribution of I_b) for the "photon burst" method is slightly more complicated. In the presence of background noise only, the sum, S, of the number of photoelectrons in a given photon "burst" follows a Poisson distribution based on the mean background level such that,

$$P(S) = P(I_b=S-1) = \frac{e^{-\mu_b}(\mu_b)^{S-1}}{(S-1)!} \qquad [5.25]$$

since $S \geq 1$ count. Thus, for a certain background level, the probability of a given burst giving a false positive is

$$P(S \geq X_d) = \sum_{X_d-1}^{\infty} P(I_b) \qquad [5.26]$$

so that during the measurement time,

$$\alpha = \bar{b} \sum_{X_d-1}^{\infty} P(I_b) \qquad [5.27]$$

where

$\bar{b}$ = average number of bursts during T_m.

For a given value of μ_b and T_m, the average number of bursts can be calculated according to

$$\bar{b} = \frac{\phi_b T_m}{\sum_{S-1}^{\infty} S \cdot P(S)} \qquad [5.28]$$

The dependence of α on T_m can readily be seen from eqns. 5.27 and 5.28. However, the denominator in eqn. 5.28 ensures that α increases very slowly (compared to the simple integration method) for a given X_d as T_m increases.

The above calculations of the theoretical value of α can aid to choose a correct value for X_d in cases where the shot noise of the background is limiting. In most practical situations, however, this would need to be confirmed by performing many blank measurements and observing the effect of different X_d values on the number of false positives.

Sliding sum method

The "sliding sum" signal processing method is an intuitively obvious technique. After the raw data is collected, which consists of the counts as a function of time during T_m, a data transformation is applied in which the value sum of the number of counts over a width t_w is assigned to the middle of the time window. The window

is then moved one step and the process is repeated. For continuous monitoring of atoms with CW-LIF, the step size should be a fraction of the residence time of the atom within V_p; e.g., $\Delta t \approx \tau_r/20$. Smaller step sizes are of course better, but only up to the point where the signal processing step becomes too long. The optimum value for the duration of the moving sum is $t_w \approx \tau_r$ (and no longer than the largest possible residence time).

Peak Detection. The sliding sum peak maximum will occur when t_w and t_r exactly coincide. Thus, it would seem desirable to use the sliding sum peak maximum value as a signal of the presence or absence of the analyte atom. The distribution of peak maximum will follow the distribution of I_t; thus, application of the SAD theory from the previous section is straightforward. When the maximum exceeds X_d (chosen based on the values of α, μ_b and T_m), then the sliding sum peak is presumed to be due to the presence of an atom in V_p. In a similar manner, peak maxima can be used to evaluate the detection efficiency and determine if the method is truly SAD.

A problem with using the peak value as an indicator of I_t will occur when the analyte concentration is high enough so that there are problems with peak overlap; ie, there is more than one atom in V_p at a given time. Sliding sum peak detection for counting N_p during T_m is only practical when there is a very small probability that such an overlap will occur.

False positives with sliding sum peak detection. Calculation of the theoretical value of α when using sliding sum peak detection is complicated; a good first

approximation can be calculated with the use of the Gamma distribution (if a Poisson distribution of the background can be assumed) if X_d is large enough that $P(I_b > X_d)$ is negligible. The details will not be given here, but the most practical method of determining α for given values of X_d, ϕ_b, T_m, and t_w is from the distribution of peak maxima from repeated blank measurements. Theoretically, the values of α from this method and the "photon burst" method are very similar for the same conditions. A comparison of the number of false positives for these two methods will be shown in chapter 8.

Peak area detection. The problem with overlapping peaks when using peak heights of the sliding sums was mentioned above. One method of alleviating this problem is to simply use the integrated peak area of sliding sum peaks as the "signal"; when the residence times of two atoms overlap, the resulting peak will be longer and the area will be the sum of the contributions of the signal due to both atoms.

A single photoelectron count in the raw data array results in a contribution of $t_w/\Delta t$ counts to the resulting sliding sum peak area as the window is moved passed, where Δt is the step size. Thus, a cluster of I_t counts (due to analyte atoms and background noise) will result in a peak of area $(t_w/\Delta t)I_t$. In general, the distribution of peak areas, I_a, will have the following characteristics

$$\bar{I}_a = \left(\frac{t_w}{\Delta t}\right) \bar{I}_t$$
$$\sigma_a = \left(\frac{t_w}{\Delta t}\right) \sigma_t \qquad [5.29]$$

where

σ_a = standard deviation of peak area.

The advantage of using peak area detection instead of peak heights is that, with no loss of information or detection efficiency, higher concentrations of analyte can be analyzed. The total peak area from overlapping atoms is a measured of the number of atoms which contributed to the peak. The theory from the counting precision can be directly applied in this situation in order to count the number of atoms which contribute to a given sliding sum peak; i.e., it may be possible to precisely count the number of atoms contributing to a given peak (in addition to the total number, N_p, which pass through V_p during T_m) if the sensitivity is high enough.

Overall Efficiency of Detection

Much of this chapter has been concerned with detection efficiency; indeed, an SAD method is defined essentially as a method which has almost unity detection efficiency. However, it is important to recall the ϵ_d applies only to atoms which interact with the laser beam. A high detection efficiency does not necessary result in a technique with a corresponding low LOD in terms of bulk concentration of analyte in the sample, since it is quite possible that most of the analyte atoms in the sample never interact with the laser beam. A better parameter to indicate the detection power of a laser-based method is the overall efficiency of detection [80, 81], ϵ_o, which is given by a product of efficiency terms:

$$\epsilon_o = \epsilon_a \epsilon_p \epsilon_t \epsilon_d \qquad [5.30]$$

where

ϵ_a = the efficiency of atomization,

ϵ_p = the spatial probing efficiency,

ϵ_t = the temporal probing efficiency, and

ϵ_d = the detection efficiency of atoms which interact with the laser.

The atomization efficiency describes the probability that an analyte atom in the sample will be converted into free atoms in an energy level suitable for interaction with the laser. In the case of molecules, this term is the probability that the analyte molecules in the sample will be prepared (perhaps by a chemical reaction to tag the molecules with a fluorophore) in a state suitable to produce an analyte-specific signal. The spatial probing efficiency, ϵ_p, describes the probability that the free analyte atoms will pass through V_p, the portion of the analyte "volume" probed by the laser. The temporal probing efficiency, ϵ_t, is the probability that an atom which passes through V_p will interact with the laser. This fraction of analyte atoms is determined by the duty cycle of the laser and the length of T_m. Finally, the detection efficiency is of course a familiar term by now; this term in the above equation takes into account the probability of detecting a signal above the background noise level.

Figure 16 depicts the various stages of a typical laser-based analytical measurement. Note that the detection efficiency, ϵ_d, as defined earlier, only comes into play at the last stage. We have discussed "SAD" methods in this chapter, but

fig. 16 indicates the difference between SAD in V_p and true single atom detection within the sample. For such a feat to be possible, ϵ_o must be nearly unity. Figure 16 also shows clearly that increasing ϵ_r or ϵ_d at the expense of any other term in eqn. 5.30 will not necessarily result in a more sensitive analytical technique, even if SAD is achieved thereby. For example, focusing the laser beam may result in a higher value for ϵ_d but may decrease ϵ_p and result in a lower value for ϵ_o.

Conventional LOD for SAD Methods

The scope of a given SAD method can be used to determine the value for LOD in terms of bulk analyte concentration if the overall efficiency of detection is known. Obviously, for the maximum value for T_m over which SAD is possible (ie the scope of the method), it is possible to detect every atom which appears within V_p and interacts with the laser. If we have knowledge of the amount of sample consumed during T_m and have reasonable estimates of the efficiency terms in eqn. 5.30 then it seems that we should be able to calculate the value of the LOD in terms of bulk concentration of analyte in the sample, rather than in terms of atoms which interact with the laser.

If the product $\epsilon_p\epsilon_t\epsilon_a$ is known for an SAD method and is much less than unity, then the value for the LOD of the technique is

$$LOD = (\epsilon_a\epsilon_p\epsilon_t)^{-1} \qquad [5.31]$$

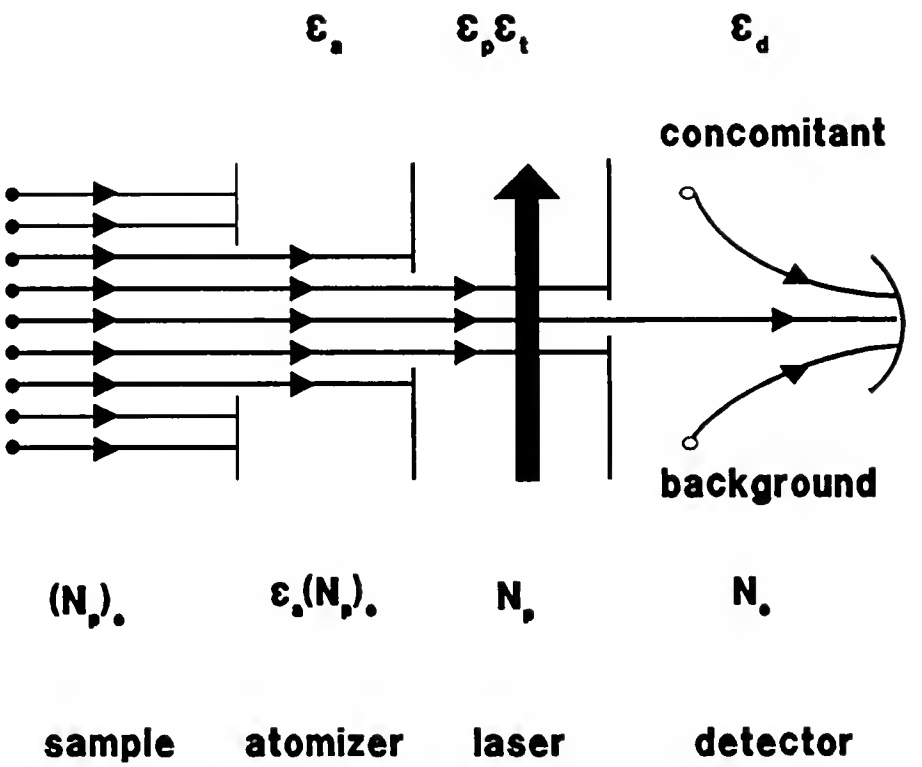

Figure 16. The overall efficiency of detection of an analytical method.

in terms of atoms of analyte per volume of sample consumed during T_m. Note that when analyzing large samples which continuously flow through V_p (as opposed to discrete sample amount), the value of LOD in terms of bulk concentration of analyte per sample analyzed will be improved through the use of larger values of T_m, even though the method may no longer be considered SAD. The reason for this improvement, of course, is that the amount of sample analyzed increases linearly with T_m while (in the shot noise limit) the noise of the background has a square root dependence on T_m.

CHAPTER 6
EXPERIMENTAL

Monte Carlo computer simulations of simple analytical experiments were used as a means for demonstration and verification of the theoretical work set forth in chapters four and five. These simulations, particularly those based on the SAD model, were also helpful in the formulation of the theory which has been presented. The intention of experiments based on these computer simulations is not to perform an exhaustive study of all aspects of the models discussed, but merely to prove their validity and provide some insight into their usefulness. This chapter will outline the general form of some of the programs which were used in these simulations; more details will be given when appropriate.

General

All Monte Carlo simulations were carried out on IBM-compatible microcomputers which were equipped with either a 25 MHz 80386 CPU and a 80387 math co-processor chip, or a 20 MHz 80286 CPU with a 80287 co-processor. All programs were written and compiled in Microsoft QuickBASIC (version 4.5, Microsoft Corp., Redmond, WA). Algorithms to generate random numbers according to normal distributions and Poisson distributions were written according

to guidelines presented by Knuth [88]; these routines are also presented in the Appendix, and are based on QuickBASIC's pseudo-random number generator.

Simulations to Investigate the Variance of the LOD

Chapter 4 presented the concept of the calculated LOD of an analytical procedure as a variable estimator of the true, unknown LOD of the technique. Two different types of models were used to investigate the properties of the LOD estimator given by eqn. 4.2, in light of eqns. 4.9 and 4.10: (1) a generic situation with arbitrary standards and various background noise levels; and (2) a model based upon conditions found in the trace analysis of metals by electrothermal atomization in a commercial graphite furnace and laser-induced fluorescence detection of the analyte atoms (ETA-LIF). The ETA-LIF model conditions were based on the recent analysis of thallium at the sub-femtogram level [89]. The variation of the LOD estimate was determined under different experimental conditions; specifics will be given when appropriate.

Experimental Determination of Shot Noise

In order to simulate conditions of a typical ETA-LIF experiment, it was necessary to have a knowledge of the shot noise in a photomultiplier for a given anodic current output. Although in most cases the shot noise can be calculated theoretically using well-known formulas [90], in the case of boxcar detection the task is considerably more difficult since the "effective" electronic bandwidth is unknown.

An experimental estimate of the relationship between output signal and shot noise was found in the following manner.

An LED was used as a light source due to its very stable output; thus, any flicker component in the source was minimized. A monochromator was tuned to the maximum of the LED, and various calibrated neutral density filters were placed between the LED source and the entrance slit of the monochromator. A terminator of 1.2 kΩ was used to convert the anodic current of the photomultiplier (model R928, Hamamatsu Corporation, Bridgewater, NJ) to a voltage; the signal was amplified 20X by a voltage amplifier (Evans model 4163, Evans Associates, Berkeley, CA) and input into a boxcar averager (SRS model SR250, Stanford Research Systems, Sunnyvale CA). The boxcar was internally triggered at 50 Hz, and a gate of 300 ns was used. Various values for the averaging was used: last sample, 3 and 10 averages. More averages were not attempted because an overly large time constant would be inappropriate for the transient pulses in ETA-LIF. The conditions chosen above closely mimic those which are found in a typical ETA-LIF experiment.

The shot noise is proportional to the square root of the mean output anodic current; the proportionality constant was determined by linear least-squares fit to a plot of the variance *vs.* the anodic current. The fitted line relating shot noise and anodic current was used to find the shot noise at any signal level in the simulations of ETA-LIF conditions.

Experimental Variation in Estimated LOD

Using the model conditions for the background, sensitivity and signal noise, a computer program was written which would calculate s_b and slope for 1000 calibration curves, and estimate the LOD according to eqn. 4.2 for each one. The observed value of $S_{\hat{LOD}}$ calculated from the 1000 values of $\hat{LOD}$ can be compared to the theoretical value predicted by eqn. 4.10. In addition, the performance of confidence intervals about the estimated LOD can be evaluated by how often the true LOD value falls within the interval. The following steps give a brief outline of the algorithm used:

1. The model parameters were defined: true values for the sensitivity, background mean and standard deviation, and calibration standards. Thus, the "true" value for the LOD is known.
2. The signal level for each calibration standard was "measured". For both generic and ETA-LIF models, the noise on the signal was assumed to be normally distributed.
3. The slope and expected standard error in the slope were calculated with either unweighted or weighted least-squares regression, using conventional formulas [20].
4. For each of the 1000 "experiments", a number of separate "measurements" were taken of the blank using the normal random number generator.

Estimates of σ_b were calculated from the results; however, the blanks were not included in the calibration curve.

5. For each experiment, the LOD and σ_{LOD} values were estimated according to eqns. 4.2 and 4.10, and a 95% confidence interval was formed assuming either a normal distribution of estimated LOD values or with the use the χ^2 tables, as in eqn. 4.11. If the "true" LOD was not within the interval, then this fact was noted.
6. The estimated variance, S_{LOD}, from the 1000 estimates of the true LOD values was calculated.

As noted earlier, two models were used for the experimental simulations of calibration curves and blank measurements: a generic model to examine the behavior of eqns. 4.9 and 4.10 under various conditions, and a model based on the determination of thallium by ETA-LIF. These models will now be described.

Simulations using a generic model

The general validity of eqn. 4.10 was investigated using an arbitrary model. The effect of increasing slope error and decreasing numbers of blank measurements (i.e., increasing either term in eqn. 4.9 which contribute to σ_{LOD}) was investigated to determine the range within which the expressions may be used. The model conditions are as follows:

Standards (x-axis): 220, 240, 260, 280, 300 (arbitrary units).

Sensitivity: 1.

All measurements exhibited homogeneous variance, σ^2. The value of σ determines the LOD and the value of CV_a in eqn. 4.9. Two different trends were followed to determine their effect on the calculated and observed value of S_{LOD}: first the slope error was gradually increased by increasing the value of σ (and the true LOD) while the number of blank measurements was held constant at twenty. Next, the number of blank readings used to estimate s_b was varied while the value of σ was held constant.

Simulations using an ETA-LIF model

A model based on the determination of thallium by ETA-LIF was used to demonstrate eqn. 4.10 in a slightly more realistic setting. The sensitivity was 2.5 mV/fg (peak detection). The limiting noise was either the photomultiplier dark current (in which case the true LOD would be 0.12 fg) or laser-induced scatter/fluorescence (LOD = 1.367 fg). Wei et al. have reported that in the second case, the noise is white in nature [91]; it is assumed here to be due to photomultiplier shot noise, and the magnitude is calculated as explained in the experimental section. The noise on the "signal" was due to two sources: (1) photomultiplier shot noise, as just described, and (2) injection imprecision of the sample. The first contribution was important at lower concentrations. The second contribution was assumed to have a value of 5% RSD. The program would calculate the signal for a given standard as follows: first the true injected amount of sample would be calculated by assuming a normal distribution (5% RSD) centered on the true standard value. The mean signal for this injected amount was calculated from the true (model) sensitivity, and the

actual "measured" signal was normally distributed around the mean with a variance due to photomultiplier shot noise.

Weighted least squares fitting was used for all program runs in which a calibration curve was used to determine the sensitivity. It is important in practice to determine whether weighted or unweighted least squares is necessary. The second term in eqn. 4.9 will not be a good estimation of the slope coefficient of variation if unweighted least squares is incorrectly used to fit heteroscedastic data.

There were three different types of simulations run with the ETA-LIF model. In the first case, ten standards were each "measured" once. The standards covered 5 orders of magnitude from 50 fg to 1 ng injections into the furnace. These values are realistic for the analysis of thallium, which is present at very low levels in the environment -- contamination of the standards is not a problem. Weighted least squares regression was used with the weights equal to the inverse of the true variance of the signals at each concentration. In the second run, only 3 standards covering 2 orders of magnitude (1 pg - 100 pg) were used, but each was measured four times to provide estimates for the weights which should be used in weighted least squares regression. This is a more realistic situation than the case in the first run, where the true weights were known. In the final run, calibration curves were not used but instead a single calibration standard (1 pg) was measured four times to provide an estimate for the sensitivity to use in estimating the LOD by eqn. 4.2. The CV_a term in eqn. 4.9 was estimated by accounting for the error in both signal and background averages, and then using eqn. 2.14 to estimate σ_a.

Simulations of SAD by LIF

Chapter 5 presented a general model of an SAD technique by laser spectroscopic methods, and outlined various associated concepts of SAD methods based on this model. In Alkemade's original work on SAD theory [79, 80], the possibility of detecting single atoms in the presence of noise was ignored, and an SAD method was considered possible only in the absence of noise (i.e., at the intrinsic-noise limit). In this work, a more general model broadens the definition of a true SAD method to include the presence of noise; however, SAD is only possible under these conditions by a nondestructive technique. The computer simulations which will be presented emphasize this fact by modeling an SAD method based on cyclic LIF of atoms flowing through the laser beam. Many of the aspects of SAD in the presence of noise presented in chapter 5 will be illustrated using these simulations.

Models for the Interaction Time with the Laser

The simulations for SAD by cyclic LIF were based on an experiment in which the analyte species flow through the probe volume and interact with the laser, which is a CW laser. The simulations can be classified into two types, according to the method used to calculate the residence time, t_r, of an atom within V_p; these models will be called the Simple and the Cylindrical Probe models. In all cases, it was assumed that ϕ_s was constant throughout V_p. All other assumptions of the general SAD model presented in chapter 5 apply.

Simple model

In simulations based on the simple model, it was assumed that the value of t_r, and hence t_i, is constant for all atoms which enter V_p. In this situation, the variable I_t is a Poisson variable, and the "extra" variance term in eqn. 5.13 is zero. Such a situation can occur with pulsed laser LIF experiments or in situations where the shape of V_p is such that the analyte atoms have (almost) constant t_r values for any path through V_p -- e.g., if a cylindrical lens was used to focus the laser in a line across the analyte stream, or the analyte flow was constricted so that it all flowed through the center of an unfocused or expanded laser beam (e.g.,sheath flow). The use of spatial masking to shape V_p might also decrease the variation in t_r to a very low value.

Cylindrical probe volume model

The purpose of this model is not necessarily to provide a more realistic simulation of typical experimental conditions but to demonstrate the effect of a non-zero "extra" variance in eqn. 5.13. In this model, the extra variance is due to a variable interaction time with the laser beam. The model is based on an experiment such as was shown in figure 9 in chapter 5, in which the probe volume as defined by the laser beam and the collection optics (with a slit as a limiting aperture) is a cylinder.

In this model, it is assumed that t_i is a variable that depends on the path of an individual atom through V_p. The situation used in the simulations, along with labelled axes, is shown in figure 17. Effects due to diffusion, flow profiles and

velocity distribution are neglected; all atoms enter V_p with the same velocity in the z-direction, v_z. Both v_x and v_y components of the velocity are assumed to be zero. The atoms are spread uniformly throughout the analyte volume, V_a, which flows past V_p during T_m. Since the number of atoms within this volume will vary according to a Poisson distribution, the number of atoms which interact with the laser, N_p, would normally also follow a Poisson distribution in an experiment following this model. The Cartesian coordinate system shown in fig. 17 has its origin in the center of V_p; if the position (x,y) of the atom within V_a is such that $x \leq x_p$ and $y \leq r_p$ then this atom interacts with the laser. For an atom which enters V_p, the value of t_i is dependent only on the position along the y-axis (since $v_x = v_y = 0$).

For this model, it is easy to see that the probing efficiency is given by

$$e_p = \frac{4x_p r_p}{\pi r_a^2} \qquad [6.1]$$

The interaction time of an atom which enter V_p can also easily be calculated for the Cylindrical V_p model according to

$$t_i = \frac{2}{v_z}\sqrt{(r_p^2 - y^2)} \qquad [6.2]$$

Note that t_i depends only on the (uniformly random) position of the atom along the y-axis. It is assumed that y is uniformly distributed within V_p[1]; under these conditions, the mean value of t_i can be calculated to be

---

[1]the condition necessary for this is that $r_p \leq (r_a^2 - x_p^2)^{1/2}$.

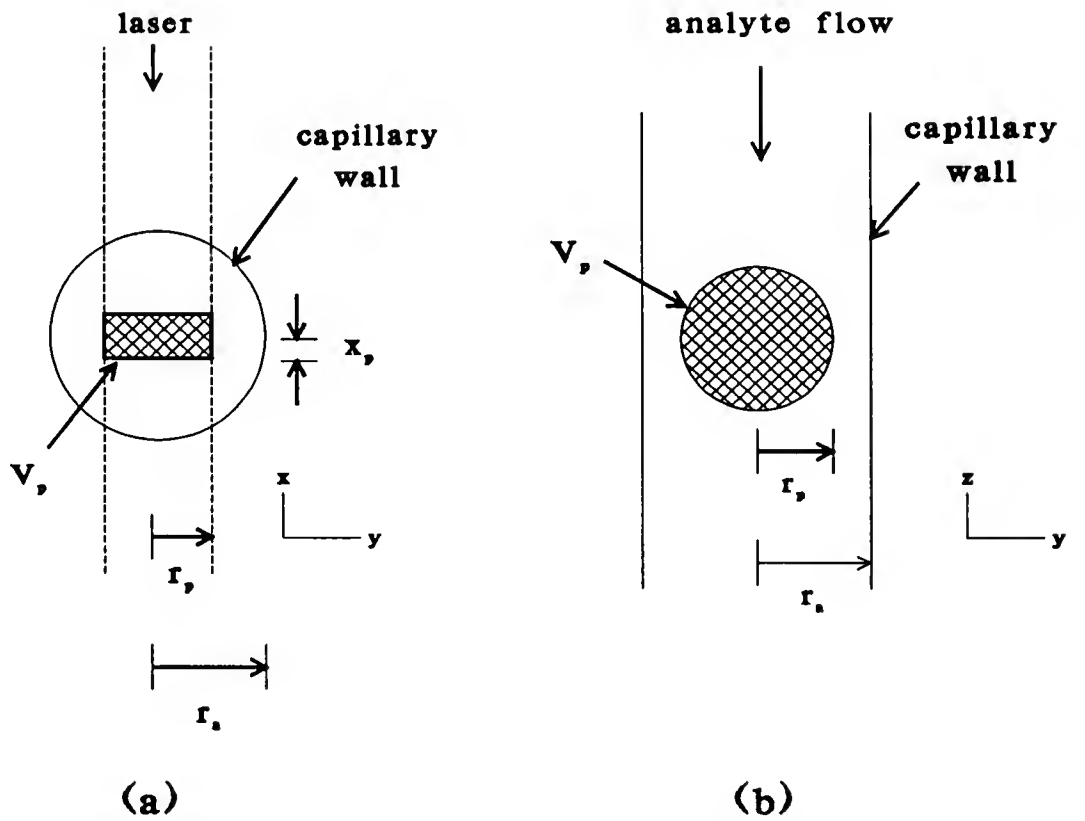

Figure 17. Basis of the Cylindrical V_p Model used in computer simulations.

$$\tau_i = \left(\frac{\pi}{2}\right)\frac{r_p}{v_z} \qquad [6.3]$$

In light of the Cylindrical V_p model, the Simple model with fixed t_i as described above can be viewed as a "rectangular" V_p model with $v_x = v_y = 0$ and constant v_z, as above. Comparisons between the two models were made by choosing and r_p (or v_z) in eqn. 6.3 such that τ_i for the Cylindrical V_p model is equal to the fixed value of t_i assumed in the Simple model -- in this manner the mean signal per atom, $\bar{i}_s$, remained the same for both models.

General Outline of Simulations

For either of the models described, the general format of a typical simulation used to generate the raw data (detected photons as a function of time) was as follows:

1. The model parameters, T_m, ϕ_b, ϕ_s, X_d, were defined. The signal detection limit, X_d, was set by the values of ϕ_b, T_m and the desired α; different values of X_d were often chosen to investigate the effects on the number of false positives.
2. Values for N_p and t_i were chosen or calculated. Although N_p would normally follow a Poisson distribution in an SAD experiment, it was usually fixed at a given value for the computer simulations. The value of t_i was assigned according to the model used; if a Cylindrical V_p model was used, then it was

calculated according to eqn. 6.2 with the position on the y-axis a uniform random variable between $-r_p$ to r_p.

3. The contribution of the background noise was added to the data matrix. The number of counts due to the noise varied according to a Poisson distribution with a mean of $\phi_b T_m$. If this mean was high enough (above 50), a normal distribution was used to approximate the Poisson distribution. The detection times for each of these photoelectrons was then generated according to a uniform random distribution between 0 and T_m.
4. The entry time of each N_p atom into V_p was randomly chosen from a uniform distribution. The signal due to each of these atoms was a Poisson variable with mean $\phi_s t_i$, where t_i was calculated for each atom according to the model used. The signal counts were uniformly distributed during the atom's residence time within V_p.

Once the raw data file was generated according to this procedure, any signal processing method could be chosen with an appropriate value of t_w. One of the advantages of using a computer simulation such as the one above to investigate SAD theory is that the number N_p could be fixed, something which may be impossible to achieve in an SAD experiment. The number of "positives" -- signals at or above X_d -- could be compared to the true number of N_p. This ability was necessary to investigate the behavior of the counting precision, RSD_c, at various values of ϕ_s, ϕ_b

and N_p. Also, the performance of the signal processing, the sliding sum and photon burst methods, could be more easily evaluated.

In many instances, simpler versions of the above simulation were used. For example, when investigating RSD_c the entire raw data file was not necessary; only the analyte signal was of interest. In such cases, the value of I_t with the analyte in the probed region, was a Poisson variable with mean $\mu_b + N_p\phi_s t_i$, and X_d was chosen according to the value of μ_b. This is similar to the situation of the "simple integration" signal processing presented in chapter 5, with the value of N_p fixed at a given level.

CHAPTER 7
INVESTIGATING THE VARIABILITY OF THE LIMIT OF DETECTION

Introduction

In chapter 4, the variability of the calculated LOD of an analytical procedure was explained to be the result of two factors: true changes in the population parameters of the procedure (such as sensitivity and background noise) and the imprecision of the sample statistics used to estimate the true (unknown) LOD of the system. In this chapter computer simulations are used to investigate the magnitude and nature of this second source of fluctuation in estimated LOD, and particularly to illustrate the limitations and uses of eqns. 4.9 and 4.10 derived in chapter 4.

The first set of simulations investigate the validity of the derived equations with various magnitude of contribution from the two terms in eqn. 4.9. These experiments use the generic model presented in chapter 6. The application and utility of these equations in a typical analysis of ultra-trace levels of thallium by ETA-LIF is demonstrated by the second set of simulations.

Effect of Increasing Values of Slope Error

The effect of increasing values of slope error on observed and calculated S_{LOD} in simulations run using the generic model is shown in table 2. The program takes 30 blank "measurements" for each simulation. The value of the parameters σ_b and CV_a are shown in the first two columns. The entries in the third column are the average value and standard deviation of $\hat{LOD}$ calculated for 1000 calibration curves. The true LOD value and calculated σ_{LOD} (using eqn. 4.10 with the population parameters) are shown in column four. The confidence intervals shown in the table are calculated from tables of the χ^2 distribution or with the formula $\hat{LOD} \pm 2S_{LOD}$. The percentage of runs in which the true LOD value lies below the lower limit are given in the column labelled "lower"; the percentage above the upper limit are given in the next column. The expected values in both columns is about 2.5%.

The agreement between the predicted and actual behavior of the LOD estimated by eqn. 4.10 is quite close while the slope error remains relatively small. Above a value of CV_a of roughly 10%, the χ^2 confidence intervals begin to show a noticeable deviation from the expected values; at this point, however, the observed and calculated values of S_{LOD} still largely agree. The final two runs, however, show a marked departure of the observed S_{LOD} from the value predicted by eqn. 4.10; this is due to the approximate nature of the propagation of errors approach since the LOD estimate is non-linearly related to the slope value. Note that at higher values of CV_a, the $2S_{LOD}$ intervals seem to perform better than the χ^2 intervals, since the

Table 2

Generic case: effect of increasing σ_b (homogenous variance)

σ_b	CV_a	LOD estimate[a]	LOD calc'd[b]	χ^2 intervals[c]		$2S_{LOD}$ intervals[d]	
				lower	upper	lower	upper
1	1.6%	2.98 0.39	3.00 0.40	2.5%	1.5%	0.6%	5.4%
2	3.2%	5.97 0.77	6.00 0.81	2.7%	1.7%	0.1%	4.2%
3	4.7%	8.91 1.20	9.00 1.13	3.5%	1.3%	0.3%	3.2%
5	7.9%	14.92 2.38	15.00 2.30	5.9%	3.6%	0.8%	6.0%
7.5	11.9%	22.72 3.97	22.50 3.98	8.7%	4.8%	0.8%	5.8%
10	15.8%	30.63 6.31	30.00 6.17	12.5%	6.0%	0.7%	5.4%
12.5	19.8%	38.94 11.31	37.5 8.9	16.9%	10.0%	0.7%	8.1%
15.0	23.7%	49.74 47.40	45.0 12.2	21.3%	13.1%	1.3%	8.9%

[a]calculated with eqn. 4.2 for each loop. First number in each entry is the average of 1000 loops; second is the observed standard deviation.

[b]theoretical values calculated with eqns. 4.1 and 4.10.

[c]The χ^2 confidence intervals are calculated for each loop from the χ^2 tables with 29 degrees of freedom and α = 2.5% on either side.

[d]95% intervals calculated using eqn. 4.10 and eqn. 4.2 for each loop.

CV_a term in eqn. 4.9 begins to become more important. In the next section there will be more discussion on the two types of intervals.

Effect of Increasing Number of Blank Measurements

For this next set of simulations using the generic model, the value of CV_a was kept at about 3% while N, the number of blank measurements, was increased. The results are shown in table 3; the calculated S_{LOD} in the third column is the average of the 1000 estimates for each value of N in the first column. It appears that for all values of N, the variability of the LOD estimate is well predicted by eqn. 4.10. One aspect of table 3 is immediately obvious: the LOD estimates shown in column two are all negatively biased compared to the true LOD values listed in the third column. Upon examination of eqn. 4.2, however, the bias in the LOD estimate is perfectly logical, since the sample standard deviation is a biased estimator of the population standard deviation (although the sample variance is unbiased) [92]. Thus, *the calculated LOD is a biased estimator of the true LOD* of the analytical procedure. The bias is worse with fewer degrees of freedom; this is one reason for choosing a relatively large number of blank measurements to calculate s_b. However, the bias was small relative to the value of S_{LOD} at any value of N used; hence, the decrease in S_{LOD} with increasing N is still the biggest motivation for a large number of blank measurements when estimating the LOD.

The confidence intervals obtained here with the χ^2 distribution are superior to those obtained by assuming a normal distribution of the LOD estimate; however,

Table 3

The effect of increasing numbers of blank measurements on LOD estimates (CV_a kept at 3%)

N	LOD estimate[a]	LOD calc'd[b]	χ^2 intervals[c]		$2S_{LOD}$ intervals[d]	
			Lower	Upper	Lower	Upper
3	5.37 2.74	6.00 2.69	1.7%	2.2%	0.0%	21.5%
5	5.60 2.02	6.00 1.99	2.4%	2.2%	0.0%	16.5%
10	5.82 1.29	6.00 1.38	1.9%	1.6%	0.0%	7.5%
15	5.88 1.11	6.00 1.13	2.3%	1.4%	0.2%	6.6%
20	5.96 0.95	6.00 0.98	2.5%	2.3%	0.2%	5.2%
30	5.96 0.76	6.00 0.80	2.9%	1.5%	0.5%	4.4%

[a]from eqn. 4.2.

[b]from eqns. 4.1 and 4.10.

[c]from χ^2 tables with N-1 degrees of freedom.

[d]from eqns. 4.2 and 4.10 for each loop.

the latter intervals become more acceptable as N increases to values of 15 or better. The performance of the confidence intervals based upon the normal distribution was at first puzzling; even when N or CV_a were increased to the point where the distribution of $\hat{LOD}$ was well characterized by a normal distribution (e.g., $N \geq 30$) the performance of the confidence intervals did not improve. In all cases, there was a larger fraction of cases where the true LOD value was larger than the upper confidence limit; at the same time, in very few cases was the true LOD value less than the lower confidence limit.

The distribution of the 1000 values of $\hat{LOD}$ with 30 blank measurements are shown in figure 18, along with a Gaussian distribution centered around the true LOD value and with a standard deviation predicted by eqn. 4.10. As can be seen, the deviation from a normal distribution is only slight. Indeed, values of the χ^2 distribution above 30 degrees of freedom are commonly calculated by assuming a normal distribution. And yet, there is asymmetry in *all* simulations when $2S_{LOD}$ confidence intervals are used -- the true LOD tends to be above the upper confidence limit more than expected. This behavior is all the more puzzling since the slight asymmetry shown in the figure is skewed to the right, and would tend to suggest that the opposite trend would prevail, i.e., the true LOD would be less than the lower confidence limits of the extra $\hat{LOD}$ values on the upper wing of the distribution.

The behavior can be understood by realizing that, as shown in eqn. 4.10, the estimated value S_{LOD} (and hence the size of the confidence interval) depends on the

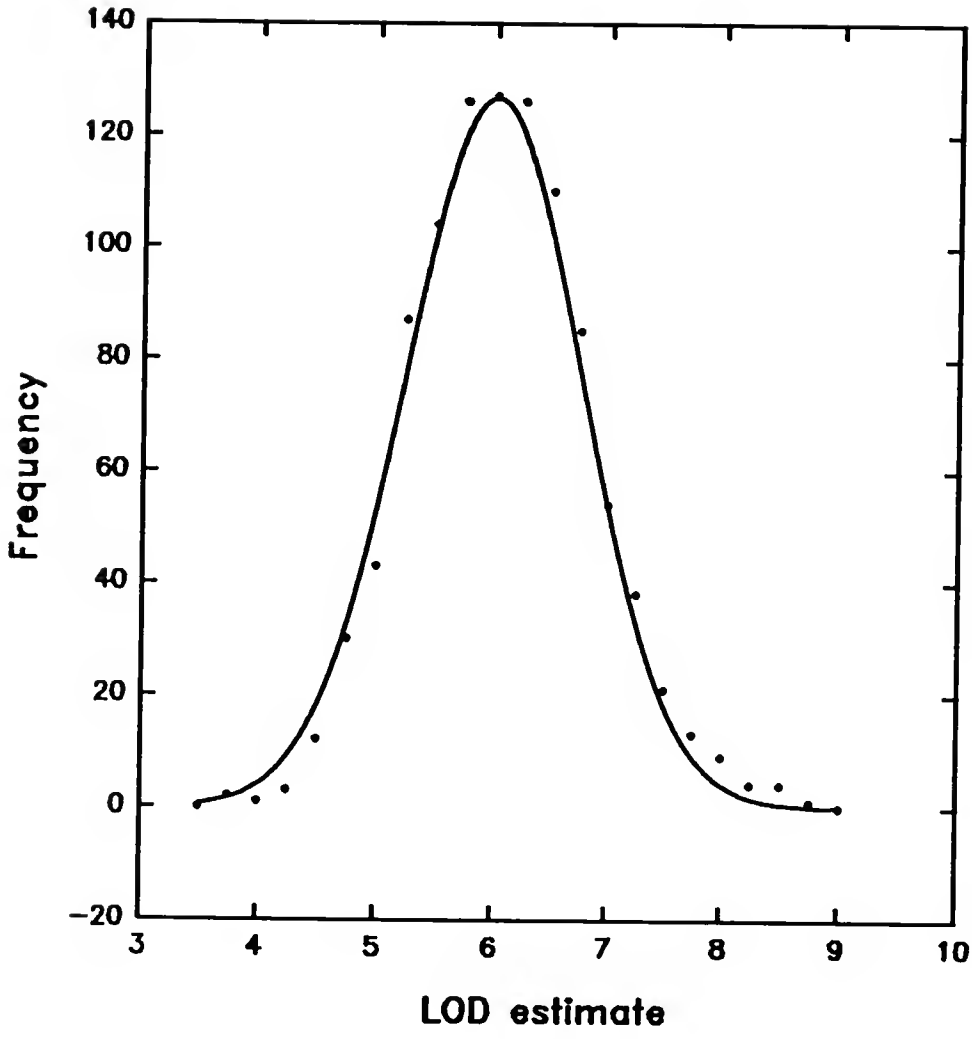

Figure 18. Histogram of calculated LOD values from 1000 calibration curves. The symbols represent observed frequency of LOD estimates with 30 blank measurements and CV_a = 3%. The curve is a normal distribution with μ = LOD and a value of σ_{LOD} calculated by eqn. 5.10.

magnitude of the estimated LOD. Remember that confidence intervals are constructed around the calculated value of $\hat{LOD}$; the true value of LOD is unknown. Values of $\hat{LOD}$ on the lower tail of the distribution in fig. 18 have smaller confidence intervals than the values on the upper tail; thus, a disproportionate number of values on the lower side of the distribution of $\hat{LOD}$ will have confidence intervals which do not include the true mean of the distribution (ie the true LOD). Likewise, values on the right wing of the distribution will have larger confidence intervals and a larger number of these values will include the true LOD value within the interval.

Using confidence intervals calculated from χ^2 tables gives the best confidence intervals in the cases shown in table 3; however, using $\hat{LOD} \pm 3S_{LOD}$ confidence intervals is almost certain (>99% from past experience) to contain the true value LOD, and may be more appropriate when the CV_a term is large, as can be seen in table 2. In addition, in some cases, very large values for N might be possible depending on the source of the limiting background noise; for example, if the background noise is not sample related but is due to, for example, laser scatter, s_b can be measured with very large degrees of freedom. In this case, as long as CV_a is low enough, the confidence interval can easily be calculated by using $3S_{LOD}$ limits from eqn. 4.10.

Application to ETA-LIF

There are two sources of noise on a given calibration point in any ETA experiment: noise due to variation of the signal (y-value) and noise due to imprecise

injection (variation in x-value). It is normally stated in any textbook on regression that least-squares estimation of the regression parameters assumes that there is no error in the x-axis. In many cases in analytical chemistry, it is assumed that errors in the independent variable are negligible compared to the range of this variable; hence, any random errors in the calibration standards are ignored. However, for some of the cases described here with ETA-LIF this assumption is not valid.

Berkson [93] has noted a special class of situations when errors in both variables can still be treated as a simple least-squares regression. When the x-variable can be controlled, then any random error in the independent variable can be attributed to an additional random error component in the dependent variable. Berkson's case has been discussed by Mandel [71] and Neter et al. [94] and should apply in this case even though the error is not constant but linearly proportional to the magnitude of the independent variable. Table 4 shows the magnitudes of the two error components -- due to signal shot noise and injection imprecision -- and the calculated and observed total noise in the signal at each calibration standard. Since the observed noise closely follows the calculated values, it appears that Berkson's model does indeed apply to ETA-LIF (when the error in the injected amount is randomly distributed about the expected value); additionally, it is obvious that shot noise in the signal is quickly overshadowed by the injection imprecision for the parameters used in this model.

Table 5 shows the results of the ETA-LIF simulation run under the three conditions described in the experimental section. The calculated value for S_{LOD}

Table 4

Observed and calculated noise on signal in ETA-LIF model; run 1(a) (10 standards, dark current limited)

Conc (pg)	Observed signal,noise (V)	Expected signal,noise (V)	Shot noise (V)	Conc flicker (injection) (V)
0.05	0.125 9.32×10^{-3}	0.125 9.24×10^{-3}	6.81×10^{-3}	6.25×10^{-3}
0.1	0.249 1.525×10^{-2}	0.250 1.575×10^{-2}	9.59×10^{-3}	1.25×10^{-2}
0.5	1.248 6.633×10^{-2}	1.250 6.603×10^{-2}	2.13×10^{-2}	6.25×10^{-2}
1	2.509 0.134	2.500 0.129	3.01×10^{-2}	0.125
5	12.499 0.623	12.500 0.629	6.71×10^{-2}	0.625
10	24.957 1.251	25.000 1.254	9.50×10^{-2}	1.250
50	125.10 6.16	125.00 6.25	0.212	6.25
100	250.40 12.67	250.00 12.50	0.300	12.50
500	1.252×10^{3} 62.474	1.250×10^{3} 62.504	0.671	62.50
1000	2.510×10^{3} 125.00	2.500×10^{3} 125.00	0.949	125.00

Table 5

Estimating LOD for Thallium in ETA-LIF

Case[a]	LOD estimate[b]	LOD calc'd[c]	χ^2 intervals[d]		$2S_{LOD}$ intervals[e]	
			lower	upper	lower	upper
1(a)	0.119 0.019	0.120 0.019	2.4%	2.0%	0.1%	5.6%
1(b)	1.343 0.216	1.367 0.219	2.4%	2.0%	0.4%	5.9%
2(a)	0.119 0.019	0.120 0.020	3.4%	1.6%	0.2%	4.9%
2(b)	1.351 0.218	1.367 0.221	2.8%	2.2%	0.4%	4.7%
3(a)	0.118 0.019	0.120 0.020	2.4%	2.5%	0.2%	4.9%
3(b)	1.352 0.223	1.367 0.224	3.6%	1.5%	0.4%	5.5%

[a]Case 1 uses weighted linear regression with 10 standards and the true weights known; case 2 uses only three standards and measures each 4 times to estimate the weights; case 3 only measures one standard four times to estimate the sensitivity. In all cases, (a) is dark current limited, and (b) is laser-induced shot noise limited (ie, due to scatter or fluorescence). See the experimental section for more details.

[b]from eqn. 4.2.

[c]from eqns. 4.1 and 4.10.

[d]from χ^2 tables with 19 degrees of freedom.

[e]from eqns. 4.2 and 4.10 for each loop.

shown in the third column is the average of the individual estimates of each of the 1000 calibration curves. It is easily seen that eqn. 4.10 predicts the observed variation in the LOD estimate quite well; by examining the relative magnitudes of the terms in eqn. 4.9, in all cases, the first term dominates, and the variation in LOD is caused for the most part by the imprecision in the s_b estimate (N = 20 in all simulations here). This fact is taken advantage of in the final case (3a and 3b): only one standard is measured to estimate the sensitivity of the method with no loss in efficiency of the LOD estimate. Thus, when changing various parameters of the analytical system (e.g., laser excitation lines used, monochromator slit width, etc.) to improve the LOD, only one standard need be measured to calculate the new LOD with no loss in precision of the estimate, as long as it is known that the calibration function is linear up to the standard used.

All of the above calculations of $\hat{LOD}$ have used the IUPAC recommendation for the confidence factor (i.e., k = 3). It is instructive to compare the true LOD of the ETA-LIF model using k=3 with the "calibration band" approach of calculating the detection limit, depicted in fig. 4 in chapter 2, and using a confidence factor given by eqn. 2.16. For run 2(a) (only three standards in the calibration set), calculation of the confidence factor according to eqn. 2.16 gives the true value of LOD at 0.16 fg, as opposed to 0.12 fg. However, the value of S_{LOD} calculated was 0.02, and the upper tolerance limit (2σ) is 0.16 fg -- i.e., 95% of the values of calculated LOD estimates using k = 3 will be in the interval 0.08-0.16 fg. Clearly, ignoring the variation in $\hat{LOD}$ (due in this case to the variation in s_b) is at least as serious as

ignoring the calibration error. Actually, using only three standards has magnified the confidence factor using the "calibration band" approach; with a larger number of standards in a calibration curve with ETA-LIF, the value of σ_{LOD} will easily overshadow the calibration error. It should be emphasized that even when using different values of confidence coefficients eqns. 4.9 and 4.10 are still valid indicators of the variability of the calculated LOD due to the imprecision in the sample estimators.

Conclusions

In this chapter, the effect of two parameters (the estimated sensitivity and blank standard deviation) on the quality of the calculated $\hat{LOD}$ as an estimator of the true (unknown) LOD has been investigated. When optimizing or comparing analytical techniques by using the value of $\hat{LOD}$, it is necessary to be aware of these factors; in addition, when quick estimates of the LOD are needed during optimization, judicious and careful use of eqns. 4.9 and 4.10 allow an evaluation of the quality of the estimate.

It cannot be overemphasized that the fluctuations in the LOD estimate as presented in this chapter, and chapter 4, are due solely to the imprecise nature of the sample statistics s_b and a_0 for the background noise and analytical sensitivity, respectively. Long-term drift, day-to-day or even hourly fluctuations in the population parameters themselves could certainly account for a much larger variation in calculated LOD values for a given analytical procedure. However, there is clearly

value in knowing the estimated magnitude of S_{LOD} as discussed in this chapter since the two sources of variation can be separated, in addition to assessing the effect of the measurement protocol used to estimate the LOD on S_{LOD}.

CHAPTER 8
INVESTIGATING THE PROCESS OF SINGLE ATOM DETECTION WITH LASER-INDUCED FLUORESCENCE

Introduction

The purpose of this chapter is to illustrate the concepts of SAD presented in chapter 5 for the case of detection by cyclic LIF. Detection by cyclic LIF is an example of a nondestructive detection method; the advantage of a technique based on nondestructive detection is that SAD is possible even in the presence of noise. The general outline of the computer simulations used in this chapter were presented in chapter 6; the full program used to generate the raw data, as well as the signal processing methods used and the algorithm for generating random numbers according to a Poisson distribution, is presented in the Appendix.

In all simulations in this chapter, unless noted, T_m = 8000 units and t_r = 20 units.[1] All times (and corresponding mean flux values) given in this chapter are in terms of arbitrary time units. To provide a basis of comparison for possible SAD methods based on flowing atoms/molecules through V_p, it has been reported that τ_r = 10-100 μs for atomic beam experiments [63, 76] and τ_r = 1-10 ms for SAD experiments with flowing solutions [66, 68].

[1]or τ_r = 20 units for the Cylindrical V_p model

The first sections of this chapter will illustrate a few of the more basic concepts of SAD from chapter 5. The basic idea of ϵ_d will be presented for the intrinsic-limited case, and then SAD in the presence of noise will be illustrated. In addition, the precision of counting atoms will be calculated theoretically and compared to observed values from the computer simulations. Finally, the consequences of a variable t_r will be demonstrated through the use of computer simulations based on the Cylindrical Probe model. For the demonstration of these concepts, all considerations regarding the entry times of atoms into V_p, and the detection times of individual photoelectrons, were ignored. This situation would be found, for example, if the simple integration method was used, in which the total number of counts during T_m were taken as the signal. All values of X_d, ϕ_s, and ϕ_b quoted in these sections will be based on simple integration as the signal processing method, with T_m = 8000 and t_r = 20 units. Another possible scenario where detection times and atoms' entry times into V_p would be unimportant is when a pulsed dye laser (pulse lengths 10-100 ns) where used (since $t_i << \tau_r$); in such cases, t_i would be the pulse duration and the number of photoelectrons from each laser pulse would be measured.

The application of SAD theory to the task of monitoring atoms/molecules flowing through V_p by CW-LIF will be demonstrated through the use of the full computer simulations to generate raw data files (which consist of the detection times of photoelectrons, which are due to either atoms passing through V_p or due to background noise). The photon burst and sliding sum signal processing methods will

be used on the data, and compared. In addition, the effect of T_m -- the "scope" of the SAD method -- will also be illustrated through these simulations.

Detection Efficiency at the Intrinsic Noise Limit

If the value of ϕ_b is so low that $\mu_b \leq \alpha$ during the desired T_m then there is no reason not to simply integrate the signal over T_m. For T_m = 8000 units this would correspond to $\phi_b \leq 1.75 \times 10^{-7}$ counts (unit time)$^{-1}$ for $\alpha \leq 0.0014$. At the intrinsic noise limit, the value of X_d is 1 single count during T_m. Table 6 presents the observed detection efficiency, ϵ_d, for various values of ϕ_s; the Simple Model was assumed, with constant ϕ_s, and t_r = 20 units. The value of N_p was fixed at 1 atom for 8000 measurements; when the signal was at least one count then the atom is "detected" during T_m.

This simulation represents a test of the Poisson number generator as much as an illustration of SAD at the intrinsic limit. Table 6 presents the expected and observed values of ϵ_d, $\bar{i}_s$, and σ_t. As expected for a Poisson detection process, the observed mean and variance of the signal due to the single atoms are almost equal for all values of ϕ_s. SAD is achieved at the 95% confidence level if $\bar{i}_s$ = 3 counts/atom, and at the 99.86% confidence level if $\bar{i}_s$ = 6.6 counts/atom, as predicted from table 1 and eqn. 5.19. It is important to realize that the detection of individual atoms is possible for all these conditions; the value of ϵ_d as a measure of the effectiveness of a near-SAD technique is clearly illustrated.

Table 6

Detection Efficiency at the Intrinsic Limit

Sensitivity		Observed		Detection efficiency	
True mean (count/atom)	ϕ_s[a]	average (count)	variance $(count)^2$	expected	observed
0.1	0.005	0.0853	0.0852	9.52%	8.16%
0.5	0.025	0.5124	0.5149	39.35%	39.99%
1.0	0.050	1.0090	1.0105	63.21%	63.33%
3.0	0.150	3.0093	2.9628	95.02%	95.28%
6.6	0.330	6.6526	6.4640	99.86%	99.84%
9.0	0.450	8.9946	8.8835	99.99%	99.99%

The value of X_d for the above table is 1 count; an atom is "detected" if a signal of at least one count is detected when N_p = 1 atom. The value of ϕ_s assumes t_i = 20 time units. The values of the expected detection efficiency are taken from Poisson distribution tables.

[a]The signal flux has units of count $(atom)^{-1}$ $(time\ unit)^{-1}$

SAD in the Presence of Noise

Once the level of noise during T_m becomes significant, then the value of X_d must increase to keep the probability of false positive at the desired level. The inefficiency of the simple integration signal processing method in the presence of noise has already been mentioned; two alternative methods will be illustrated later in this chapter. However, if ϕ_b is still fairly low, and discrete samples are analyzed (low values of T_m), then the simplicity of the method may be desirable. The process of detecting single atoms in the presence of noise with simple integration is illustrated in table 7 for various values of ϕ_s and X_d, assuming the Simple Model with integration over T_m = 8000 units and with t_r = 20 units. All values of X_d, X_g, α and ß shown in the table are taken from tables of the Poisson distribution [86]. Detection at two different significance levels are illustrated, represented by the two different pairs of values for X_d and X_g for each noise level. In the first row of value of μ_b, α and ß are chosen to be approximately 5%, while these probabilities are kept around 0.14% for the second row.

Choosing the signal detection limits, X_d and X_g: The signal detection limit, X_d, for a given noise level is chosen so as to keep the probability of false positive during T_m (denoted by α) below a pre-defined level. However, due to the discrete nature of X_d, it is not possible to choose α at any level, since α takes on discrete values for different X_d. The exact values of α for the chosen X_d are shown in the fourth column in the table. The nature of choosing X_d at low levels of noise is clearly indicated: it is rarely possible to choose α to be exactly the value desired (5%

Table 7

Detection and guaranteed detection of atoms
in the presence of noise

μ_b	ϕ_b	X_d	α	X_g	β	Observed ϵ_d	
						$\phi_s t_i = X_d - \mu_b$	$\phi_s t_i = X_g - \mu_b$
1	0.00125	4	1.90%	7.8	4.85%	57.19%	95.58%
		6	0.06%	16	0.14%	54.78%	99.88%
2.5	0.00313	6	4.20%	10.5	5.04%	55.55%	94.94%
		9	0.11%	21	0.11%	54.93%	99.93%
5	0.00625	10	3.18%	16	4.33%	54.68%	95.50%
		14	0.07%	28	0.13%	52.79%	99.89%
10	0.01250	16	4.87%	23	5.20%	54.10%	94.29%
		22	0.07%	39	0.12%	52.30%	99.95%

All units are in counts, except for ϕ_b, which is in counts (time unit)$^{-1}$.

or 0.14%); instead, upper tolerance must be defined, and α chosen to be below these levels. Naturally, similar considerations hold for X_g and ß; the value of X_g (which is defined in terms of X_d by the procedure outlined in chapter 5) is chosen so that ß is as close to the desired value as possible.

When the sensitivity of the technique was such that the signal distribution was centered at X_d (S/N $\approx$ 2-3), the observed detection efficiency values at the various levels of noise were those given in column six in the table. Due to the asymmetry of the Poisson distribution, the expected value of ϵ_d is slightly higher than 50%. It is obvious that true SAD, as defined in chapter 5, is not achieved at these sensitivities. On the other hand, when the sensitivity is such that the mean of the distribution of I_t is exactly X_g, then the expected value of ϵ_d is 1-ß (required for SAD); comparison of the values of ß and the observed ϵ_d show that this was indeed the case.

Counting Precision

Counting at the Intrinsic Limit

The difference between the signal measurement precision, RSD_m, and the counting precision, RSD_c, when a given number of atoms pass through V_p during a measurement, was illustrated in figures 13 and 14 in chapter 5. Calculation of the theoretical value of RSD_c, for fixed values of N_p, $\bar{i}_s$, and μ_b, is represented by eqns. 5.21-5.24. The theoretical values are computed in the case of Poisson distribution of I_t with a simple computer program, since the manual computation can be rather

tedious. Particularly, the minimum value of the sensitivity necessary to achieve a certain pre-defined counting precision, is of interest as a comparison to the sensitivity necessary for SAD.

A computer simulation can be used to compare the observed value of RSD_c with the theoretically calculated values, since in a computer simulation the number of atoms probed can be held constant for any number of measurements. In the simulations, the measured number of atoms, N_m, are computed for each measurement according to eqn. 5.21; the standard deviation of N_m is then used to calculate the observed value of RSD_c and comparisons to the theoretical value can be made. Table 8 shows the results of 8000 measurements at the intrinsic limit for various values of $\bar{i}_s$ and N_p, along with comparisons to the theoretical values for both RSD_c and RSD_m.

A number of interesting observations can be made from table 8. First of all, in all cases the observed and calculated values of RSD_c agreed very well. The column with a sensitivity of 6.6 counts/atom represents the requirement of SAD at the 0.14% confidence level; clearly, RSD_c is higher than 0.1 (the desired precision) for $N_p < 16$ atoms. This observation illustrates that fact that a sensitivity which is necessary to achieve SAD may not be sufficient to count any number of atoms with precision; at lower analyte concentrations the counting precision is quite high.

Another interesting observation involves the difference between RSD_m and RSD_c. As predicted by eqn. 5.20, the value of RSD_m decreases as N_p increases. However, the values of RSD_c at low numbers of probed atoms is markedly different

Table 8

Counting precision, RSD_c, at the intrinsic limit: comparison of theoretical and observed values

N_p	Sensitivity (counts/atom)											
	6.6			34			35			100		
	RSD_m	RSD_c		RSD_m	RSD_c		RSD_m	RSD_c		RSD_m	RSD_c	
		Obs	Calc		Obs	Calc		Obs	Calc		Obs	Calc
1	.389	.339	.366	.171	.054	.049	.169	.051	.052	.100	.000	.000
2	.275	.293	.294	.121	.099	.099	.120	.095	.095	.071	.012	.010
3	.225	.238	.238	.099	.102	.101	.098	.099	.099	.058	.019	.021
4	.195	.211	.212	.086	.096	.095	.085	.093	.093	.050	.026	.028
5	.174	.184	.185	.077	.088	.088	.076	.086	.086	.045	.033	.032
10	.123	.127	.128	.054	.061	.061	.053	.061	.060	.032	.034	.034
15	.101	.103	.103	.044	.048	.048	.044	.047	.048	.026	.030	.030
20	.087	.089	.089	.038	.041	.041	.038	.040	.040	.022	.026	.026

from the expected RSD_m, and increases to a maximum value before once again decreasing with increasing N_p. From both the calculated values of RSD_c and the simulations, the value of $(\bar{i}_s)_c$ necessary for $RSD_c \leq 0.1$ is approximately 35 counts/atom at the intrinsic limit. This value is roughly 5-6 times the necessary sensitivity for true SAD.

Finally, the comparison of RSD_m and RSD_c at 100 counts/atom is interesting since this is the sensitivity predicted for precise counting on the basis of RSD_m only. As was illustrated in figure 13, the counting precision at this sensitivity is much greater than predicted by RSD_m for small numbers of atoms, since the overlap between distributions of different values of N_p is slight.

Counting in the Presence of Noise

The presence of increasing levels of background noise during T_m will tend to broaden the signal distributions, I_t, for fixed values of N_p; hence, it is expected that RSD_c will increase as well for a given sensitivity at the analyte concentration level. Table 9 reflects the increased signal variance in increased levels of $(\bar{i}_s)_c$ necessary to achieve precision counting at the same levels of μ_b as shown in table 7. It is interesting to note, through comparison of tables 7 and 9, that the value of $(\bar{i}_s)_c$ does not increase nearly as quickly as the minimum sensitivity required for SAD in the "simple integration" case.

Table 9

Counting precision in the presence of noise

μ_b (counts)	$(i_s)_c$ (counts/atom)	N_p (atoms)	RSD_c	
			Calc'd	Observed
1	35	3	0.0995	0.1001
2.5	36	3	0.0982	0.0985
5	37	3	0.0976	0.0991
10	39	2	0.0969	0.0940

The minimum sensitivity (counts/atom) -- both theoretical and observed values -- needed to precisely count atoms at all levels is given above. The value of RSD_c and the corresponding N_p represent the most imprecise counting levels.

"Extra" Variance in the Cylindrical Probe Model

In the discussion thus far, it has been assumed that ϕ_s and t_i were both constant for all atoms which enter V_p. However, variance in either of these two parameters results in "extra" variance in the total signal distribution, I_t, as predicted in eqn. 5.13. Simulations based on the Cylindrical V_p model were specifically formulated to investigate this process by making the residence time, t_r, a variable depending on the path of the atom through the cylindrically-shaped probe volume. In such a situation, the total variance of the signal, σ_t^2, is given by

$$\sigma_t^2 = \bar{I}_t + (N_p\phi_s)^2\sigma^2(t_i) \qquad [8.1]$$

A simulation based on the Cylindrical V_p model at the intrinsic limit (simple integration of signal over T_m) was run 8000 times for several values of τ_r for $t_i = t_r$ (CW-LIF) and ϕ_s = 1 count (atom)$^{-1}$ (time unit)$^{-1}$. Table 10 shows the results of the simulations. The observed values s_t^2 and $s^2(t_r)$ are given in the table; the value of $s_2(t_r)$ was used as an estimate for $\sigma^2(t_r)$ in eqn. 8.1 to calculate the expected total signal variance. The calculated values of σ_t^2 compare very well to the observed values for all simulations. There was good agreement for simulations with varying levels of N_p and ϕ_s as well (although the results are not shown here).

The larger signal variance due to variation in t_r can be clearly seen in figure 19 for 8000 loops of the simulation with values of $\bar{i}_s$ = 12.35 counts/atom and N_p = 1 atom. The observed distribution of I_s (intrinsic case) and the Poisson distribution which would be expected with fixed t_r are shown in the figure.

Table 10

Comparison of observed and calculated signal variance for the Cylindrical V_p model

Signal average (counts)	Total Signal Variance, σ_t^2		Residence Time, t_r	
	observed	calculated	average	variance
1.00	1.05	1.08	1.00	0.08
2.53	3.04	3.05	2.51	0.51
4.98	6.93	6.98	4.99	2.01
7.44	11.70	11.95	7.47	4.54
10.09	17.99	18.20	10.00	7.97
15.02	33.49	33.35	15.01	18.32
19.92	51.55	52.00	19.91	32.06
50.37	246.02	246.36	50.26	195.18

The value of ϕ_s was held constant at 1 count $(atom)^{-1}$ $(time\ unit)^{-1}$. The units of t_r are arbitrary time units.

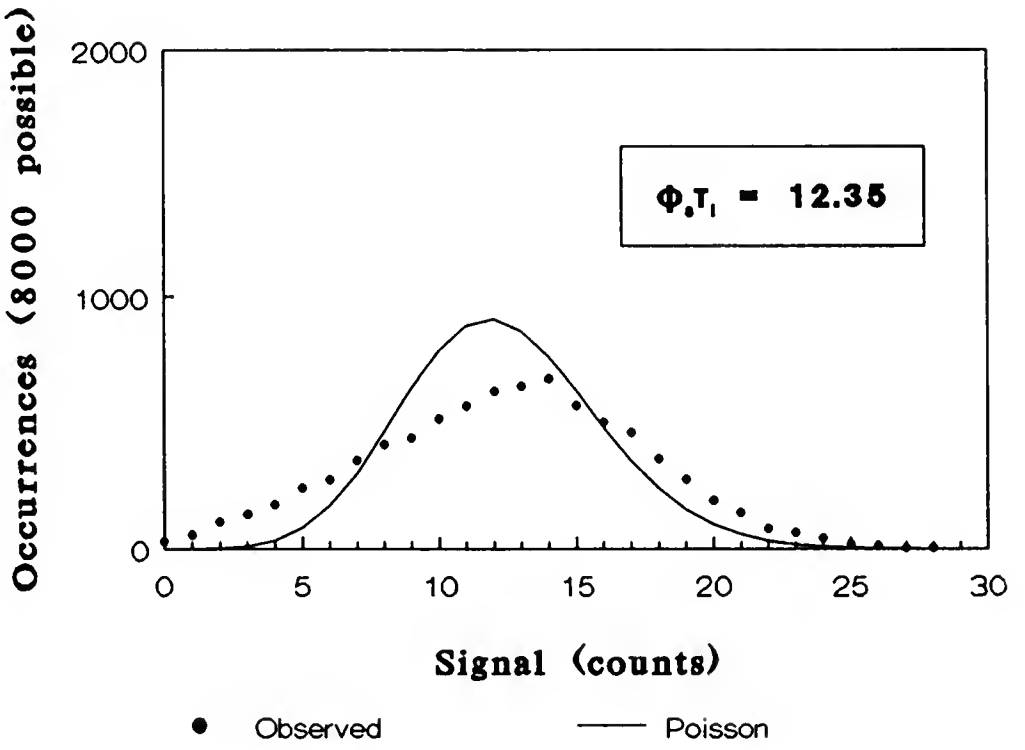

Figure 19. Comparison of the observed signal distribution I_t with $N_p = 1$ (8000 measurements) for the Cylindrical Probe Model with the Poisson distribution which would be expected for the same S/N level for the Simple Model.

The consequences of variable t_i can be easily understood from eqn. 8.1 in light of the discussion of ϵ_d and RSD_c thus far. Obviously, an increased variance would decrease ϵ_d and increase RSD_c, the latter particularly since the total signal variance is proportional to N_p^2. A high enough sensitivity to result in a true SAD technique for constant t_i would perhaps not be high enough if the value of $\sigma^2(t_i)$ were large; in addition, since σ_t^2 is proportional to ϕ_s^2, it might be that a rather large improvement in sensitivity would be necessary to achieve SAD. A more effective method of achieving SAD might be to decrease the "extra" variance term by decreasing $\sigma_2(t_i)$, even at a cost to S/N. Finally, the value of ϵ_d as a FOM for near-SAD methods is even more clear, since S/N does not reflect this "extra" variance. For example, the two distributions in fig. 19 each possess the same S/N ratio; if the noise level were such that X_d = 5 counts, then the detection efficiency of the Poisson-distributed I_t would be significantly higher than due to the Cylindrical V_p model.

Continuous Monitoring of Atoms with CW-LIF

The scope of an SAD method in the presence of noise is represented by the value of T_m over which it is possible to detect single atoms at the required detection efficiency. Earlier in this chapter, it was seen that, when the simple integration method is used, the required sensitivity necessary for SAD increased rapidly as ϕ_b was increased (table 7). However, since individual atoms have residence times much less than T_m, it is not surprising that the sensitivity required for SAD increases so rapidly with relatively small increases in ϕ_b.

The rest of this chapter will be concerned with monitoring atoms under the following conditions: T_m = 8000 time units, t_r = 20 units, and ϕ_b = 0.05 counts/time unit. This background level results in an average of 400 counts over T_m in the simple integration method, and a sensitivity of approximately 130 counts/atom would be necessary for SAD at the 0.1% confidence level. This is obviously a very inefficient way to detect single atoms which interact with the laser during T_m. In chapter 5, three alternative signal processing methods based on the application of a "time window", t_w, of a size comparable to t_r, were described. Two of these methods, the photon burst and the sliding sum signal processing methods, will be demonstrated for the case of near-SAD methods based on CW-LIF to detect single atoms during T_m under these conditions.[2]

The Photon Burst Method

False positives with the photon burst method; choice of X_d

The theoretical value of α for the photon burst method, for a given level of background noise, ϕ_b, can be calculated from eqns. 5.25-5.28 if the form of the distribution of I_b is well characterized. In any event, many measurements of the blank can be used to estimate the probability of type I error at any value of X_d. Table 11 shows the comparison of the observed and theoretically calculated average number of false positives during T_m for the case of a Poisson-distributed background

---

[2]The Simple model will be assumed. The effects of variation of either ϕ_s or t_i would be reduced values of ϵ_d, as discussed earlier.

(i.e., shot noise limit). The agreement between the two sets of values is satisfactory at all values of X_d. It is important to notice two significant facts:

1. The "scope" of the SAD method is still an issue; i.e., the correct value of X_d may change as T_m increases. With $t_w = t_r$, the average background count in the time window is approximately 1 count. A value of $X_d = 5$ counts would be sufficient for only one application of the time window -- i.e., $T_m = t_r$: guaranteed detection of an atom (SAD) during its transit time through the laser beam. However, even with a method based on a time window such that $t_w = t_r$, a larger value of X_d is still necessary for larger values of T_m. If $X_d = 5$ counts was still used with $T_m = 8000$ units, then a single atom could never possibly be detected against the average of 3.6 false positives due to the background noise.
2. The difference between the simple integration method and the photon burst method is striking. At $\phi_b = 0.05$, increasing X_d to 9 counts is all that is necessary to reduce the probability of false positives back to approximately the 0.1% level. Compare this value to the much higher values of X_d given above, or given in table 7 with much lower values of ϕ_b.

Detection of single atoms

Simulations of CW-LIF according to the general outline given in chapter six were performed to construct the raw data file; the photon burst method was then used on this array of detection time of photoelectrons during T_m. The value of N_p was fixed at 1 atom for every measurement -- in other words, one single atom

Table 11

Calculated and observed false positives
using the "photon burst" signal processing method

X_d (counts)	Average number of false positives	
	observed	calculated
5	3.628	3.797
6	0.693	0.73195
7	0.107	0.11881
8	0.014	0.01663
9	0.001	0.00203

Distribution of background counts is Poisson. Conditions of measurements: T_m = 8000 time units; t_w = 21 time units; ϕ_b = 0.05 counts/unit time. The observed number of false positives is the average of 1000 measurements.

entered and exited V_p sometime during T_m. During the course of a measurement, a burst was considered "detected" if there were at least 9 counts in the burst; it has already been established that it is very unlikely that the background noise level would cause a burst to be detected at this level during T_m.

Table 12 shows the expected and observed results for 1000 measurements at two different sensitivity levels. The distribution of the number of detected bursts from the 1000 measurements are shown, along with the expected values. The first sensitivity level results in SAD if $T_m = t_r$ -- i.e., the atom would always be detected during its transit through V_p. The use of this sensitivity in the simulation clearly demonstrates the limited scope of SAD at that sensitivity: even though SAD at this sensitivity is possible with $T_m = t_r$, SAD is not possible at this increased value of T_m. The second sensitivity corresponds to the value of X_g with $X_d = 9$ counts ($\beta = 0.1\%$), and would result in near-certain detection of the atoms in all 1000 measurements if the burst values followed a Poisson distribution.

In comparing the expected and observed values it appears that the value of ϵ_d is somewhat less than expected for both cases, and there are a number of cases of "double counts," in which there are two detected photon bursts rather than the expected one due to N_p alone. The expected number of false positives is expected to be very low (1-2 for 1000 measurements), as has already been established. Thus, the double bursts must both be due to the presence of the analyte atom in some manner.

Table 12

Simulations of CW-LIF with photon burst signal processing:
Distribution of detected photon bursts

Number of "detected" photon bursts	ϕ_s[a] = 0.665		ϕ_s[a] = 1.000	
	Observed	Expected	Observed	Expected
0	102	53	7	1
1	862	947	867	999
2	36	0	124	0
3	0	0	2	0

Conditions: Simple Model (fixed ϕ_s and t_r) with T_m = 8000 time units, t_r = 20 time units, t_w = 21 time units, X_d = 9 counts. A photon burst must have a sum of at least 9 counts to be "detected" above the noise. One thousand measurements were taken.

[a]units of ϕ_s are: counts $(\text{atom})^{-1}$ $(\text{time unit})^{-1}$.

Figure 20 explains the discrepancy in both ϵ_d and double peaks. The upper portion of the figure was used to first explain how the photon burst method works in chapter five. Obviously, in the particular situation shown in fig. 20(a), if the sensitivity is high enough for SAD, then the probability is high that this particular burst would be detected since t_w contains all the detected photons due to the atom. However, a single spurious background count can result in the splitting of the photon burst due to the analyte atom; an example is shown in fig. 20(b). In the figure shown, the signal due to the atom is spread out over two separate bursts due to the single noise count. In such situations, depending on the number of signal photons emitted and the exact positioning of the time windows, there is a possibility that either both bursts containing the signal are detected, or that neither one is. At higher sensitivities (i.e., very near to SAD conditions), then it is more likely that the divided signal will result in a "double count" than in no detected burst at all; on the other hand, at lower sensitivities, there is a greater chance that the analyte atom is not detected at all. The results shown in table 12 reflect both of these trends.

Thus, the use of the photon burst method comes with these complications. The effect of the "double counts" may not be too critical if the analyte concentration is so low that it is unlikely that two analyte atoms enter V_p so close together. In such a situation, it might be assumed that two closely-spaced bursts such as represented in the figure were due to single atoms. However, the problem becomes worse with both increased noise and increasing analyte concentration.

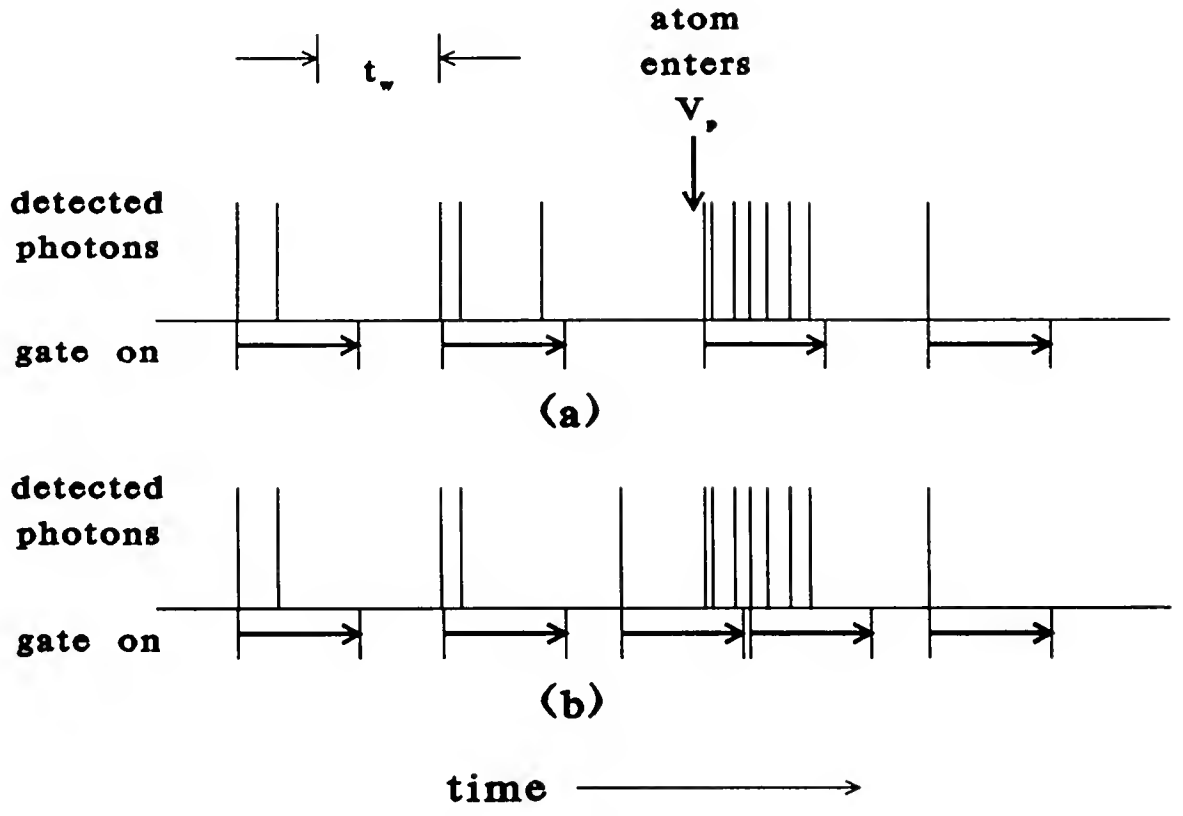

Figure 20. Possible complication with photon burst method.
(a) normal operation of photon burst, in which a single burst contains the entire signal emitted by an analyte atom.
(b) complication: splitting of the emitted burst from an atom due to the background noise count.

Sliding Sum: Peak Height Detection

False positives

The number of false positives -- the number of sliding sum peaks with peak heights of at least X_d counts -- are very similar to the corresponding values in the photon burst method. For larger values of X_d, the Gamma distribution can be used to calculate the theoretical value of α, but the method is somewhat tedious and is only an approximation. Experimental determination of α is the best method to set X_d. With X_d = 5 counts, an average of 4.621 false positives were observed with 1000 measurements at ϕ_b = 0.05 counts/time unit and t_w = 21 time units; this value is slightly higher than the corresponding photon burst level. At X_d = 9 counts, the calculated value of α is 0.00372; there were three false positives observed in 1000 measurements when X_d was set at this level. This value of the signal detection limit was used for the sliding sum signal processing.

Detection of single atoms

One thousand measurements with N_p fixed at 1 atom were run at the same two sensitivity values as was used for the photon burst method. The results and expected values (same as in photon burst case) are given in table 13. Unlike in the case of the photon burst method, there seems to be no problem with decreased values for ϵ_d, indicating that peak heights tend to follow a Poisson distribution. In the case of the higher sensitivity, however, there are still a few double counts. In almost all cases, these extra peaks were found to be due to a "shoulder" on the peak due to the analyte atom, in which the value fell below X_d and then increased again

Table 13

Simulation of CW-LIF with sliding sum signal processing
Distribution of detected peaks

Number of "detected" sliding sum peaks	ϕ_s[a] = 0.665		ϕ_s[a] = 1.000	
	Observed	Expected	Observed	Expected
0	58	53	1	1
1	942	947	983	999
2	0	0	16	0
3	0	0	0	0

Conditions: Simple Model (fixed ϕ_s and t_r) with T_m = 8000 time units, t_r = 20 time units, t_w = 21 time units, and X_d = 9 counts. Sliding sum peak heights of 9 counts or higher are considered "detected." One thousand measurements were taken.

[a]units of ϕ_s are: counts $(atom)^{-1}$ $(time\ unit)^{-1}$.

due to a single background count outside of t_r. In these cases it was obvious that the peak was due to only a single atom present in V_p, and the double counts were more an artifact of the signal processing algorithm used to count "detected" peaks.

Unlike the photon burst method, the sliding sum peak maxima can be easily used to form a picture of the signal distribution due to single analyte atoms. If the analyte concentration is kept very low, then it is unlikely that there are two atoms in V_p at any one time. In such a situation, all the sliding sum peak maxima at or above X_d will be due to single atoms. At the peak maximum, t_w will be centered so that the window contains t_r, so that the distribution of maxima at or above X_d provides insight into the distribution of I_s. Figure 21 shows such a distribution for a simulation of a near-SAD CW-LIF method: $\bar{i}_s$ = 9 counts/atom, μ_b = 1.05 counts during t_w, so that the distribution of peak maxima should have a Poisson distribution (the Simple model was used) with a mean of 10.05 counts. Both the observed and expected distributions are shown in the figure, and match quite well. In a normal experiment, the use of curve fitting techniques applied to this distribution of heights may make it possible to obtain estimates of both $\bar{i}_s$ and σ_t.

Sliding Sum: Peak Area Detection

The possibility of using peak areas of sliding sum peaks rather than peak heights was discussed in chapter five. Although the use of peak areas will not be demonstrated with the computer simulations, the possibility should be included as a brief discussion. It may seem intuitively more obvious to use peak height detection

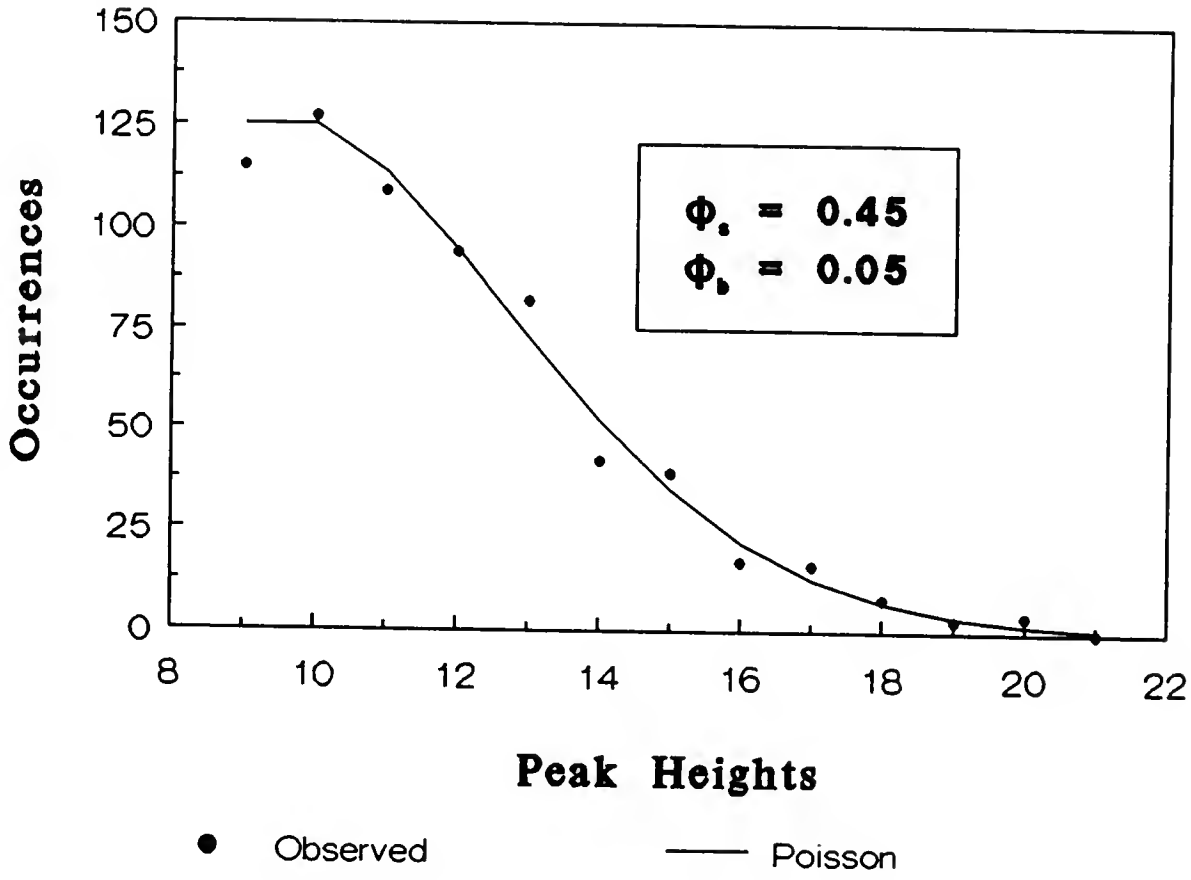

Figure 21. Distribution of sliding sum peak heights due to single atoms above the detection limit. The theoretical Poisson distribution of detected photons above X_d is also shown.

of the raw data transformed by the sliding sum signal processing method, but in actual fact there is no loss in information when using the peak areas as the signal rather than peak heights (see eqn. 5.29), and there is one important advantage to be gained, which will now be addressed.

As with the photon burst method, the peak height method suffers when there is overlap between atoms residing in V_p. In such a situation, it is not easily to count the atoms which pass through V_p. The advantage gained by using the peak areas rather than their heights is that atoms with overlapping residence times within V_p can be easily treated; the total area due to the peak encompassing both atoms is due to the total sum of the signal due to the atoms. In such cases, the total number of atoms which contribute to a given peak is calculated by equation 5.21 for N_m; all the concepts of the counting precision, RSD_c, also apply in this situation.

Note that as the analyte concentration increases further -- to the point where V_p very often contains at least one analyte atom -- it might be more practical to revert to the simple integration method once it is certain that the analyte signal is easily detectable above X_d.

Comparison of Signal Processing Methods

There have been a total of four possible signal processing methods which have been mentioned thus far in this work which can be applied to SAD methods: the "simple integration" method (with $T_m > t_r$), and the three time window methods: the sequential time window (with $t_w \approx t_r/20$), the photon burst and the sliding sum (peak

or area) methods. It is difficult to state unequivocally which of these is "better," since the performance of these is highly dependent on the conditions and the requirements of the experiment to be performed.

The process of simply integrating the signal during T_m may be desirable for small discrete sample or for the application of SAD methods to larger analyte concentrations, as has been mentioned. The advantage of simplicity is obvious; in addition, the signal can be processed in real time. However, any desired temporal information of the entry/exit times of individual atoms into V_p is restricted by the duration of T_m.

If the sensitivity of the SAD method is very high, then the possibility of sequential application of small time windows over T_m should be investigated. If SAD is possible during t_w, then the atoms can be monitored in real time as they cross through V_p. Obviously, this is the best situation one can hope for in an SAD method.

For methods in which the sensitivity is low enough to desire to increase t_w to about the level of t_r, then two possible methods have been addressed in this chapter, and some of their strengths and weaknesses have been demonstrated. The two main advantages of the photon burst method are the fact that it can be a real-time method [63] and that it is fairly uncomplicated. However, the application of this method to higher levels of analyte concentration or background noise is complicated by the presence of double counts due to single atoms. In addition, there is some loss in

detection efficiency of near-SAD methods due to the "splitting" of atom's photon burst.

The sliding sum method is a fairly powerful signal processing method to apply to near-SAD techniques. There is no loss of detection efficiency and information can be gained about the distribution of the analyte signal due to single atoms. In addition, the use of peak areas allows the application of this method to atom counting even at relatively high concentrations of analyte. The main disadvantages are that the method is computationally more complex than any of the others -- particularly for long measurement times -- and the method cannot be used in real-time.

Mention should be made of one other signal-processing method which has been used to detect photon bursts due to single atoms: autocorrelation of the raw data collected over T_m [66, 68]. Use of an autocorrelator is relatively simple and yet supplies good evidence of SAD if the analyte concentration is low enough that there are no more than one atom in V_p at a given time. Another advantage of this method is that the autocorrelogram can supply a good estimate of τ_i if T_m is long enough and the noise is low enough. However, there are problems in attempting to use the autocorrelation function in attempting to measure the total number of atoms which have passed through V_p during T_m [68].

There was no intent in this work to attempt to cover all possible signal-processing methods which can be applied to the raw data from an SAD experiment using CW-LIF. There are many more complicated signal processing

schemes or moving filters that might be useful. The intent in this chapter was merely to demonstrate that for all of these the detection theory presented in chapter five for the general SAD model is still applicable in these instances.

Conclusions

The main goal of this chapter was to use simple Monte Carlo simulations to illustrate the application of the concepts introduced in chapter five to specific numerical examples of SAD and near-SAD methods. What has become evident during the course of these experiments, however, is that such simulations can be very valuable in clarifying some of the subtleties of SAD techniques. Some of the examples seen in this chapter are the presence of the "extra" variance with the Cylindrical V_p model, the scopes of SAD methods, and the behavior of the two signal processing methods chosen.

However, the SAD theory presented, and the computer simulations used, are only as good as the model upon which they are based. A brief look at some of the assumptions inherent in the general SAD model as presented is warranted. The assumptions of Poisson processes for both the background noise and the detection process are not serious obstacles. It is quite likely that in many situations the first assumption is not valid; however, some assumption of the form of I_b had to be made, and a distribution other than a Poisson merely signifies that a different value of X_d must be chosen.

The assumption of a Poisson detection process is usually valid in the time frame of most experiments. However, the characteristics of Poisson processes must be kept firmly in mind. The presence of metastable traps, detector "dead" time, or space-charge effects can all alter the distribution of the detection process. In addition, clustering effects or other interatomic or intermolecular forces can alter the distribution of N_p.

Perhaps the biggest assumption in the general SAD model is that the probe volume is well-defined. In most analytical experiments, it is usually the case that the boundaries of the probe volume are rather vague due to either the collection/detection efficiency of laser-induced events in the atoms, or the spatial characteristics of the laser-beam itself. For example, a common method of describing the radius of a laser beam involves the use of the 1/e distance -- i.e., the distance at which the intensity decays to 1/e of its peak value. However, the laser beam obviously still has some intensity at values beyond this distance, and atoms "outside" the laser might still be detected. Likewise, in LIF experiments, the collection efficiency of most optical systems is a function of the distance of the emitter from the central axis of the system, and any abrupt "line" to define V_p is a gross simplification.

The concept of the detection efficiency itself is obviously only as well defined as the probe volume, despite the fact that the requirement for a method to be considered SAD has been given in terms of this FOM. It may often be more sensible to speak of an "effective" probe volume within which almost all detected events are likely to occur. In such cases, it may be impossible to achieve very high detection

efficiencies, since it will always be possible for an atom to skirt the edges of the ill-defined "effective" V_p.

The assumptions of the Simple model of course depend upon a very sharply-defined probe volume, within which ϕ_s is almost constant, and outside of which ϕ_s is effectively zero. Although difficult to achieve in practice, such a situation might often be desirable since the "extra" variance of the signal will be reduced, with consequent improvement in ϵ_d and RSD_c. Some of the possible methods to reduce variance include laser beam expansion, the use of spatial filters and apertures, and good collection optics (reduction of optical aberration); as mentioned earlier, decrease of the variance of the signal may more than compensate for any loss in S/N.

Despite the rather idealized nature of the general SAD model, many of the concepts of the theory of SAD based upon this model are of value to the laser spectroscopist. Even the analytical chemist interested only in ultra-trace analysis by laser-based techniques should be aware of many of the concepts presented for SAD, even if there is no desire to count individual atoms, since: (a) there may be few atoms or molecules of analyte being actively probed by the laser at the signal detection limit; and (b) the background noise is frequently reduced to very low levels, near the intrinsic limit. Of course, the analytical or physical chemists who are actually concerned with measuring signals or properties dealing with single atoms struggle with concerns which do not arise in more conventional experiments; the formulation of the general SAD model and the related concepts have illustrated this

fact most clearly, and might be used to advantage in the evaluation or optimization of any (near-)SAD technique.

APPENDIX
RANDOM NUMBER GENERATORS

The following two functions were used to generate random numbers in Microsoft QuickBASIC. Random numbers from a normal distribution were obtained from the following function, which accepted the desired mean and standard deviation as the input:

```
FUNCTION RndNorm! (mean!, StanDev!)
  DO
    RandomA! = 2! * RND - 1!
    RandomB! = 2! * RND - 1!
    Radius2! = RandomA! ^ 2 + RandomB! ^ 2
  LOOP UNTIL Radius2! < 1!                    'Mod. #2
  Deviate! = RandomA! * SQR((-2! * LOG(Radius2!)) / Radius2!)
  RndNorm! = mean! + Deviate! * StanDev!
END FUNCTION
```

This next function returned integers from a Poisson distribution:

```
FUNCTION Poisson% (mean!)
   p! = EXP(-mean!)
   N% = 0
   q! = RND
   DO UNTIL q! < p!
      q! = q! * RND
      N% = N% + 1
   LOOP
   Poisson% = N%
END FUNCTION
```

REFERENCES

1. IUPAC, Pure Appl. Chem., 1976, 45, 101-103.

2. Royal Society of Chemistry, Analyst, 1987, 112, 199-204.

3. H. Kaiser, Two Papers on the Limit of Detection of a Complete Analytical Procedure, 1969, Jafner Publishing Company, Inc. (New York).

4. L.A. Currie, Anal. Chem., 1968, 40, 586-592.

5. A.L. Wilson, Talanta, 1970, 17, 21-29.

6. A.L. Wilson, Talanta, 1970, 17, 31-44.

7. A.L. Wilson, Talanta, 1973, 20, 725-732.

8. M.A. Sharaf, D.L. Illman, B.R. Kowalski, Chemometrics, Chemical Analysis: A Series of Monographs on Analytical Chemistry and its Applications, P.J. Elving and J.D. Winefordner ed, 1986, Wiley-Interscience (New York).

9. R.L. Anderson, Practical Statistics for Analytical Chemists, 1987, Van Nostrand Reinhold Co. (New York).

10. D.L. Massart, B.G.M. Vandeginste, S.N. Deming, Y. Michotte, L. Kaufman, Chemometrics: a Textbook, Data Handling in Science and Technology, B.G.M. Vandeginste and L. Kaufman ed, 1988, Elsevier (Amsterdam).

11. J.C. Miller, J.N. Miller, Statistics for Analytical Chemistry, Ellis Horwood Series in Analytical Chemistry, R.A. Chalmers and M. Masson ed, 1988, 2nd ed, Ellis Horwood Limited (Chichester, England).

12. P.A. St. John, W.J. McCarthy, J.D. Winefordner, Anal. Chem., 1967, 39, 1495-1497.

13. L.A. Currie, "Detection: Overview of Historical, Societal, and Technical Issues," Detection in Analytical Chemistry, L.A. Currie ed, 1988, American Chemical Society (Washington DC), 1-62.

14. G.L. Long, J.D. Winefordner, Anal. Chem., 1983, 55, 712A-724A.

15. J.N. Miller, Analyst, 1991, 116, 3-14.

16. P.W.J.M. Boumans, Spectrochim. Acta, 1978, 33B, 625-634.

17. R.E. Walpole, R.H. Myers, "Sampling Distributions of Means," Probability and Statistics for Engineers and Scientists, 1989, 4th ed, Macmillan (New York), 210-215.

18. IUPAC, Spectrochim. Acta, 1978, 33B, 242-245.

19. R.E. Walpole, R.H. Myers, "Chebyshev's Theorem," Probability and Statistics for Engineers and Scientists, 1989, 4th ed, Macmillan (New York), 104-106.

20. N.R. Draper, H. Smith, Applied Regression Analysis, 1981, 2nd ed, John Wiley & Sons, Inc (New York).

21. R.H. Myers, Classical and Modern Regression with Applications, The Duxbury Advanced Series in Statistics and Decision Sciences, M. Payne ed, 1990, 2nd ed, PWS-Kent Publishing Co. (Boston).

22. R.L.J. Watters Jr., R.J. Carroll, C.H. Spiegelman, Anal. Chem., 1987, 59, 1639-1643.

23. R. de Levie, J. Chem. Ed., 1986, 63, 10-15.

24. A. Hubaux, G. Vos, Anal. Chem., 1970, 42, 849.

25. C.A. Clayton, J.W. Hines, P.D. Elkins, Anal. Chem., 1987, 59, 2508-2514.

26. D.G. Mitchell, J.S. Garden, Talanta, 1982, 29, 9210929.

27. L. Oppenheimer, T.P. Capizzi, R.M. Weppelman, H. Mehta, Anal. Chem., 1983, 55, 638-643.

28. M. Alden, U. Westblom, J.E.M. Goldsmith, Opt. Lett., 1989, 14, 305-307.

29. U. Westblom, S. Agrup, M. Alden, H.M. Hertz, J.E.M. Goldsmith, Appl. Phys. B, 1990, 50, 487-497.

30. T. Hirschfeld, Appl. Opt., 1976, 15, 2965-2966.

31. G.S. Hurst, M.H. Nayfeh, J.P. Young, Appl. Phys. Lett., 1977, 30, 229-231.

32. G.I. Bekov, V.S. Letokhov, O.I. Matveev, V.I. Mishin, Opt. Lett., 1978, 3, 159-161.

33. G.S. Hurst, M.G. Payne, S.D. Kramer, C.H. Chen, Phys. Today, 1980, Sept, 24-29.

34. G.S. Hurst, J. Chem. Ed., 1982, 59, 895-899.

35. G.S. Hurst, M.G. Payne, Principles and Applications of Resonance Ionization Spectroscopy, 1988, IOP Publishing Ltd. (Philadelphia).

36. V.S. Letokhov, Laser Photoionization Spectroscopy, 1987, Academic Press Inc. (Orlando FL).

37. D.J. Wineland, W.M. Itano, Phys. Lett., 1981, 82A, 75-78.

38. W.M. Itano, J.C. Bergquist, D.J. Wineland, Science, 1987, 237, 612-617.

39. W.P. Ambrose, W.E. Moerner, Nature, 1991, 349, 225-227.

40. W.E. Moerner, L. Kador, Phys. Rev. Lett., 1989, 62, 2535-2538.

41. W.E. Moerner, New J. Chem., 1991, 15, 199-208.

42. M. Orrit, J. Bernard, Phys. Rev. Lett., 1990, 65, 2716-2719.

43. G.S. Hurst, M.G. Payne, S.D. Kramer, S.H. Chen, R.C. Philips, S.L. Allman, G.D. Alton, J.W.T. Dabbs, R.D. Willis, B.E. Lehmann, Rep. Prog. Phys., 1985, 48, 1333-1370.

44. G.S. Hurst, M.H. Nayfeh, J.P. Young, Phys. Rev. A., 1977, 15, 2283-2292.

45. D.J. Wineland, J.C. Bergquist, W.M. Itano, J.J. Bollinger, C.H. Manney, Phys. Rev. Lett., 1987, 59, 2935.

46. G.I. Bekov, V.S. Letokhov, V.N. Radaev, J. Opt. Soc. Am. B, 1986, 2, 1554-1559.

47. D.L. Pappas, D.M. Hrubowchak, M.H. Ervin, N. Winograd, Science, 1989, 243, 64-66.

48. G.I. Bekov, V.S. Letokhov, O.I. Matveev, V.I. Mishin, Sov. Phys. JETP, 1978, 48, 1052-1056.

49. G.I. Bekov, V.S. Letokhov, V.I. Mishin, JETP Lett., 1978, 27, 47-51.

50. G.I. Bekov, E.P. Vidolova-Angelova, V.S. Letokhov, V.I. Mishin, "Selective Detection of Single Atoms by Multistep Excitation and Ionization through Rydberg States," Laser Spectroscopy IV, vol. 21 in "Springer Series in Optical Sciences," H. Walther and K.W. Rothe ed, 1979, Springer (Berlin), 283-294.

51. S.D. Kramer, C.E. Bemis Jr, J.P. Young, G.S. Hurst, Opt. Lett., 1978, 3, 16-18.

52. S.D. Kramer, J.P. Young, G.S. Hurst, M.G. Payne, Opt. Comm., 1979, 30, 47-50.

53. M. Maeda, Y. Nomiyama, Y. Miyazoe, Jap. J. Appl. Phys., 1981, 20, L5-L8.

54. A.T. Tursunov, N.B. Eshkabilov, Sov. Phys. Tech. Phys., 1984, 29, 93-94.

55. G.S. Hurst, Anal. Chem., 1981, 53, 1448A-1456A.

56. V.S. Letokhov, Sci. Am., 1988, Sept., 54-59.

57. V.I. Balykin, V.S. Letokhov, V.I. Mishin, Appl. Phys., 1980, 22, 245-250.

58. N.J. Dovichi, J.C. Martin, J.H. Jett, M. Trkula, R.A. Keller, Anal. Chem., 1984, 56, 348-354.

59. W.M. Fairbank Jr., T.W. Hansch, A.L. Schawlow, J. Opt. Soc. Am., 1975, 65, 199-204.

60. J.A. Gelbwachs, C.F. Klein, J.E. Wessel, Appl. Phys. Lett., 1977, 30, 489-491.

61. G.W. Greenlees, D.L. Clark, S.L. Kaufman, D.A. Lewis, J.F. Tonn, Opt. Comm., 1977, 23, 236-239.

62. J.H. Jett, R.A. Keller, J.C. Martin, B.L. Marrone, R.K. Moyzis, R.L. Ratliff, N.K. Seitzinger, E.B. Shera, C.C. Stewart, J. Biolmol. Struct. Dynam., 1989, 7, 301.

63. D.A. Lewis, J.F. Tonn, S.L. Kaufman, G.W. Greenlees, Phys. Rev. A, 1979, 19, 1580-1588.

64. W. Nagourney, J. Sandberg, H. Dehmelt, "Quantum Jumps and Laser Spectroscopy of a Single Barium Ion Using "Shelving"," Laser Spectroscopy VIII, vol. 55 in "Springer Series in Optical Sciences," W. Persson and S. Svanberg ed, 1987, Springer (Berling), 114-115.

65. D.C. Nguyen, R.A. Keller, J.H. Jett, J.C. Martin, Anal. Chem., 1987, 59, 2158-2161.

66. K. Peck, L. Stryer, A.N. Glazer, R.A. Mathies, Proc. Natl. Acad. Sci. USA, 1989, 86, 4087-4091.

67. E.B. Shera, N.K. Seitzinger, L.M. Davis, R.A. Keller, S.A. Soper, Chem. Phys. Lett., 1990, 174, 553-557.

68. S.A. Soper, E.B. Shera, J.C. Martin, J.H. Jett, J.H. Hahn, H.L. Nutter, R.A. Keller, Anal. Chem., 1991, 63, 432-437.

69. W.B. Whitten, J.M. Ramsey, S. Arnold, B.V. Bronk, Anal. Chem., 1991, 63, 1027-1031.

70. A. Hald, Statistical Theory with Engineering Applications, 1952, Wiley (New York).

71. J. Mandel, The Statistical Analysis of Experimental Data, 1984, Dover Publications, Inc. (New York).

72. R.E. Walpole, R.H. Myers, "Estimation," Probability and Statistics for Engineers and Scientists, 1989, 4th ed, Macmillan (New York), 231-285.

73. V.I. Balykin, G.I. Bekov, V.S. Letokhov, V.I. Mishin, Sov. Phys. Usp., 1980, 23, 651-677.

74. H. Falk, Prog. Analyt. Atom. Spectrosc., 1980, 3, 181-208.

75. G.M. Hieftje, J. Chem. Ed., 1982, 59, 900-909.

76. V.S. Letokhov, "Photoionization Detection of Single Atoms," Laser Photoionization Spectroscopy, 1987, Academic Press Inc. (Orlando), 93-116.

77. N. Omenetto, B.W. Smith, J.D. Winefordner, Spectrochim. Acta, 1988, 43B, 1111-1118.

78. J.D. Winefordner, B.W. Smith, N. Omenetto, Spectrochim. Acta, 1989, 44B, 1397-1403.

79. C.T.J. Alkemade, Appl. Spectrosc., 1981, 35, 1-13.

80. C.T.J. Alkemade, "Detection of Small Numbers of Atoms and Molecules," Analytical Applications of Lasers, E. Piepmeier ed, 1986, Wiley-Interscience (New York), 107-162.

81. C.L. Stevenson, J.D. Winefordner, Chemtracts - Anal. Phys. Inorg. Chem., 1990, 2, 217-262.

82. R.E. Walpole, R.H. Myers, "Gamma and Exponential Distributions," Probability and Statistics for Engineers and Scientists, 1989, 4th ed, Macmillan (New York), 164-169.

83. R.E. Walpole, R.H. Myers, "Poisson Distribution and the Poisson Process," Probability and Statistics for Engineers and Scientists, 1989, 4th ed, Macmillan (New York), 131-136.

84. N. Omenetto, J.D. Winefordner, Prog. Anal. At. Spectrosc., 1979, 2, 1-183.

85. N. Omenetto, B.W. Smith, L.P. Hart, Fresenius Z. Anal. Chem., 1986, 324, 683.

86. E.C. Molina, Poisson's Exponential Binomial Limit, 1947, 4th ed, D. van Nostrand Company Inc. (New York).

87. R.E. Walpole, R.H. Myers, "Mathematical Expectation," Probability and Statistics for Engineers and Scientists, 1989, 4th ed, Macmillan (New York), 79-108.

88. D.E. Knuth, "Random Numbers," The Art of Computer Programming, 1969, 1st ed, vol. 2, Addison-Wesley (Reading, MA), 1-118.

89. B.W. Smith, P.B. Farnsworth, P. Cavalli, N. Omenetto, Spectrochim. Acta, 1990, 45B, 1369-1373.

90. E. Voigtman, J.D. Winefordner, Prog. Analyt. Atom. Spectrosc., 1986, 9, 7.

91. G.-T. Wei, J.P. Dougherty, F.R. Preli Jr., R.G. Michel, J. Anal. At. Spectrosc., 1990, 5, 249.

92. H. Mark, J.W. Jr., Spectroscopy, 1989, 4, 56-58.

93. J. Berkson, J. Amer. Statistical Assn., 1950, 45, 164.

94. J. Neter, W. Wasserman, M.H. Kutner, "Simultaneous Inferences and other Topics in Regression Analysis -- I," Applied Linear Statistical Models, 1985, Richard D. Irwin, Inc. (Homewood, IL), 147-176.

BIOGRAPHICAL SKETCH

Christopher Leonidas Stevenson was born in Cleveland, Ohio, on October 4, 1964. Upon graduation from Sanderson High School in Raleigh, NC, he attended the University of North Carolina at Chapel Hill, receiving his Bachelor of Science in Chemistry in 1986. In August, 1986, he entered the Graduate School at the University of Florida in Gainesville.

I certify that I have read this study and that in my opinion it conforms to acceptable standards of scholarly presentation and is fully adequate, in scope and quality, as a dissertation for the degree of Doctor of Philosophy.

James D. Winefordner, Chairman
Graduate Research Professor of Chemistry

I certify that I have read this study and that in my opinion it conforms to acceptable standards of scholarly presentation and is fully adequate, in scope and quality, as a dissertation for the degree of Doctor of Philosophy.

Anna Brajter-Toth
Associate Professor of Chemistry

I certify that I have read this study and that in my opinion it conforms to acceptable standards of scholarly presentation and is fully adequate, in scope and quality, as a dissertation for the degree of Doctor of Philosophy.

Richard A. Yost
Professor of Chemistry

I certify that I have read this study and that in my opinion it conforms to acceptable standards of scholarly presentation and is fully adequate, in scope and quality, as a dissertation for the degree of Doctor of Philosophy.

Daniel Talham
Assistant Professor of Chemistry

I certify that I have read this study and that in my opinion it conforms to acceptable standards of scholarly presentation and is fully adequate, in scope and quality, as a dissertation for the degree of Doctor of Philosophy.

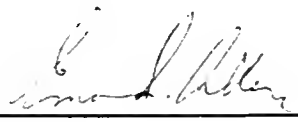

Eric Allen
Professor of Environmental Engineering

This dissertation was submitted to the Graduate Faculty of the Department of Chemistry in the College of Liberal Arts and Sciences and to the Graduate School and was accepted as partial fulfillment of the requirements for the degree of Doctor of Philosophy.

December 1991

Dean, Graduate School